DEPARTMENT OF THE INTERIOR
U.S. GEOLOGICAL SURVEY

Sediment properties related to prediction of embedment and penetration depth of objects into the seafloor off the Farallon Islands, California

by

William J. Winters[1] and James S. Booth[1]

Open-File Report 87-600

Prepared in cooperation with the
U.S. Environmental Protection Agency under
interagency agreement DW14931699-01

[1]Woods Hole, Massachusetts 02543

October 1987

CONTENTS

ABSTRACT

This report presents the findings of a laboratory testing program that was performed on three short sediment cores that were obtained at different water depths south west of the Farallon Islands. Results from index property, consolidation, and triaxial compression strength tests enabled an evaluation to be made of the relative penetrability of the sediment at the three sites. The importance of the geotechnical tests for determining the suitability of seafloor sediments for radioactive waste disposal is also discussed.

INTRODUCTION

Both high-level and low-level nuclear wastes are produced by many government and private organizations within the United States. Disposing of some types of waste within the seafloor may be feasible if adequate burial depth is achieved.

This report presents a geotechnical methodology for predicting the relative penetrability of seafloor sediment by objects free-falling or propelled through the water column. Furthermore, the test results may provide insight into bottom sediment behavior that affects hole closure after full penetration by an object has occurred.

It is not the intent of this report to show a detailed example of how sediment properties are used to predict penetration depth. Examples of such procedures have been published elsewhere: Rocker (1985); Beard (1984); Valent and Lee (1976); True (1974); and Schmid (1969).

Index, consolidation, and shear-strength tests were performed on three sediment cores obtained south west of the Farallon Islands, Calif. (Table 1, Fig. 1) to show how geotechnical tests can be used to assess the penetration potential of seafloor material. The area has not been actively used as a dumpsite since 1965 (Schell and Sugai, 1980). Although numerical penetration depths are not presented in this report, the relative penetrability of the three sites is discussed. The test results can also be applied to many other projects involving the seafloor.

Six main sections are included in this report: (1) shipboard sampling, shipping, and storage of geotechnical samples; (2) a description of the test methods; (3) results of the laboratory testing; (4) discussion and comparison of test results; (5) discussion of geotechnical test results as predictors of the penetration depth of canisters; and (6) conclusions and recommendations for future investigations.

SHIPBOARD SAMPLING, TRANSPORTATION, AND STORAGE

Two box cores were obtained at each of three stations aboard the National Oceanic and Atmospheric Administation (NOAA) R/V DAVID STARR JORDAN in December 1985. Three polycarbonate liners (approximately 9.3 cm O.D., 8.9 cm I.D., and 30 cm long) sharpened at one end were pushed into one box core from each station at sea. One of those sediment cores from each station was preserved for geotechnical testing (Table 1). The geotechnical cores were capped and taped at both ends and stored vertically. The bottom was also dipped in molten wax to reduce the potential for pore-water drainage. The

Table 1. Core locations, water depths, and sediment intervals.

Core	Latitude Longitude	Approximate Water Depth (m)	Sediment Interval (m)
BC-1	37°28.4'N 123°01.8'W	516	0 - 0.240
BC-3	37°33.9'N 123°07.75'W	1007	0 - 0.260
BC-5	37°35.9'N 123°14.0'W	1494	0 - 0.265

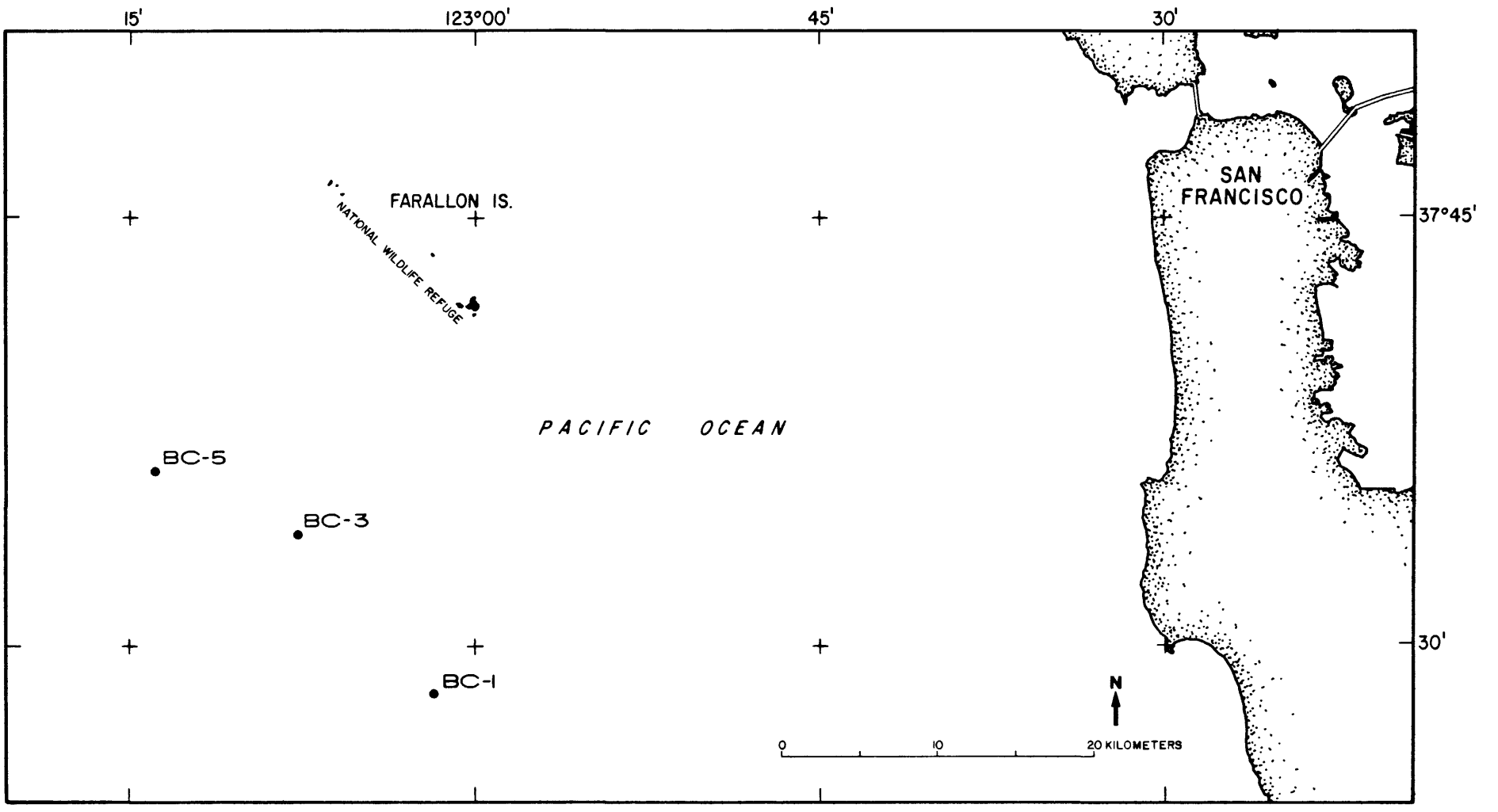

Figure 1. Station location map.

cores were then shipped to Woods Hole, Mass within a padded container that maintained a cool temperature by means of frozen ice packs. Care was taken to prevent the frozen packs from contacting the sediment at any time.

In Woods Hole, the cores were visually inspected and vertically stored inside a refrigerator at an approximate temperature of $4^{o}C$. No pull-apart zones or tension cracks were observed in the sediment through the translucent liner walls. However, the sediment may have been severely disturbed during shipment. The cores were shipped with a space between the top sediment surface and the top cap, and the presence of sediment adhering to the inside of the top caps when delivered indicated that the cores may have been placed on their side or even rotated end-over-end during transit.

METHODS

Three main types of tests were performed: (1) index property, (2) consolidation, and (3) shear strength. The core was partitioned for testing as shown in Figure 2.

Index properties provide information on general engineering behavior. Often, more sophisticated parameters that bear directly on penetration or embedment (such as effective stress friction angle (ϕ') or strength to overburden stress ratio (s_u/σ'_{vo}) can be approximated by utilizing correlations that are based on index properties.

Methods for index-property measurements followed the recommendations of ASTM, with the following exceptions: water contents were measured from samples oven dried at 50^{o}; liquid limits were determined using the fall-cone penetrometer method (Head, 1980, p. 69-73); and grain specific gravity values were calculated using an air comparison pycnometer with helium as the purge and chamber gas. All data were corrected for salt content assuming a salinity of 35 ppt and bulk samples (i.e., unsieved) were used for all tests. Details of each test procedure are given in Winters and Booth (1986) or Winters (1986).

Constant rate-of-strain consolidation (CRSC) tests were performed within triaxial chambers, utilizing 63.5-mm-diameter and 18.9-mm-high samples, according to methods given in Winters and Booth (1986) or Winters (1986). Consolidation test data are used to evaluate: (1) the stress history of the sediment, i.e., how the assumed present in situ stress state compares with previous geologically-induced stresses; (2) the amount of settlement or compressibility that can be expected from engineering loading; and (3) the rate at which consolidation will occur. Compressibility is influenced by stress history and is related to penetration susceptibility; very compressible sediment is probably easily penetrated. Additionally, parameters related to the permeability of the sediment are derived. Permeability can be used to predict a rate of radionuclide migration through the sediment.

The most important set of measurements that bear on penetration are those related to shear strength. Numerous methods are available to determine shear strength parameters; in this study, the laboratory miniature-vane-shear test and the triaxial-compression test were performed according to guidelines presented in Winters and Booth (1986) or Winters (1986). Vane-shear tests were attempted at the top and bottom of each core (Fig. 2), using a Wykeham-

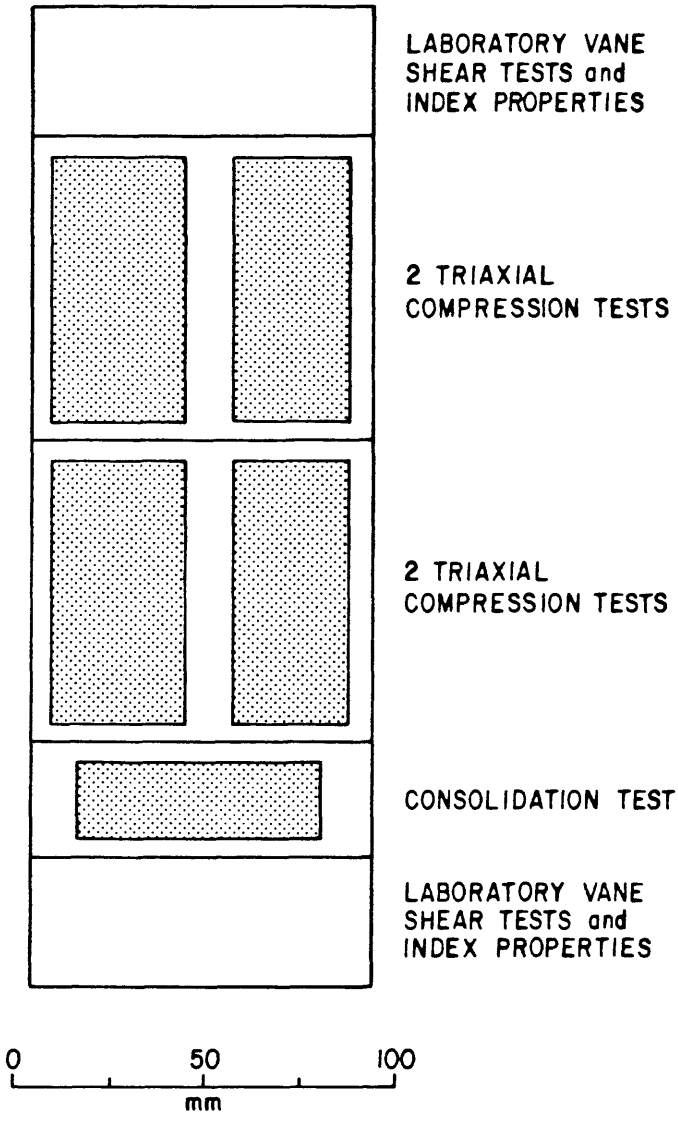

Figure 2. Longitudinal view of a sediment core showing relative positions of samples used for laboratory geotechnical tests.

Farrance vane-shear machine equipped with a 12.7-mm-high by 12.7-mm-diameter vane and a 25.4-mm by 25.4-mm vane, at a rotation rate at the top of the machine's spring of approximately 84°/minute. A lack of sediment precluded our using the larger size vane at some locations and the vane shear tests performed on core BC-1 were judged invalid because the coarse grain size permitted partial drainage of pore water during the test.

We performed triaxial tests to allow extrapolation of undrained-shear-strength measurements to depths below the level of sampling, assuming uniform sediment conditions with subbottom depth and a constant normally consolidated stress history. Such extrapolation is an important goal because the sediment available for testing in this study was obtained from a shallow subbottom depth. The triaxial tests further define the drained-effective-stress strength envelope.

All of the approximately 35-mm-diameter by 70-mm-high triaxial samples were back pressured to about 300 kPa and three of the four triaxial samples from each core were isotropically consolidated overnight to different effective stresses (σ'_c) representative of vertical effective stresses of possible field conditions involving projectile penetration (approximately 70, 140, and 210 kPa). The fourth sample was not consolidated, but subjected instead to a cell pressure equal to the back pressure. After consolidation was complete, the triaxial test samples were vertically loaded at a constant rate of strain without drainage while axial force, vertical displacement, cell pressure, and pore pressure measurements were recorded.

RESULTS OF SEDIMENT PROPERTY MEASUREMENTS

Index properties

Water contents (w), ranging from 226% in core BC-5 to 32% in core BC-1, decreased with subbottom depth in all cores. Liquid limits, w_L, varied from 90% in core BC-5 to 39% in core BC-1. Plastic limits, w_P, ranged from 30 to 40% in cores BC-3 and BC-5, however, sediment from core BC-1 was non-plastic (i.e., a plastic limit could not be determined). Plasticity index, I_P, (w_L-w_P), and liquidity index, I_L, $(w-w_P)/I_P$, results exhibit a wide range in values. Plasticity indices vary from 23% in core BC-3 to 50% in core BC-5; and liquidity indices range from 0.91 to 1.85. Results of all index propeerty tests are presented in Table 2.

The Atterberg Limits results as plotted on a plasticity chart (Casagrande, 1948) are shown in Figure 3. The data from core BC-3 plot parallel to and slightly below the A-line indicating the sediment can be classified as a silt with high (w_L>50%) compressibility. Because the data from core BC-5 predominantly plot above the A-line, inorganic clay with high plasticity is probably the main sediment component (Peck and others, 1974, p. 22).

Grain density values (ρ_s) ranged from 2.59 to 2.67 g/cm^3. The results for core BC-5 (~2.60 g/cm^3) are significantly less than values considered typical of most fine-grained continental margin sediment.

The bulk density (ρ_t) equal to $[\rho_s(1+(w/100))/(1+e)]$, void ratio (e) equal to $[G_s(w/100)]$, and porosity (η) equal to $[e/(1+e)]$ values were calculated from the grain specific gravity and water content data assuming 100 percent saturation (Table 2).

Table 2. DJ-85-FI Vane Shear Strengths and Index Properties.

Core ID	Depth in core (m)	Vane size (mm)	S_{uv} (kPa)	S_{rv} (kPa)	S_t	w (%)	w_L (%)	w_P (%)	I_P (%)	I_L	G_s	ρ_t (g/cm^3)	e	η
BC-1(500m)	0.00-0.02	-	NV	NV	-	41	41	NP	-	-	2.65	1.79	1.09	0.52
	0.18-0.21	-	-	-	-	-					2.67			
	0.21-0.23	-	NV	NV	-	32	39	NP	-	-	2.67	1.90	0.85	0.46
BC-3(1000m)	0.00-0.03	-	-	-	-	111	77	37	40	1.85				
		12.7	0.5	0.1	5.2	147								
		12.7	0.6	0.2	3.0	170								
		25.4	0.7	0.4	1.9	-								
		25.4	0.7	0.4	1.8	-								
	0.03-0.11	-	-	-	-	77	60	32	28	1.61				
	0.11-0.19	-	-	-	-	60	54	30	24	1.25				
	0.19-0.22	-	-	-	-	-					2.63			
	0.22-0.25	-	-	-	-	51	53	30	23	0.91	2.65	1.70	1.35	0.57
		12.7	9.6	2.9	3.3	52								
		12.7	13.2	4.1	3.2	47								
BC-5(1500m)	0.00-0.03	-	-	-	-	124	90	40	50	1.68				
		12.7	0.8	0.2	4.0	187								
		12.7	0.9	-	-	226								
		25.4	0.9	0.4	2.4	173								
		25.4	1.7	0.7	2.3	139								
	0.03-0.11	-	-	-	-	100	77	34	43	1.53				
	0.11-0.18	-	-	-	-	79	79	35	44	1.00				
	0.19-0.22	-	-	-	-	-					2.59			
	0.22-0.25	-	-	-	-	69	69	30	39	1.00	2.61	1.57	1.80	0.64
		12.7	11.6	3.4	3.4	62								
		12.7	12.6	3.5	3.6	68								

where: NV = Test not valid (sandy sediment)
S_{uv} = Natural undrained vane shear strength
S_{rv} = Remolded undrained vane shear strength
S_t = Sensitivity (S_{uv}/S_{rv})
w = Natural water content (corrected for an assumed salinity of 35 ppt)
w_L = Liquid limit
W_P = Plastic limit
I_P = Plasticity index
I_L = Liquidity index
G_s = Grain specific gravity
ρ_t = Bulk density
e = Void ratio
η = Porosity
NP = Non-plastic

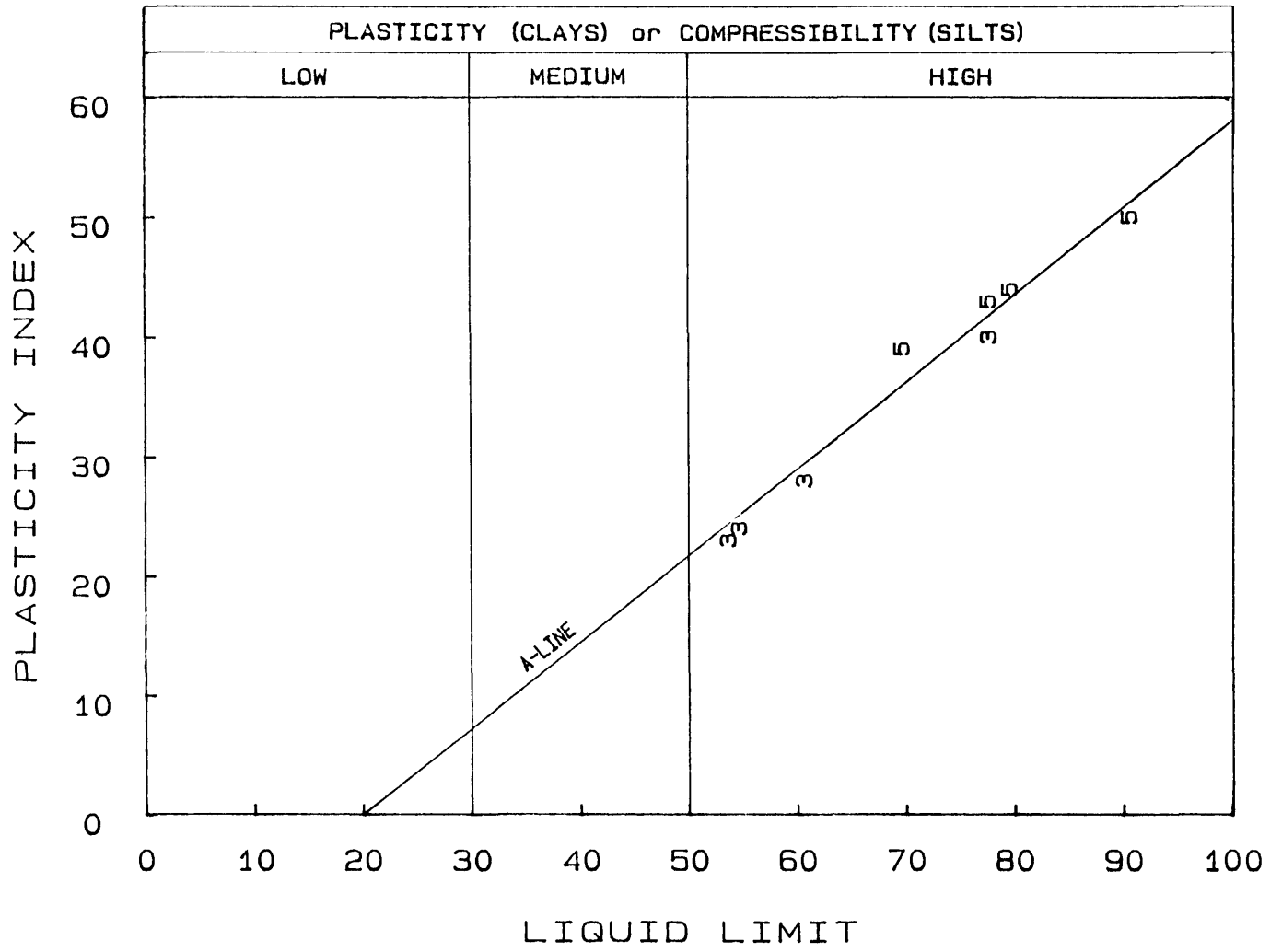

Figure 3. Plasticity chart for DJ-85-FI sediment. Data from core BC-3 are represented by a 3; data from core BC-5 are represented by a 5.

Consolidation properties

The consolidation-test results for all three cores are plotted on the same graph as void ratio (e) versus the vertical effective stress (σ'_v), (plotted on a log scale) (Fig. 4). Other consolidation test results including the coefficient of permeability (coefficient of hydraulic conductivity) (k) which may be of importance in nuclear waste disposal analyses, are listed in Table 3 and are plotted in Appendix A.

At higher stresses, the slope of the virgin e-log σ'_v line is termed the compression index (C_c) a parameter that reflects the compressibility and therefore the penetration susceptibility of sediment. The laboratory compression indices ranged from 0.12 to 0.54.

The maximum past stress (σ'_{vm}) a very important parameter that is related to the sediment's stress history is useful in determining how past geologic-loading conditions compare with present in situ stresses (Casagrande, 1936). The maximum past stresses ranged from 12 to 150 kPa (Table 3). A high maximum past stress near the seafloor indicates that cementation effects are present or that mass wasting may have exposed the penetration resistent sediment.

Strength properties

The natural vane shear strengths (s_{uv}) ranging from 0.5 to 13.2 kPa, were significantly higher at the bottom of the cores than at the tops (Table 2). The remolded shear strengths, s_{rv}, varied from 0.1 to 4.1 kPa.

The sensitivity (S_t) (equal to s_{uv}/s_{rv}) a factor related to the amount of strength loss exhibited upon remolding, ranged from 1.8 to 5.2 (Table 2). A high sensitivity promotes deeper penetration in a particular sediment because much of its natural shear strength is lost upon remolding caused by the penetration process.

Undrained shear strengths (s_u or maximum q) and friction angles (ϕ') expressed in terms of effective stresses were calculated from the triaxial test results (Table 4, Figs. 5-7, Appendix B). The friction angle is used in penetration analyses if the rate of loading is slow enough to allow pore pressure dissipation. Because penetration seldom occurs that slowly in fine-grained sediment, friction angles are primarily used in relation to coarse-grained material. Even in coarse-grained sediment penetration might be too fast to allow significant drainage. In such cases the friction angle may be used to determine the undrained shear strength using the method of Seed and Lee (1967) (Beard, 1981).

Because the samples at the two highest consolidation stresses for each core approached normal consolidation, friction angles assuming no cohesion intercept ($\phi'(c'=o)$) were calculated for them (Table 4); however, superimposing the results of all four tests from a particular core enabled the determination of a friction angle ($\phi'(c'\neq o)$) with a cohesion intercept (c') for each site. Friction angles assuming no cohesion intercept varied from 36.6 to 40.9°, whereas friction angles accompanied by a cohesion intercept ranged from 34.6 to 38.5° (Table 4).

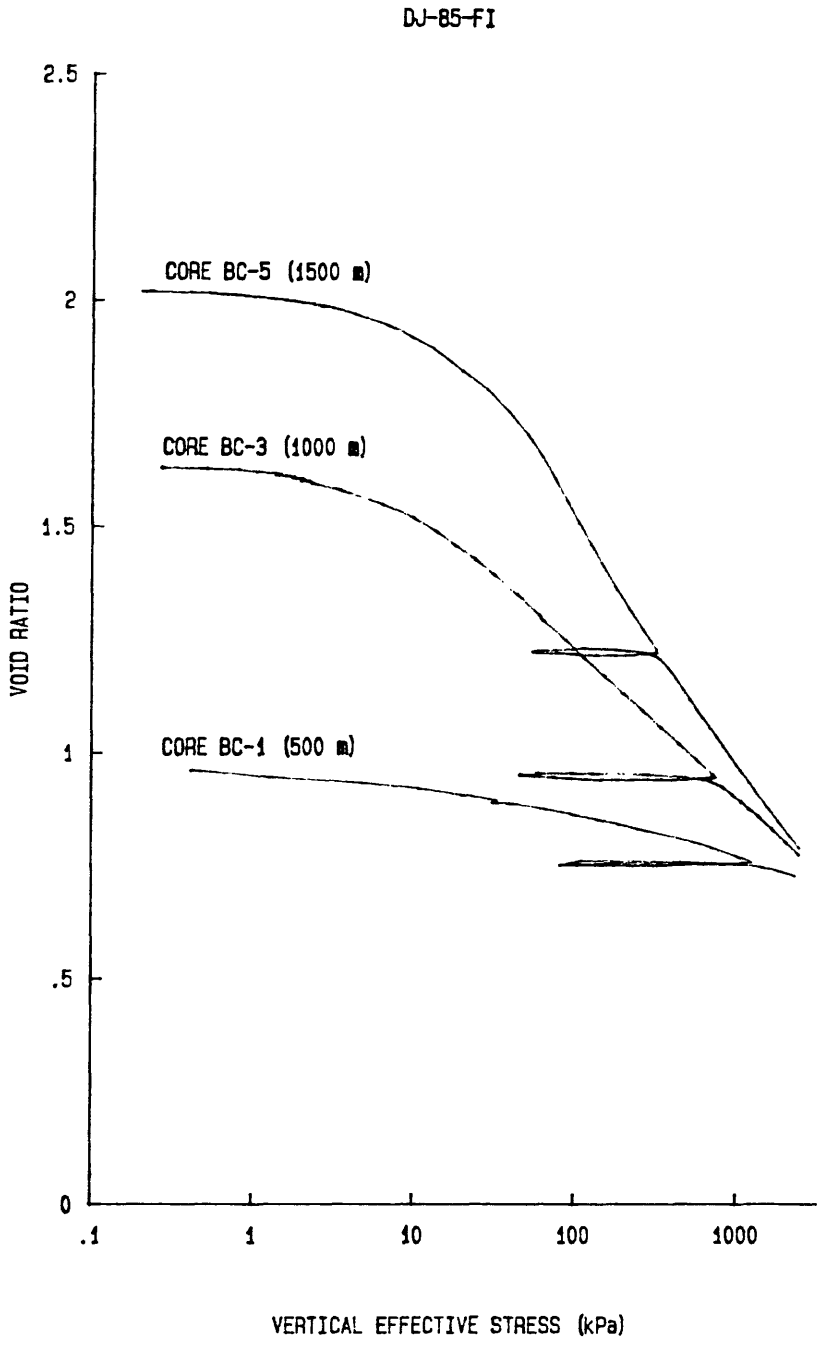

Figure 4. Void ratio versus vertical effective stress plots derived from constant rate of strain consolidation tests.

Table 3. DJ-85-FI Consolidation Test Results.

Core ID	Test No.	Depth in core (m)	w (%)	σ'_{vo} (kPa)	σ'_{vm} (kPa)	σ'_e (kPa)	OCR	C_c (ave)	C_{cf}	C_r	$c_v(\sigma'_{vo})$ (cm^2/s)	$c_v(\sigma'_{vm})$ (cm^2/s)	c_v(ave) (cm^2/s)	$k(\sigma'_{vo})$ (cm/s)	$k(\sigma'_{vm})$ (cm/s)	k(ave) (cm/s)	I_D	Comments
BC-1	CR060	0.195	36	1.57	150?	150	95	0.12	0.14	-	$8x10^{-2}$	$4x10^{-1}$	$9x10^{-1}$	$4x10^{-5}$	$6x10^{-6}$	$5x10^{-6}$	0.57	Sandy
BC-3	CR061	0.21	62	0.87	12	11	14	0.32	0.36	0.01	-	$1x10^{-2}$	$2x10^{-2}$	-	$3x10^{-6}$	$6x10^{-7}$	0.31	
BC-5	CR062	0.205	78	0.73	34	33	47	0.54	0.74	0.01	-	-	$3x10^{-3}$	-	-	$6x10^{-8}$	0.37	

Where:

w = Natural water content (corrected for an assumed salinity of 35 ppt).

σ'_{vo} = In-situ effective overburden stress.

σ'_{vm} = Maximum past vertical effective stress (determined by Casagrande (1936) method).

σ'_e = Excess vertical effective stress ($\sigma'_{vm}-\sigma'_{vo}$).

OCR = Overconsolidation ratio.

I_D = Disturbance index (determined by Silva (1974) method).

C_c (ave) = Average compression index.

C_{cf} = Corrected field compression index (determined by Schmertmann (1955) method).

C_r = Rebound-recompression index.

c_v (σ'_{vo}) = Coefficient of consolidation at the in-situ effective overburden stress.

$c_v(\sigma'_{vm})$ = Coefficient of consolidation at the maximum past vertical effective stress.

c_v (ave) = Average coefficient of consolidation for virgin compression.

k (σ'_{vo}) = Coefficient of permeability at the in-situ effective overburden stress.

$k(\sigma'_{vm})$ = Coefficient of permeability at the maximum past vertical effective stress.

k (ave) = Average coefficient of permeability for virgin compression.

Table 4. DJ-85-FI Triaxial Compression Test Results.

Core ID	Test No.	Depth in core (m)	w (%)	w_s (%)	σ'_c (kPa)	A_f	Strain at failure (%)	s_u (kPa)	s_u/σ'_c	ϕ' (c'=0) (degrees)	ϕ' (c'≠0) (degrees)	c' (kPa)
BC-1	TS008 (40)	0.140	35	44	0.0	-0.15	15.5	7.6	-	-	38.5	2.0
	TS007 (39)	0.145	37	35	69.9	-0.10	19.5	156.8	2.24	-	38.5	2.0
	TS006 (38)	0.060	35	34	145.4	-0.09	19.0	290.6	2.00	37.6	38.5	2.0
	TS005 (37)	0.060	35	40	206.9	-0.06	20.1	390.5	1.89	38.7	38.5	2.0
BC-3	TS004 (36)	0.146	67	62	0.0	0.16	18.7	12.8	-	-	34.6	9.3
	TS003 (35)	0.146	60	47	69.9	0.59	19.9	42.2	0.60	-	34.6	9.3
	TS002 (34)	0.071	74	48	147.7	0.65	20.1	78.3	0.53	39.3	34.6	9.3
	TS001 (33)	0.071	84	45	209.1	0.89	15.0	86.4	0.41	37.6	34.6	9.3
BC-5	TS012 (44)	0.145	82	79	0.0	0.05	14.1	11.0	-	-	38.2	6.6
	TS011 (43)	0.145	82	59	69.2	0.63	18.7	41.3	0.60	-	38.2	6.6
	TS010 (42)	0.065	97	47	143.1	0.99	19.7	53.6	0.37	36.6	38.2	6.6
	TS009 (41)	0.065	97	47	205.9	0.81	18.0	95.6	0.46	40.9	38.2	6.6

where: w = Natural water content (corrected for an assumed salinity of 35 ppt).

w_s = Water content during undrained shear.

σ'_c = Consolidation stress.

A_f = The coefficient of pore pressure response at failure (change in pore pressure at failure/change in deviator stress).

s_u = Undrained shear strength (maximum q during shear; $q = (\sigma_1 - \sigma_3)/2$.

ϕ' (c'=0) = Effective friction angle from an individual test assuming no cohesion intercept; the reported values are preliminary, they may be changed upon further analysis.

ϕ' (c'≠0) = Effective friction angle from a set of tests performed on similar sediment; the reported values are preliminary, they may be changed upon further analysis.

c' = Effective cohesion intercept from a set of tests performed on similar sediment; the reported values are preliminary, they may be changed upon further analysis.

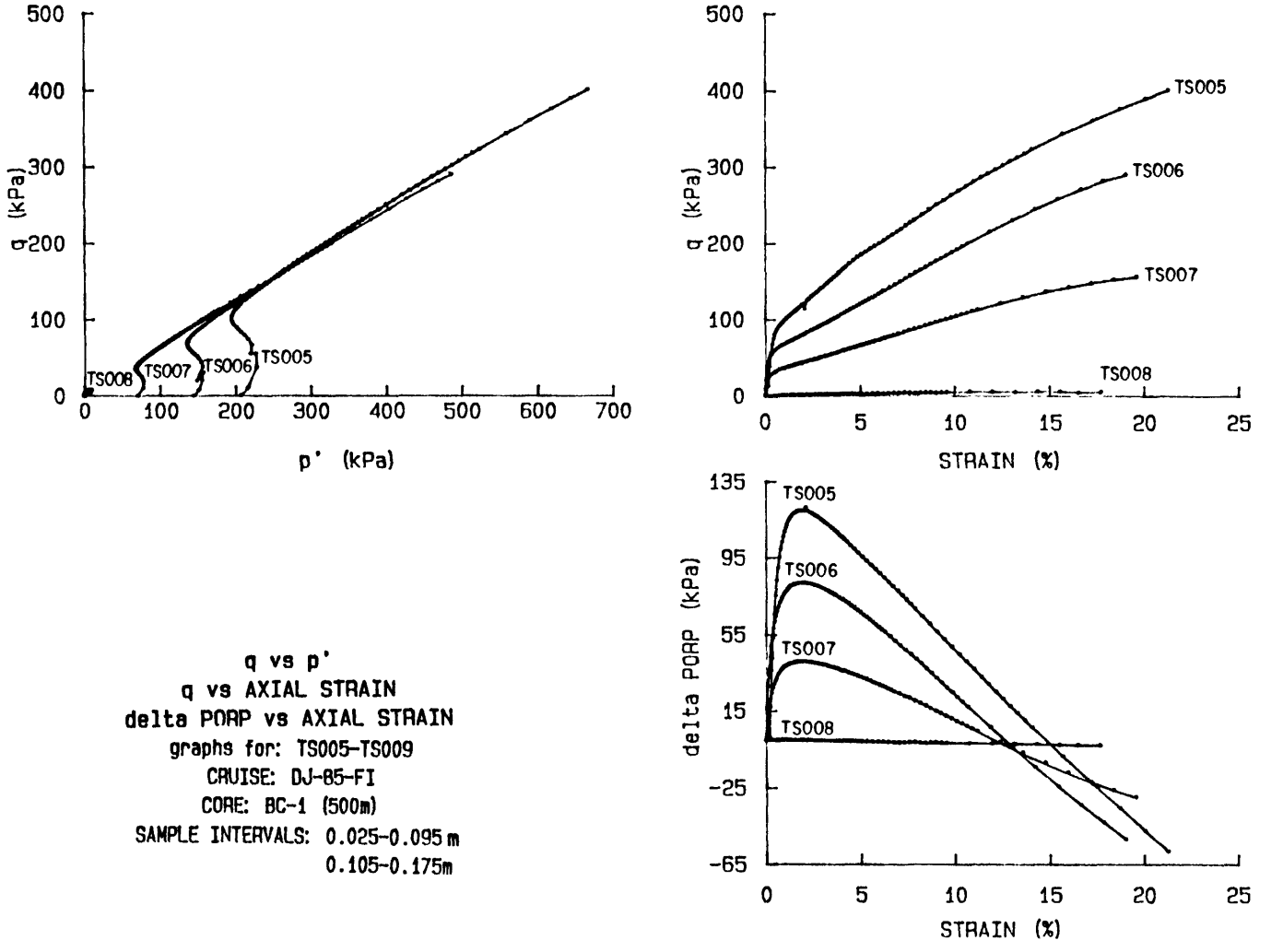

Figure 5. Triaxial compression test results for core BC-1.

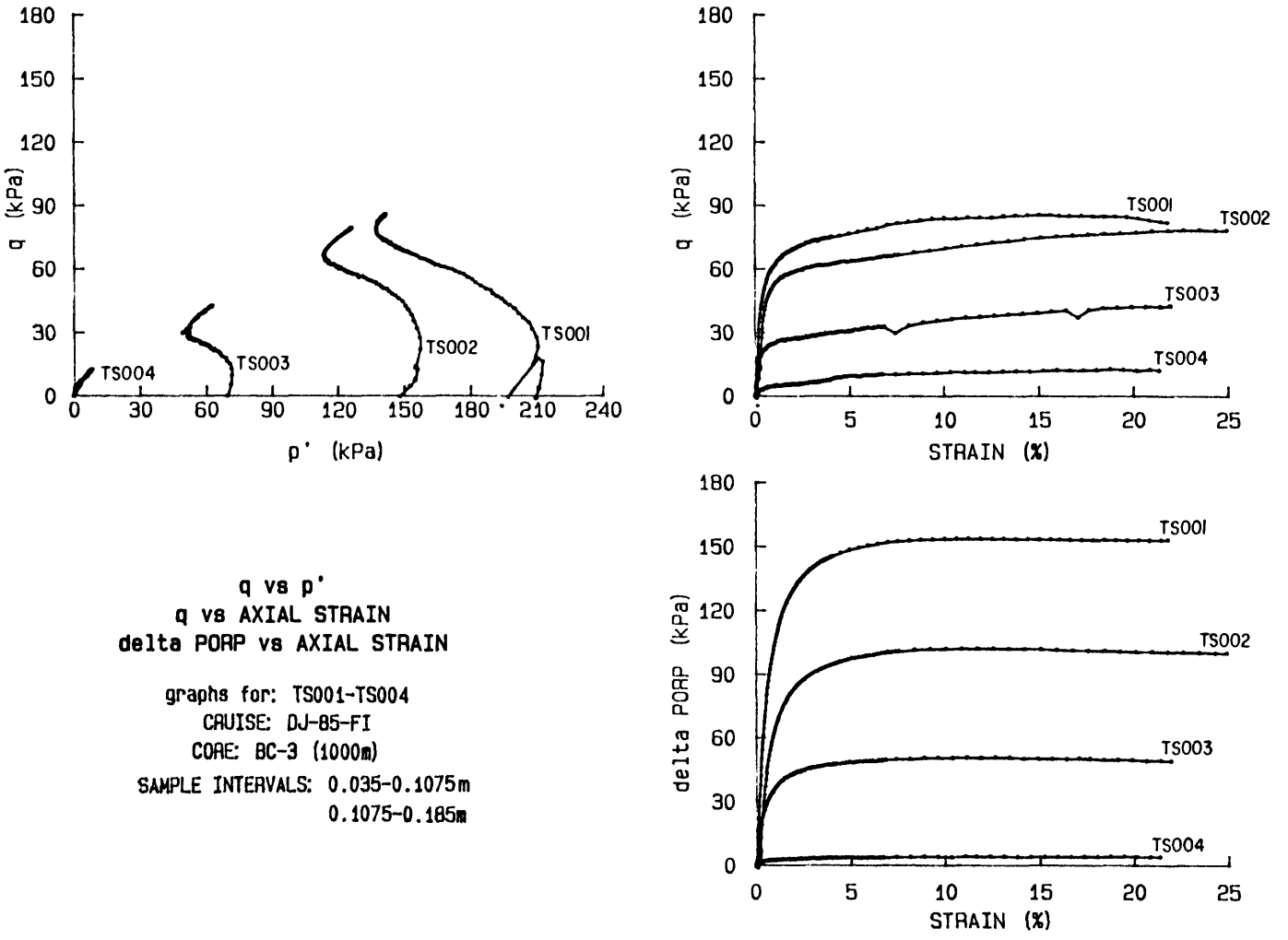

Figure 6. Triaxial compression test results for core BC-3.

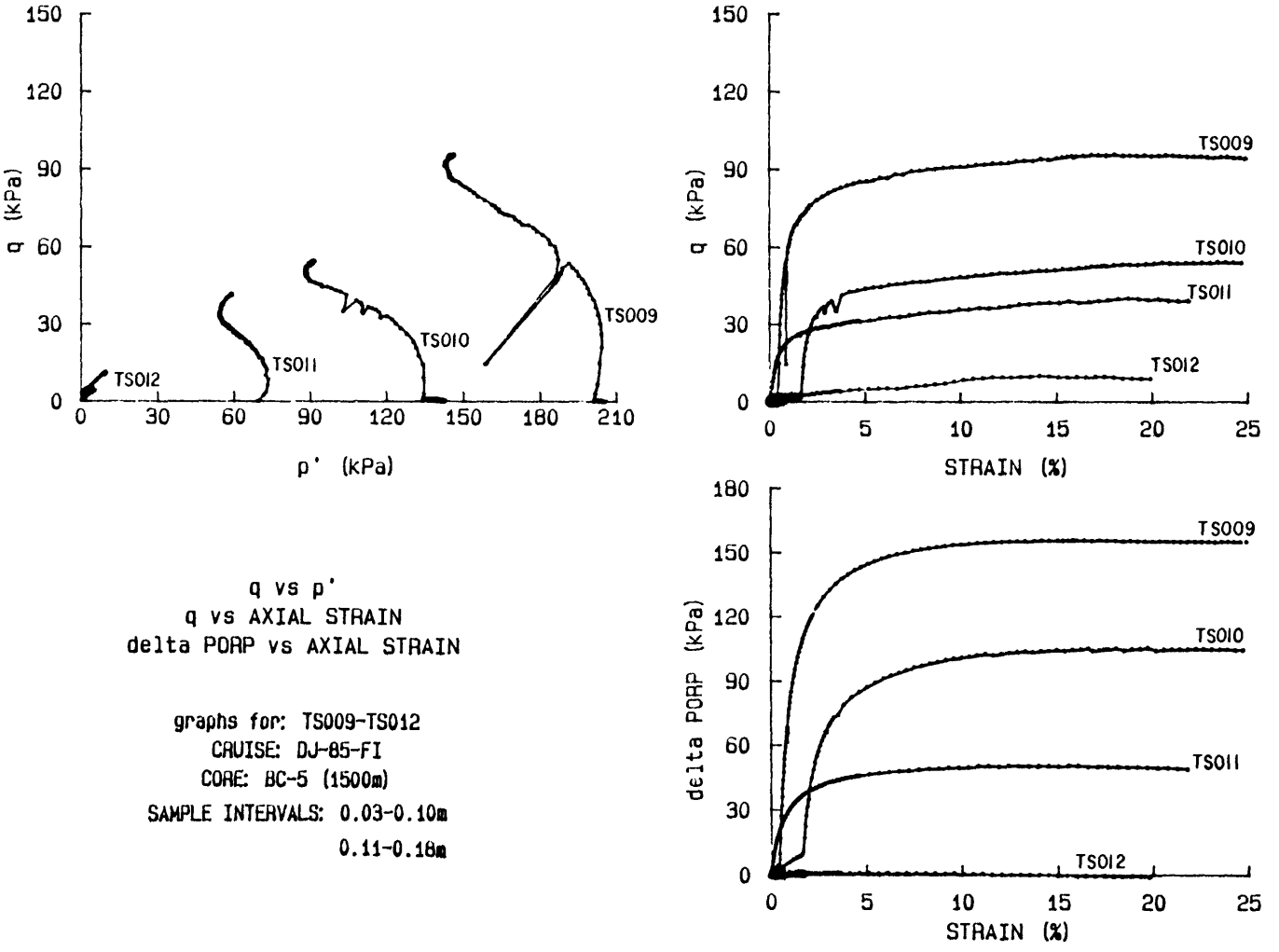

Figure 7. Triaxial compression test results for core BC-5.

The undrained shear strength is used in analyses of both coarse and fine-grained sediment for conditions where pore pressure dissipation does not occur. Undrained shear strengths varied from 7.6 kPa for an unconsolidated sample, representative of sediment strength near the seafloor to 390.5 kPa for a sample consolidated to a stress level of 206.9 kPa, reflecting an approximate subbottom depth of 24 m.

DISCUSSION OF SEDIMENT PROPERTIES

Index properties

Water content, plasticity index, and liquid limit all increase with water depth, indicating that the grain size of the sediment varies considerably and becomes finer as the water depth increases. Therefore, the sediment becomes more plastic and is probably more compressible in deeper water. The reduction in liquid limits and plasticity indices with subbottom depth imply that grain sizes may become coarser down-core or perhaps organic content decreased from biological processes.

Consolidation properties

In agreement with the index properties, the consolidation test results suggest that amounts of finer grained, more plastic, and more compressible sediment increase in greater water depths. The primary compression index (C_c) shows that low, medium-high, and high compressibility can be expected at locations represented by cores BC-1, BC-3, and BC-5, respectively.

The stress history represented by the maximum past stress (σ'_{vm}), excess effective stress (σ'_e), and overconsolidation ratio (OCR) indicate that an overconsolidated sediment is present at all locations. Because the sediment from core BC-1 is sandy, however, the test results from that sample are questionable.

The overconsolidated nature of the sediment from cores BC-3 and BC-5 may be due to a number of factors, such as compaction caused during transportation, seafloor erosional processes, or pseudo-overconsolidation (a characteristic exhibited by many surfacicial sediments throughout the world that may be caused by interparticle bonding and cementation effects; Silva and Jordan, 1984). The coefficients of consolidation (c_v) and permeability (k) both decrease with water depth, again implying that finer grain sizes are present in deeper water.

Strength properties

On the basis of the vane shear strength data (s_{uv}) the sediment at the top of cores BC-3 and BC-5 is, for engineering purposes, classified as very soft (s_u<12.2 kPa), whereas the core bottom sediments are borderline very soft to soft (Table 2) (Terzaghi and Peck, 1967, p. 30). The low strengths, in conjunction with other data, suggest that either an active depositional surface was sampled or at least that significant erosional forces are not present. The marked increase in sediment strength with depth in core may have been caused by compaction during shipping, by natural compaction, possible coarsening grain size with subbottom depth, or a combination of these factors. With one exception, the sensitivity values are all in the low range (S_t<4.0) according to the classification system of Holtz and Kovacs (1981, p.

586). Such values indicate that there is a low potential for strength loss due to remolding in situ or that the reduced s_{uv} measurements were the result of disturbance during sampling and handling.

The sandy sediment in core BC-1 possessed the highest triaxial undrained strength and the highest strength to vertical effective stress ratio (s_u/σ'_c; Table 4). The ratio for dense sand is very high compared to similar ratios for normally consolidated clay, which typically range from 0.1 to 0.6 (Holtz and Kovacs, 1981, p. 589). The s_u/σ'_c ratios for cores BC-3 and BC-5 are in the middle-to-high portion of that range, possibly because of a relatively high sand and silt content. Although we listed the s_u/σ'_c ratio in this report for comparison purposes, it is seldom used or reported for sands because the strength is not well defined if based solely on the confining stress.

The average friction angle ($\phi'(c'\neq o)$) of the BC-1 sediment is the highest of the three cores; the BC-3 sediment has a lower friction angle by 4^o and a higher cohesion intercept. The friction angle of the sediment from core BC-3 is about 5^o higher than predicted by a regression equation based on plasticity index (Lambe and Whitman, 1969, p. 307). The friction angle ($\phi'(c'\neq o)$) determined from core BC-5 is also anomalously high compared to the previously mentioned equation.

Overall, as water depth increases from core BC-1 (500 m) to cores BC-3 (1000 m) and BC-5 (1500 m), sediment grain size (determined visually) and undrained shear strength decrease. As consolidation stresses increase, analogous to increasing overburden stress at greater subbottom depths, the undrained shear strength increased in all cores (Fig. 8). The undrained shear strengths determined from the unconsolidated triaxial samples from cores BC-3 and BC-5 agree very well with the vane shear strengths obtained at the base of each respective core.

RELATION OF SEDIMENT PROPERTIES TO ESTIMATION OF EMBEDMENT AND PENETRATION POTENTIAL

Index properties

Index properties provide important information with which to assess engineering and geological behavior of sediment. For example, sediment type, stress history in fine-grained material, preliminary estimation of consolidation and strength properties, and better interpretation of more sophisticated test results can all be provided by index properties.

However, interpretations based solely on index properties often possess large degrees of uncertainty, and index properties should not invariably replace tests used to measure actual design parameters. They derive their predictive capability through applications of inexact empirical correlations that are based on numerous tests conducted on a wide variety of sediment types. Because their composition and geologic settings may differ, sediment from discrete areas of the seafloor may not fit previously determined correlations. Unless large degrees of uncertainty in the assessment of final sediment-canister interaction can be accepted, index properties alone should not be used for design purposes.

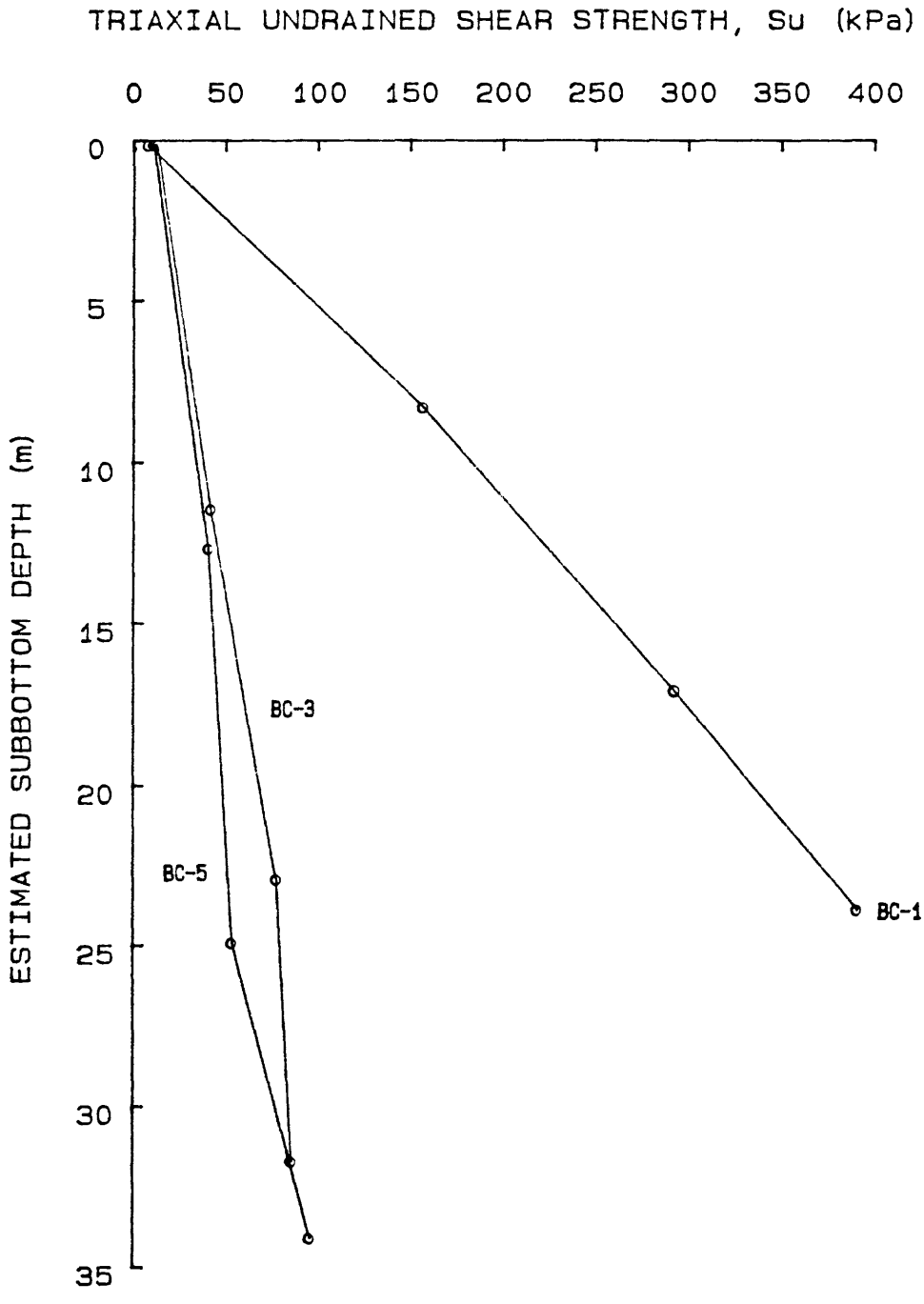

Figure 8. Triaxial test undrained shear strengths (assuming normal consolidation and homogeneous sedimentation to the depth shown) versus calculated subbottom depth for sediment obtained from cruise DJ-85-FI near the Farallon Islands.

However, once an initial set of consolidation and strength measurements are obtained from a particular area, index properties may be used to extrapolate these data to additional nearby sites, thereby reducing the need for more sophisticated testing. Such extrapolations present an economic advantage in cases where large areas of the seafloor are being considered for radioactive waste disposal.

Because the index properties for the study area (Table 2) indicate that the sediment becomes softer, finer grained, and more compressible with increasing water depth, a projectile should penetrate more deeply at greater water depths (Table 5). The index properties suggest that not only are conditions for penetration more favorable at station BC-5 than at station BC-1, the permeability of the BC-5 sediment will be lower. Low permeability can be very important to the disposal of high-level nuclear waste because it may slow radionuclide migration from the canister to the seafloor unless long-life sealed canisters are employed. However, sediment permeability may not be as critical for disposing of low-level radioactive waste because canisters may not be required to penetrate the seafloor.

Index properties can be used to determine approximate natural undrained strength parameters (s_u/σ'_v or τ_f/σ'_{vo}; Fig. 9) or remolded shear strength (Fig. 10) for fine-grained sediment and drained strength characteristics (ϕ') for fine (Fig. 11) or coarse-grained sediment (Fig. 12). Those parameters can be used to derive an estimated undrained strength profile in fine-grained sediment, similar to those shown in Figure 8, without performing strength tests; the estimated friction angles can be applied in analyses of coarse-grained materials. Using a procedure from True (1974) or Rocker (1985) (examples are shown in Figures 13 and 14) the penetration depth of an object can then be estimated for static or dynamic conditions. For further discussion of penetration of objects into the seafloor see Winters (1987).

Consolidation properties

Although consolidation properties may not be used directly for evaluating penetration depth, consolidation tests do provide meaningful data pertinent to stress history at a site. Occasionally they are useful for estimating strength in both normally consolidated and in overconsolidated sediment. High maximum past stresses near the seafloor may indicate that relatively impenetrable sediment is present.

Consolidation tests also provide a measurement of the rate at which compression occurs and the consequent change in permeability of the sediment as effective stress increases and void ratio decreases (Table 3, Appendix A). Based on a classification of coefficient of permeability values (Lambe and Whitman, 1969, p. 287), the permeability of sediment from cores BC-1, BC-3, and BC-5 is low to very low, very low, and very low to practically impermeable, respectively.

The consolidation tests performed on the Farallon Island cores indicate that compressibility increases with finer grain sizes in agreement with our interpretation of the index-property data. Therefore, the soft finer-grained sediment at sites BC-3 and BC-5 would provide much better penetration potential than the coarser sediment at station BC-1.

Table 5. Summary of sediment properties.

	BC-1	BC-3	BC-5
Grain Size	coarsest	finer	finest
Plasticity/Compressibility	medium	high	high
Consistency	-	very soft	very soft
Sensitivity (S_t)	-	low	low
Primary Compression Index (C_c)	low	medium-high	high
Permeability (k)	low-very low	very low	very low - impermeable
Penetrability	lowest	higher	highest

where: Plasticity/Compressibility is based on liquid limit (Peck and others, 1974, p. 22).
Primary Compression Index is based on an emperical relation between liquid limit and C_c (modified from Peck and others, 1974, p. 22).

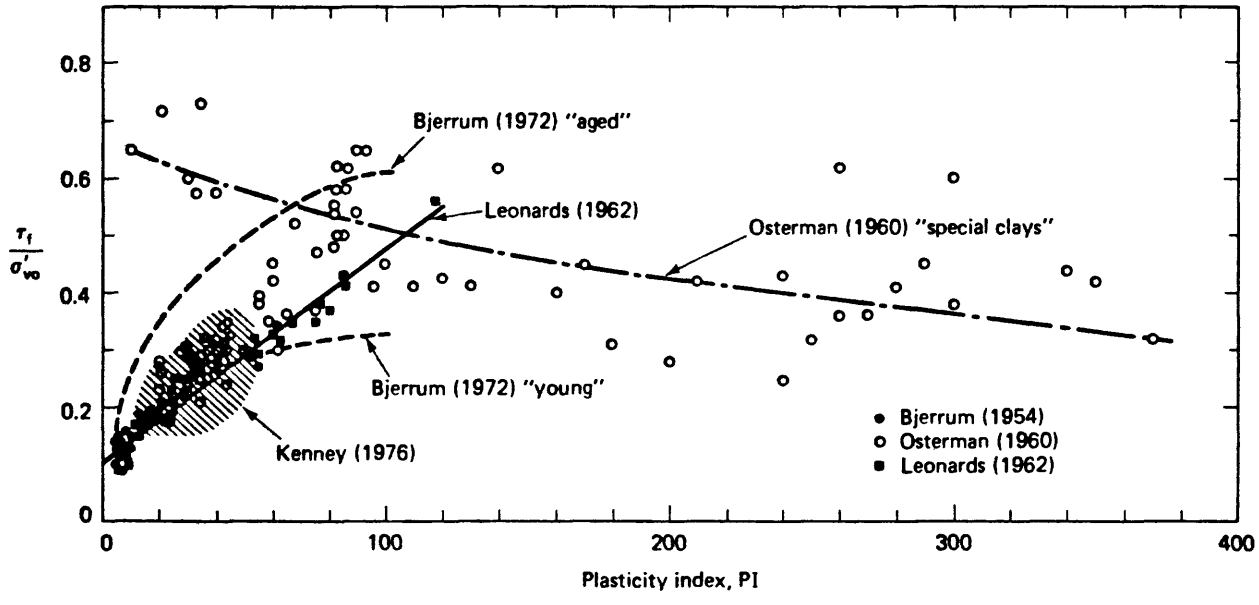

Figure 9. Relationship between undrained shear strength to overburden stress ratio, (τ_f/σ_{vo}) and plasticity index (Holtz and Kovacs, 1981, p. 589.

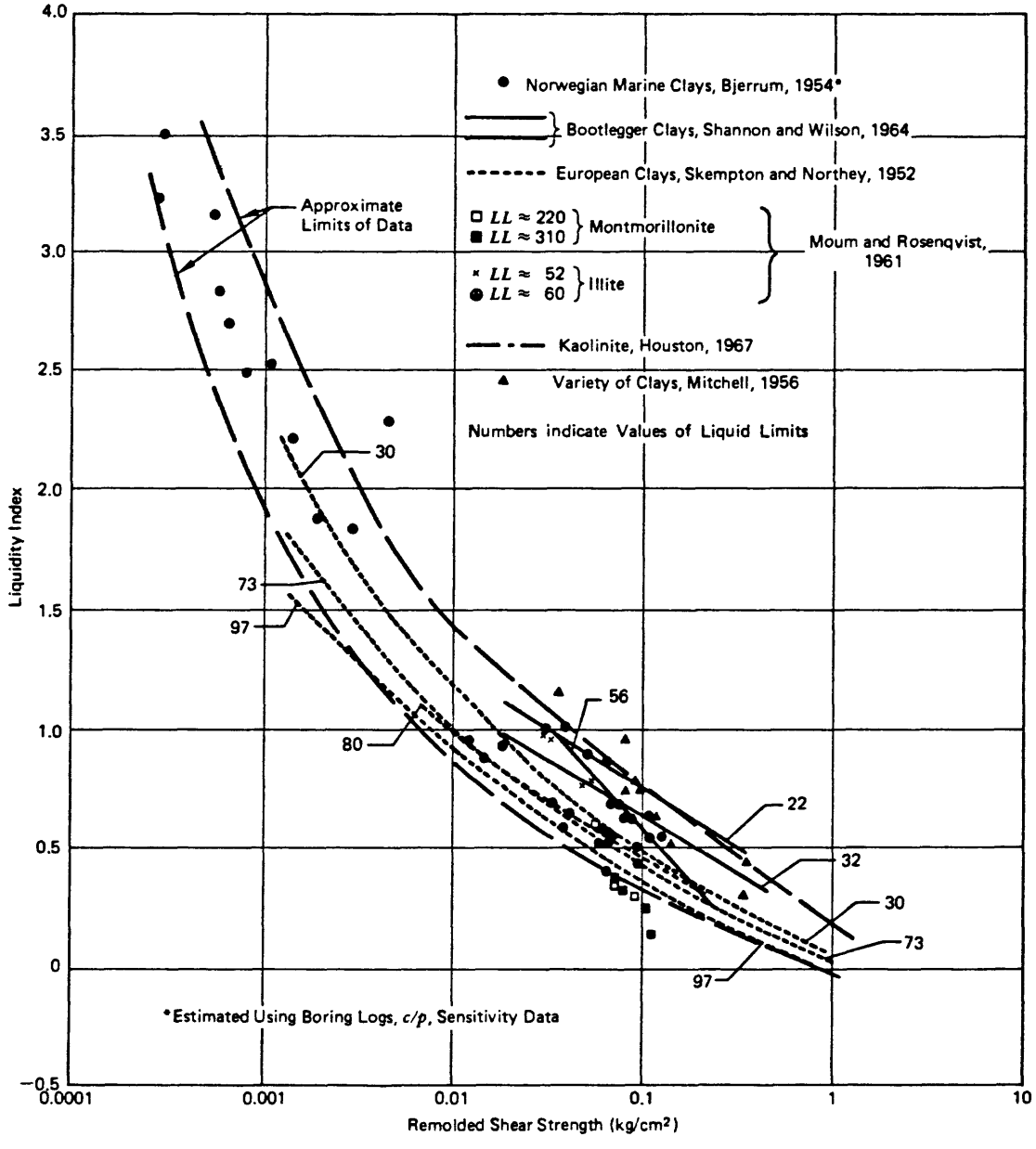

Figure 10. Relationship between liquidity index and remolded shear strength (1 kg/cm^2 = 98.0665 kPa) (Mitchell, 1976, p. 228).

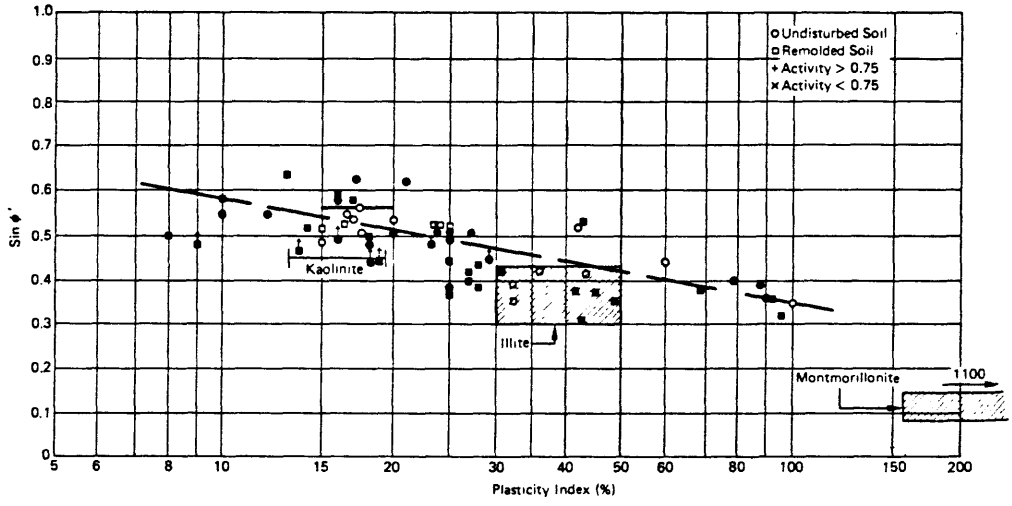

Figure 11. Relationship between sin ϕ' and plasticity index for normally consolidated soils (Kenney, 1959, Olson, 1974; cited in Mitchell, 1976, p. 284).

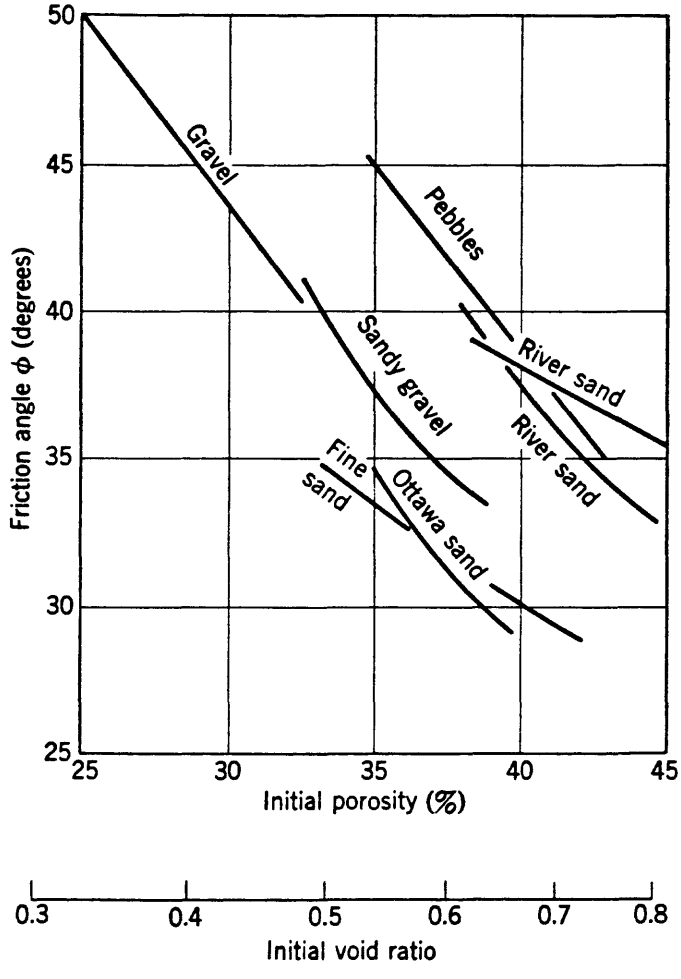

Figure 12. Relationship between friction angle and initial porosity or initial void ratio for coarse-grained soil (Lambe and Whitman, 1969, p. 146).

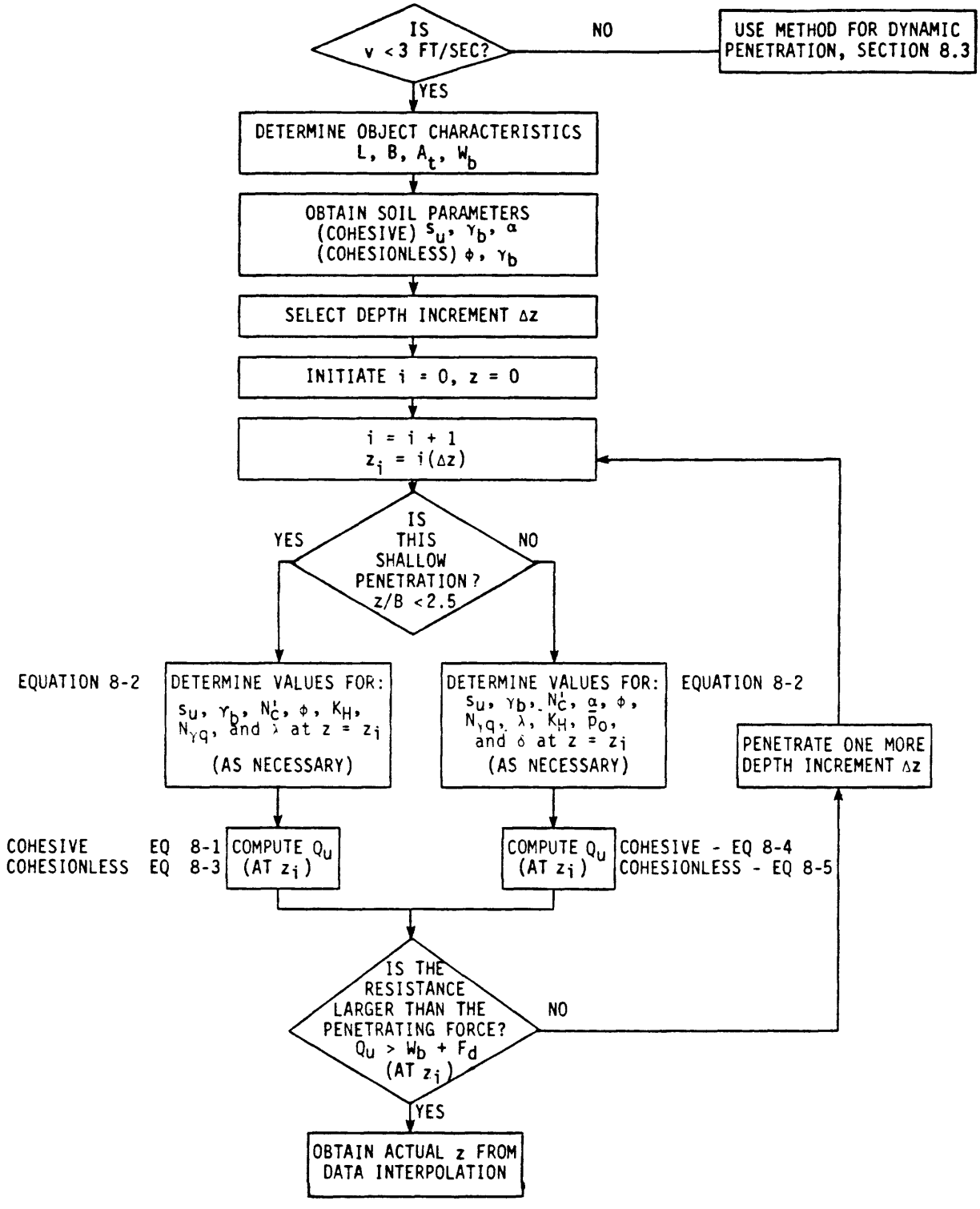

Figure 13. Calculation procedure for predicting static penetration (Rocker, 1985).

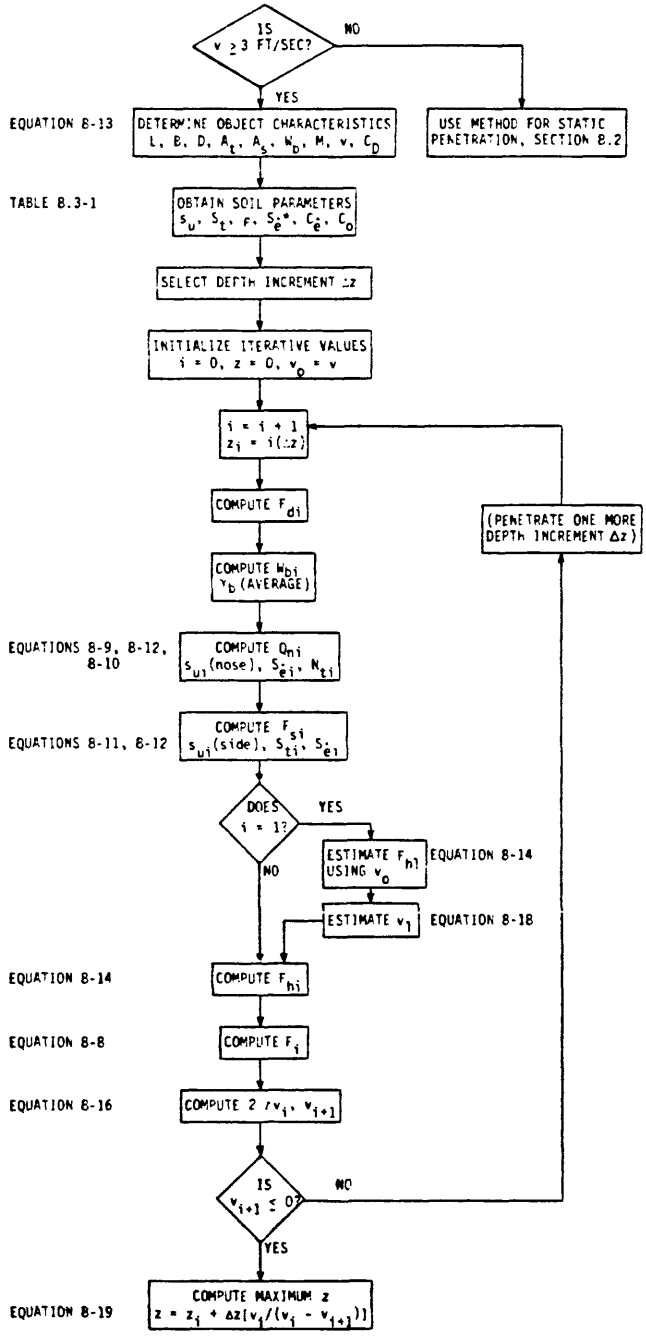

Figure 14. Calculation procedure for predicting dynamic penetration (Rocker, 1985).

Strength properties

Shear strength data, obtained from triaxial and vane shear tests or indirectly from index properties, can be used to construct a subbottom strength profile such as Figure 8. After that profile is separated into a number of subbottom sequences with changing sediment properties (typically representing a strength increase with subbottom depth), an iterative procedure (e.g. Rocker, 1985) can be used to estimate a penetration depth for a particular canister (provided the canister dynamics are known).

The strength data for the cores obtained near the Farallon Islands show that greater dynamic penetration would occur at stations BC-3 and BC-5 than at BC-1 because the strength is lower in those cores (Fig. 8, Table 4). The penetration depth in BC-1 sediment would probably be minimal because negative excess pore pressures build up during undrained shear (negative A_f values, Table 4) which increase strength. Under static penetration conditions, sediment from cores BC-3 and BC-5 has a greater potential for penetration and settlement than BC-1 material.

The undrained shear strength of sediment in the study area (Fig. 8) decreases with water depth and is higher (especially from core BC-1) than typical strength values for deep sea sediment (Fig. 15). Therefore, penetration depths will be less near the Farallon Islands than at deep-sea sites.

CONCLUSIONS AND RECOMMENDATIONS

The sediment from cores BC-3 and BC-5 is more plastic, finer grained (with a lower permeability), weaker, and is therefore more penetrable than the sandy sediment from core BC-1. Because of the lower permeability at sites BC-3 and BC-5, the sediment there would provide a more effective barrier to radionuclide migration after penetration and hole closure.

Because the material in this study area near the Farallon Islands possesses greater strength (especially at site BC-1) than typical deep-sea sediment, less penetration would occur in the sandy or silty-clayey sediment within the study area than in deeper water farther offshore where finer-grained clays may be present.

It is extremely difficult both to sample and to accurately analyze sandy sediment. Therefore, in situ methods should be used at sandy locations to assess penetration potential. Dense sands typically will allow minimal penetration; even if deeper penetration occurs, permeability characteristics would be undesirably high. Therefore, sandy areas of seafloor should be avoided when disposing of nuclear waste if the sediment is being relied upon to help contain radioactive material.

Application of the Farallon Islands core data to problems of penetration, embedment, and hole closure are limited because of sample disturbance and short core length. Future seafloor sediment investigations will obtain the maximum benefit from geotechnical analyses, if the following recommendations are followed. Longer high-quality cores should be obtained whenever possible because sediment properties measured near the seafloor surface may not adequately represent behavior below it. Two cores should be obtained at each

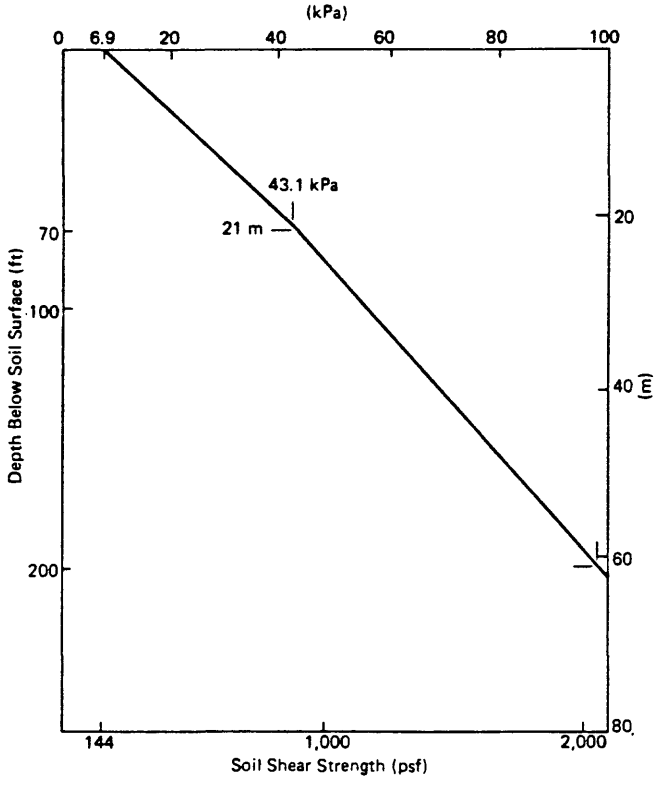

Figure 15. Typical undrained shear strength profile for normally consolidated cohesive marine sediment (Valent and Lee, 1976).

station, so that one core can be split longitudinally at sea in order to observe stratigraphy and to determine vane shear strengths and water contents at discrete intervals down core. The other core should be properly stored for later, more selective geotechnical tests. The undisturbed geotechnical cores should be cut into lengths shorter than 1.5 m and stored upright without air or water present at the top of the core. Specially designed liner cutters or supports may be needed to prevent severely disturbing the sediment.

Disturbance to the cores should be minimized. The cores should be surrounded by foam rubber or other shock- and vibration-absorbing material. A tilt indicator should be placed inside and outside the container to record any mishandling during shipping. For further discussion of shipboard handling, storage, and transport of cores see Winters and Booth (1986).

The basic tests presented in this report enable fundamental sediment properties to be evaluated. Future studies may require, additional, more specific testing, such as anisotropically consolidated triaxial tests that better model the field stress state, rapid shear tests that account for strain rate effects, and adhesion tests that measure the tendency for clayey sediment to adhere to projectiles, before the dynamic interaction between projectiles and sediment can be fully evaluated.

Laboratory geotechnical testing can be supplemented with in situ methods and equipment such as the Doppler penetrometer (Beard, 1984) to provide more direct evidence of sediment penetrability. In addition to local site investigations, regional studies can be made that utilize geophysical methods to show variation in sediment thickness and stratification, presence of gas, and morphology that can provide information useful for slope stability analyses.

ACKNOWLEDGEMENTS

The authors are grateful to the reviewers of this report, Homa Lee, Jim Robb, and Elizabeth Winget, for their valuable comments and suggestions. Steve Dickenson performed most of the laboratory testing; we thank him for his assistance throughout the writing of the report. J. Zwinakis and P. Forrestel drafted some of the figures.

Funding for this report was provided under Interagency Agreement DW 14931699-01-0 with the U.S. Environmental Protection Agency.

REFERENCES

Beard, R. M., 1981, Test results of large cylinders impacting sand and clay seafloors: Naval Civil Engineering Laboratory Technical Memorandum M-42-81-07, Port Hueneme, Calif., 22 p.

Beard, R. M., 1984, Expendable Doppler penetrometer for deep ocean sediment strength measurements: Naval Civil Engineering Laboratory Technical Report R-905, Port Hueneme, Calif., 43 p.

Bjerrum, L., 1954, Geotechnical properties of Norwegian marine clays: Geotechnique, v. 4, no. 2, p. 49-69.

Bjerrum, L., 1972, Embankments on soft ground: Proceedings of the ASCE Specialty Conference on Performance of Earth and Earth-supported Structures, Purdue University, v. 2, p. 1-54.

Casagrande, Arthur, 1936, The determination of the pre-consolidation load and its practical significance: Proceedings First International Conference on Soil Mechanics and Foundation Engineering, v. 3, Cambridge, Massachusetts, p. 60-64.

Casagrande, Arthur, 1948, Classification and identification of soils: Transactions of the American Society of Civil Engineers, v. 113, p. 901-991.

Head, K. H., 1980, Manual of soil laboratory testing, volume 1: soil classification and compaction tests: London, Pentech Press, 339 p.

Holtz, R. D. and Kovacs, W. D., 1981, An introduction to geotechnical engineering: Englewood Cliffs, N. J., Prentice-Hall, Inc., 733 p.

Houston, W. N., 1967, Formation mechanisms and property interrelationships in sensitive clays: Ph.D. thesis, University of California, Berkeley.

Kenney, T. C., 1959, Discussion: Journal of the Soil Mechanics and Foundations Division, ASCE, v. 85, no. SM3, p. 67-79.

Kenney, T. C., 1976, Formation and geotechnical characteristics of glacial-lake varved soils: Lauritis Bjerrum Memorial Volume - Contributions to Soil Mechanics, Norwegian Geotechnical Institute, Oslo, p. 15-39.

Lambe. T. W. and Whitman, R. V., 1969, Soil mechanics: New York, John Wiley & Sons, 553 p.

Leonards, G. A., ed., 1962, Foundation engineering: New York, McGraw Hill Book Company, 1136 p.

Mitchell, J. K., 1956, The fabric of natural clays and its relation to engineering properties: Proceedings of the Highway Research Board, v. 35, p. 693-713.

Mitchell, J. K., 1976, Fundamentals of soil behavior: New York, John Wiley & Sons, Inc., 422 p.

Moum, J. and Rosenqvist, I, Th., 1961, The mechanical properties of montmorillonitic and illitic clays related to the electrolytes of the pore water: Proceedings of the Fifth International Conference on Soil Mechanics and Foundation Engineering, v. 1, p. 263-267.

Olson, R. E., 1974, Shearing strength of kaolinite, illite and montmorillonite: Journal of the Geotechnical Division, ASCE, v. 100, GT 11, p. 1215-1229.

Osterman, J., 1960, Notes on the shearing resistance of soft clays: Acta Polytechnica Scandinavica, Series Ci-2, (AP 263, 1959), p. 1-22.

Peck, R. B., Hanson, W. E., and Thornburn, T. H., 1974, Foundation engineering: New York, John Wiley & Sons, Inc., 514 p.

Rocker, Karl, Jr., ed., 1985, Penetration of objects into the seafloor, chapter 8: Handbook for marine geotechnical engineering: Naval Civil Engineering Laboratory, Port Hueneme, Calif., 21 p.

Schell, W. R., and Sugai, S., 1980, Radionuclides at the U.S. radioactive waste disposal site near the Farallon Islands: Health Physics, v. 39, p. 475-496.

Schmertmann, J. H., 1955, The undisturbed consolidation behavior of clay: Transactions of the American Society of Civil Engineers, v. 120, p. 1201-1233.

Schmid, W. E., 1969, The penetration of objects into the ocean bottom: Proceedings Civil Engineering in the Oceans II, American Society of Civil Engineers, Miami Beach, FL, p. 167-207.

Seed, H. B., and Lee, K. L., 1967, Undrained strength characteristics of cohesionless soils: Journal of Soil Mechanics and Foundations Division, ASCE, v. 93, no. SM6, p. 333-360.

Shannon and Wilson, Inc., 1964, Report on Anchorage area soil studies, Alaska: Report to U.S. Army Engineer District, Anchorage, Alaska, Seattle, 300 p.

Silva, A. J., 1974, Marine geomechanics: overview and projections: in Inderbitzen, A. L., ed., Deep-sea sediments: physical and mechanical properties: New York, Plenum Press, p. 45-76.

Silva, A. J. and Jordan, S. A., 1984, Consolidation properties and stress history of some deep sea sediments, chapter 3: in Denness, Bruce, ed., Seabed mechanics: London, Graham and Trotman Limited, p. 25-39.

Skempton, A. W. and Northey, R. D., 1952, The sensitivity of clays: Geotechnique, v. 3, no. 1, p. 30-53.

Terzaghi, Karl and Peck, R. B., 1967, Soil mechanics in engineering practice: New York, John Wiley & Sons, Inc., 729 p.

True, D. G., 1974, Rapid penetration into seafloor soils: Offshore Technology Conference Paper No. 2095, Houston, Tx, p. 607-617.

Valent, P. J., and Lee, H. J., 1976, Feasibility of subseafloor emplacement of nuclear waste: Marine geotechnology, v. 1, no. 4, p. 267-293.

Winters, W. J., 1986, Geotechnical test methods for marine sediments, section H: in Booth, J. S., ed., Methods manual for sediment monitoring at deep-ocean low-level radioactive waste disposal sites: U.S. Geological Survey administrative draft report to the U.S. Environmental Protection Agency under interagency agreement DW14931699-01-0, Woods Hole, Mass., 51 p.

Winters, W. J., 1987, Embedment, penetration, hole closure, and related geotechnical tests associated with subseafloor nuclear waste disposal: U.S. Geological Survey Open-File Report 87-256, 19 p.

Winters, W. J., and Booth, J. S., 1986, Analysis of sediment behavior during seafloor embedment or penetration of waste canisters and measurement of pertinent geotechnical properties: U.S. Geological Survey administrative draft report to the U.S. Environmental Protection Agency under interagency agreement DW14931699-01-0, Woods Hole, Mass., 70 p.

NOMENCLATURE AND SYMBOLS:

A_f	The coefficient of pore pressure response at failure during a triaxial compression test (change in pore pressure at failure/change in deviator stress).
ASCE	American Society of Civil Engineers.
ASTM	American Society for Testing and Materials
BC	Box Core.
c'	The cohesion intercept expressed in terms of effective stresses determined from a number of triaxial compression tests performed on similar sediment.
C_c (ave)	Average compression index, defined as the average slope of the linear part of a consolidation curve plotted on a graph of void ratio versus log of effective stress.
C_{cf}	Corrected field compression index (determined by Schmertmann (1955) method).
C_r	Rebound-recompression index.
CR	Identification prefix for a constant rate of strain consolidation (CRSC) test.
CRSC	Constant rate of strain consolidation test.
c_v	Coefficient of consolidation.
$c_v(\sigma'_{vo})$	Coefficient of consolidation at the in-situ effective overburden stress.
$c_v(\sigma'_{vm})$	Coefficent of consolidation at the maximum past vertical effective stress.
c_v(ave)	Average coefficient of consolidation for virgin compression.
delta DVOL	The change in volume during consolidation phase of a triaxial compression test.
delta PORP	The change in pore water pressure during the shear phase of a triaxial compression test.
DELTA u	The change in pore water pressure measured from the beginning of a test.
Dev STRESS	The deviator stress or difference between the major and minor principal effective stresses ($\sigma'_1 - \sigma'_3$).
DJ-85-FI	Cruise identifier (David Jordan-1985-Farallon Islands).

du	The change in pore water pressure from the beginning of a test.
e	Void ratio, (volume of voids/volume of solids).
e_o	Initial void ratio; in-situ void ratio.
EFF STRESS RATIO	Effective stress ratio (σ'_1/σ'_3); also known as obliquity factor; it is a maximum at the point of the largest friction angle (assuming c' = o) during a triaxial test.
G_s	Grain specific gravity (corrected for a pore water salinity of 35 ppt).
I_D	Disturbance index (determined by Silva (1974) method).
I_L	Liquidity index.
I_P	Plasticity index.
k	Coefficient of permeability or coefficient of hydraulic conductivity.
kg	Kilogram.
$k(\sigma'_{vo})$	Coefficient of permeability at the in-situ effective overburden stress.
$k(\sigma'_{vm})$	Coefficient of permeability at the maximum past vertical effective stress.
k(ave)	Average coefficient of permeability for virgin compression.
km	Kilometer.
kPa	KiloPascal, kN/m^2.
LI	Liquidity index.
LL	Liquid limit.
m	Meter.
mm	Millimeter.
NP	Non-plastic.
NV	Test not valid.
OCR	Overconsolidation ratio ($\sigma'_{vm}/\sigma'_{vo}$).
ppt	Parts per thousand.
PI	Plasticity index.

p'	The vertical effective stress in a consolidation test or the normal effective stress acting on a plane inclined at 45 degrees from the horizontal in a triaxial test $(\sigma'_1 + \sigma'_3)/2$.
q	The shear stress acting on a plane inclined at 45 degrees from the horizontal in a triaxial test $(\sigma_1 - \sigma_3)/2$.
s_{rv}	Undrained vane shear strength determined from remolded sediment.
S_t	Sensitivity (s_{uv}/s_{rv}).
s_u	Undrained shear strength.
s_{uv}	Natural undrained vane shear strength.
s_v	Total vertical stress.
TC	Identification prefix for the consolidation phase of a triaxial compression test.
TS	Identification prefix for the shear phase of a triaxial compression test.
u	Excess pore water pressure or change in pore water pressure from the beginning of a test.
w	Natural water content (weight of water including salt/weight of solids; corrected for an assumed salinity of 35 ppt).
w_L	Liquid limit.
w_P	Plastic limit.
w_s	Water content of a triaxial compression test sample during undrained shear.
η	Porosity (volume of voids/total volume).
ρ_t	Bulk density.
σ'_c	The consolidation stress exerted on a triaxial test sample prior to shear.
σ'_e	Excess vertical effective stress $(\sigma'_{vm} - \sigma'_{vo})$.
σ'_v	Vertical effective stress.
σ'_{vo}	In-situ effective overburden stress.
σ'_{vm}	Maximum past vertical effective stress.

τ_f	Shear stress at failure on the failure plane (equal to s_u).
ϕ'	The effective friction angle.
$\varphi'(c=o)$	The friction angle of a sediment expressed in terms of effective stresses determined from an individual triaxial compression test assuming no cohesion intercept.
$\phi'(c \neq o)$	The friction angle expressed in terms of effective stresses determined from a number of triaxial compression tests performed on similar sediment.

APPENDIX A

Consolidation Test Results

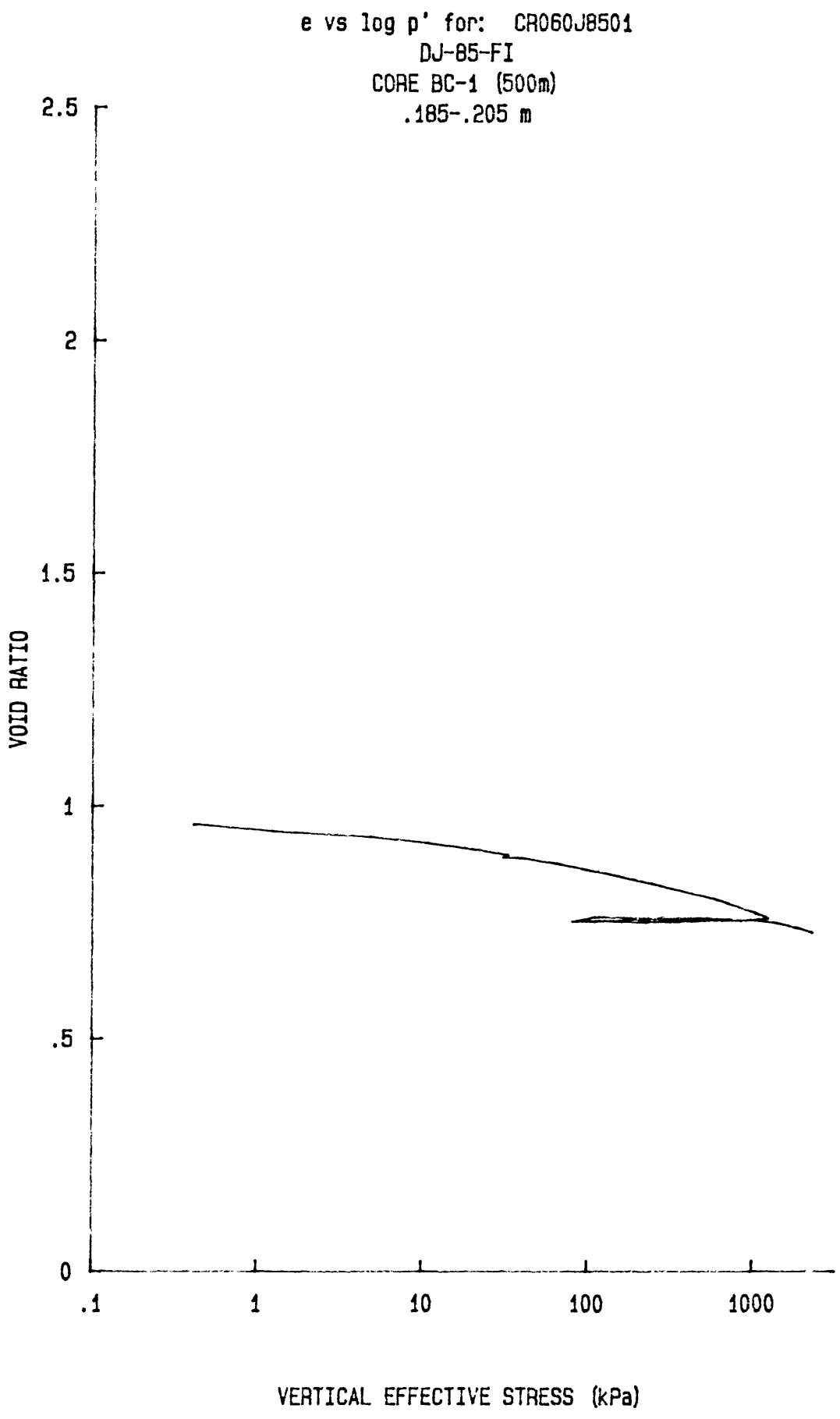
e vs log p' for: CR060J8501
DJ-85-FI
CORE BC-1 (500m)
.185-.205 m
2.5
2
1.5
1
.5
0
VOID RATIO
.1
1
10
100
1000
VERTICAL EFFECTIVE STRESS (kPa)

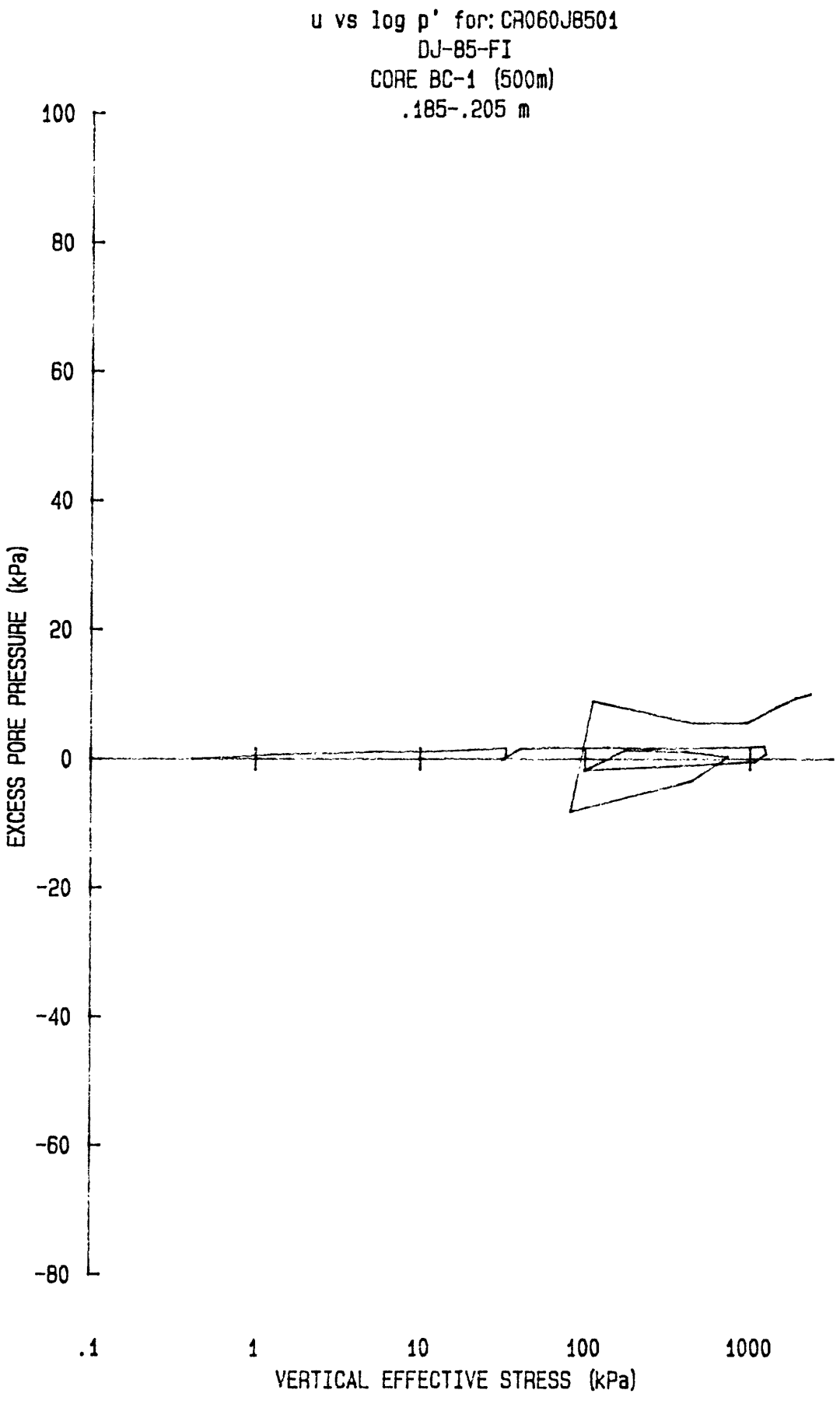
u vs log p' for: CR060J8501
DJ-85-FI
CORE BC-1 (500m)
.185-.205 m
100
80
60
40
20
0
-20
-40
-60
-80
EXCESS PORE PRESSURE (kPa)
.1
1
10
100
1000
VERTICAL EFFECTIVE STRESS (kPa)

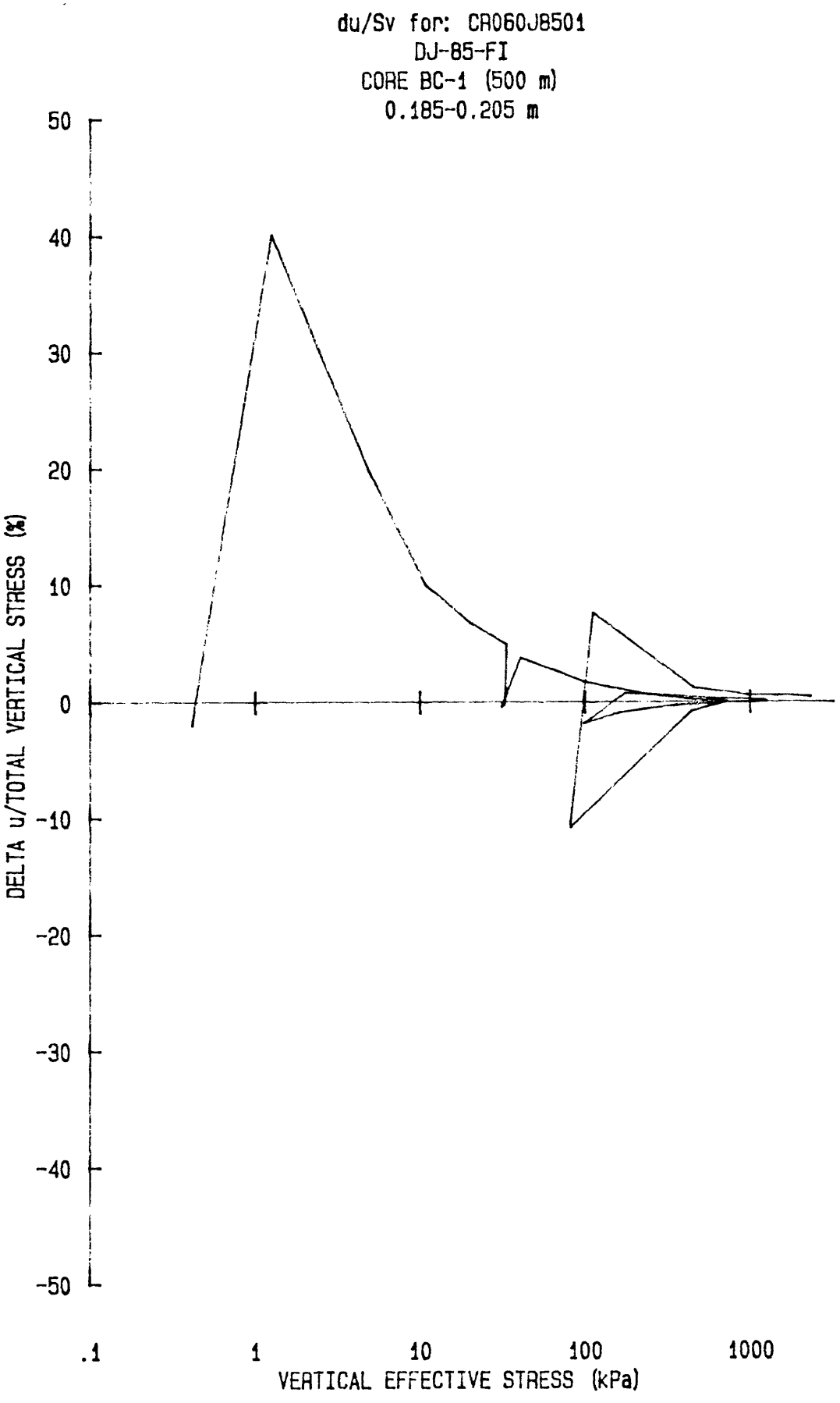
du/Sv for: CR060J8501
DJ-85-FI
CORE BC-1 (500 m)
0.185-0.205 m
50
40
30
20
10
0
-10
-20
-30
-40
-50
DELTA u/TOTAL VERTICAL STRESS (%)
.1
1
10
100
1000
VERTICAL EFFECTIVE STRESS (kPa)

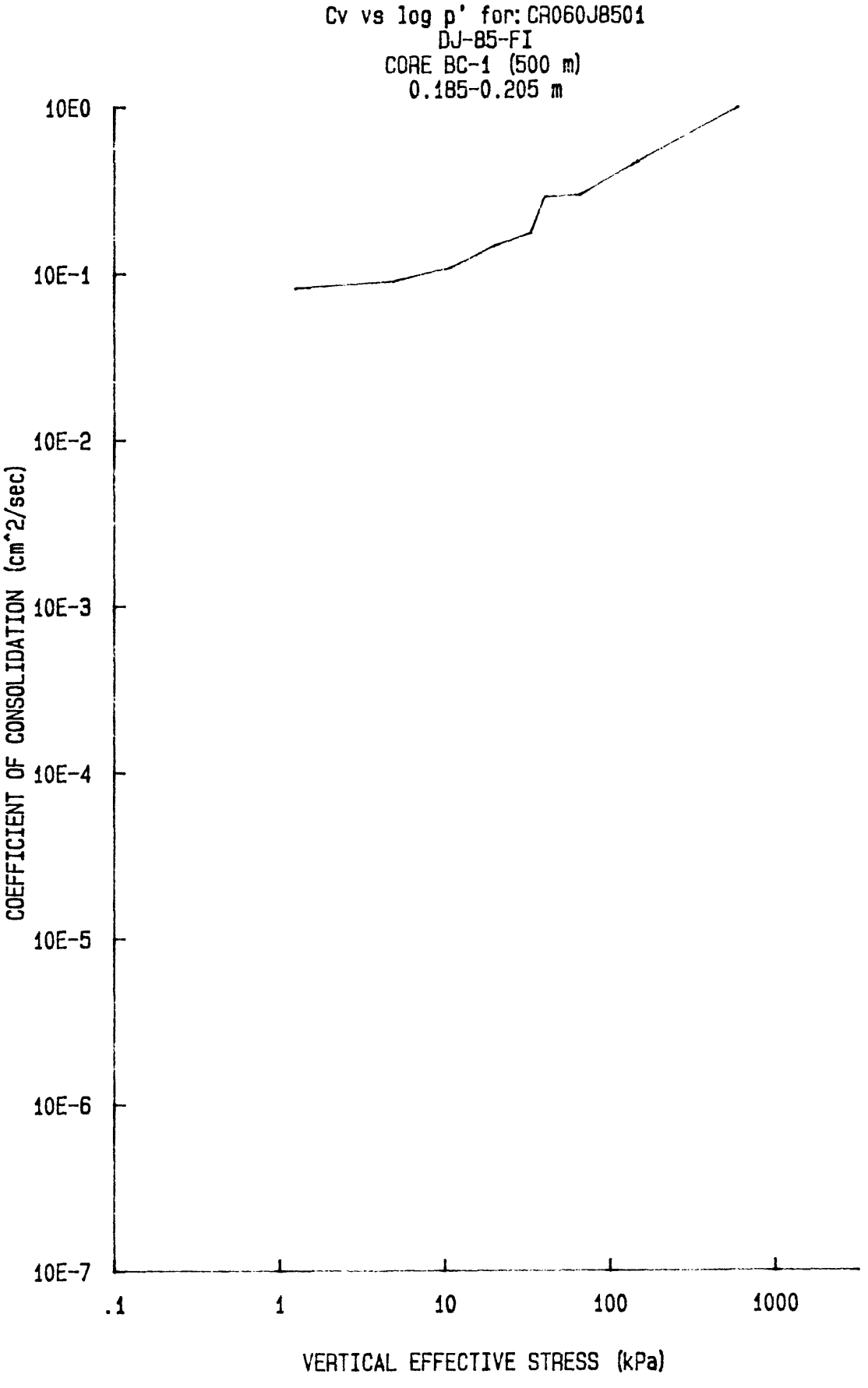
Cv vs log p' for: CR060J8501
DJ-85-FI
CORE BC-1 (500 m)
0.185-0.205 m
10E0
10E-1
10E-2
10E-3
10E-4
10E-5
10E-6
10E-7
COEFFICIENT OF CONSOLIDATION (cm^2/sec)
.1
1
10
100
1000
VERTICAL EFFECTIVE STRESS (kPa)

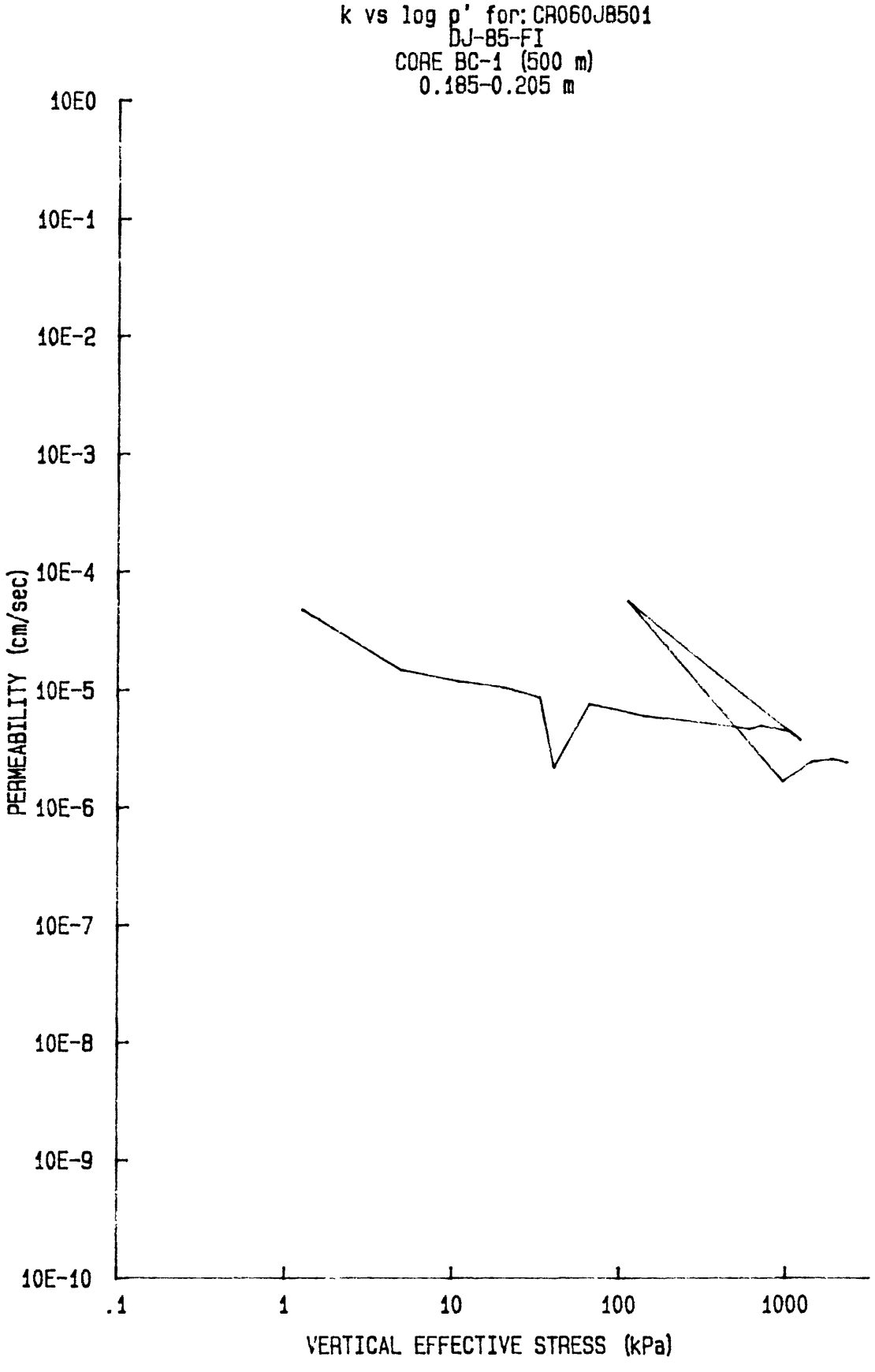
k vs log p' for: CR060J8501
DJ-85-FI
CORE BC-1 (500 m)
0.185-0.205 m
10E0
10E-1
10E-2
10E-3
10E-4
10E-5
10E-6
10E-7
10E-8
10E-9
10E-10
PERMEABILITY (cm/sec)
.1
1
10
100
1000
VERTICAL EFFECTIVE STRESS (kPa)

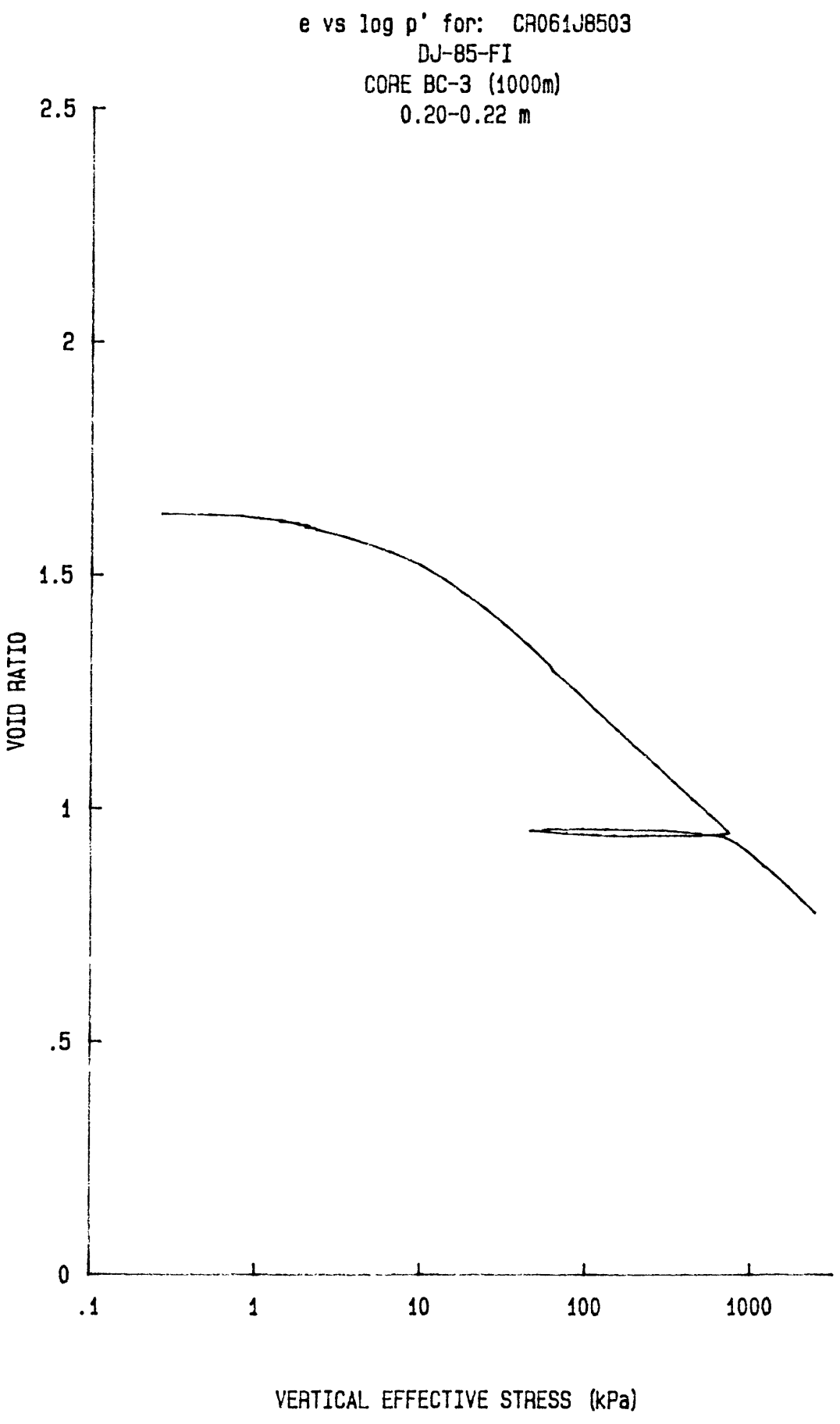
e vs log p' for: CR061J8503
DJ-85-FI
CORE BC-3 (1000m)
0.20-0.22 m
2.5
2
1.5
1
.5
0
VOID RATIO
.1
1
10
100
1000
VERTICAL EFFECTIVE STRESS (kPa)

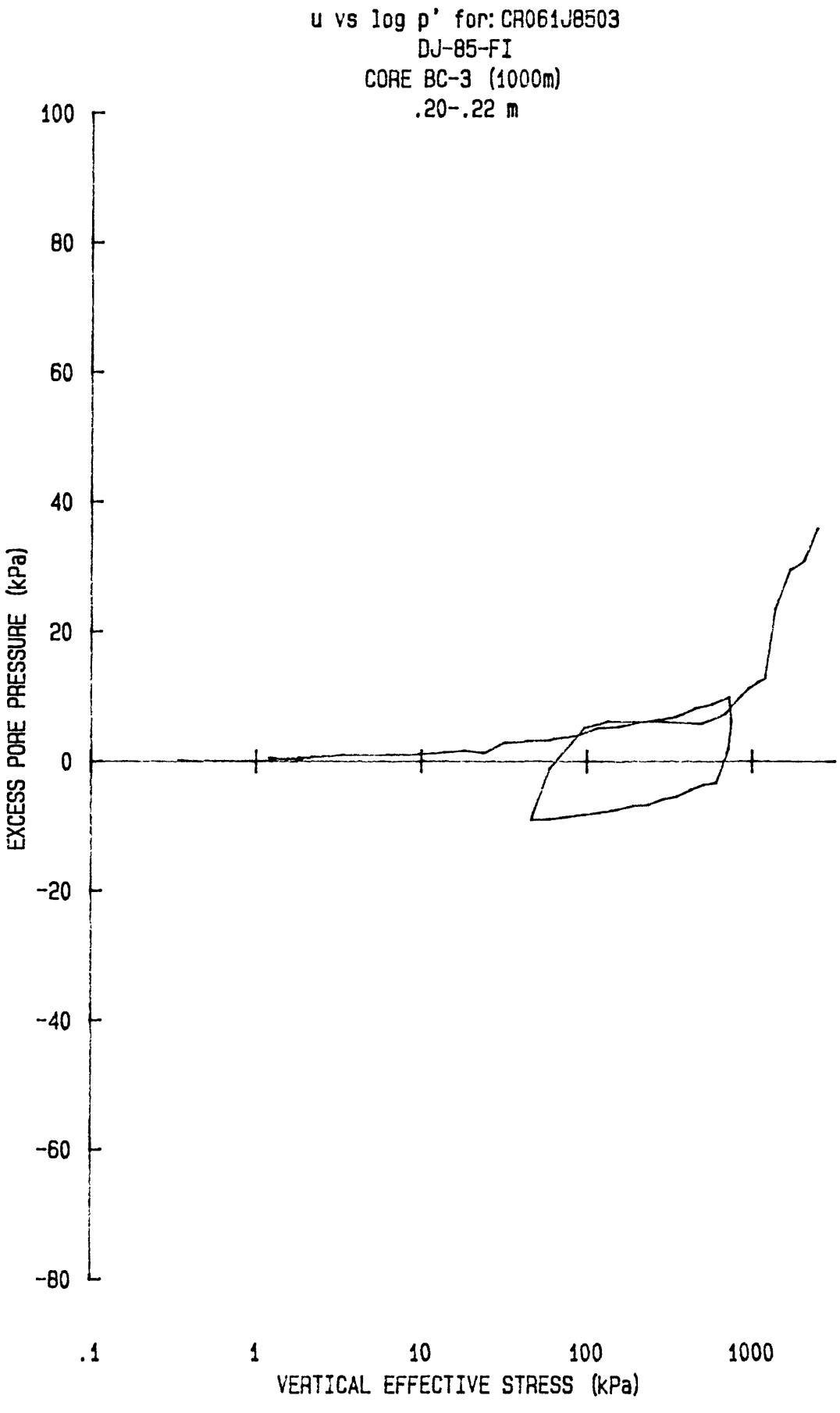
u vs log p' for: CR061J8503
DJ-85-FI
CORE BC-3 (1000m)
.20-.22 m
100
80
60
40
20
0
-20
-40
-60
-80
EXCESS PORE PRESSURE (kPa)
.1
1
10
100
1000
VERTICAL EFFECTIVE STRESS (kPa)

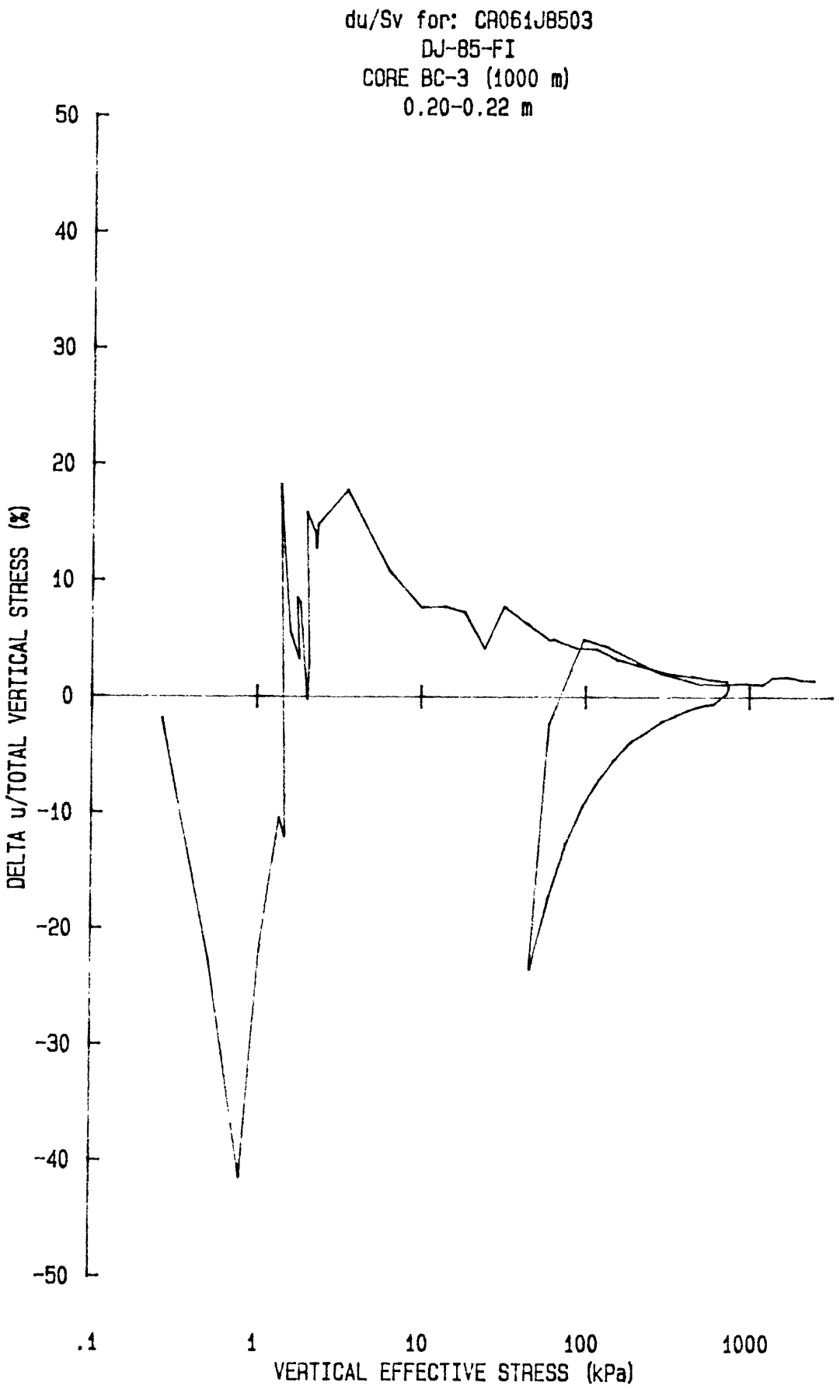
du/Sv for: CR061J8503
DJ-85-FI
CORE BC-3 (1000 m)
0.20-0.22 m
50
40
30
20
10
0
-10
-20
-30
-40
-50
DELTA u/TOTAL VERTICAL STRESS (%)
.1
1
10
100
1000
VERTICAL EFFECTIVE STRESS (kPa)

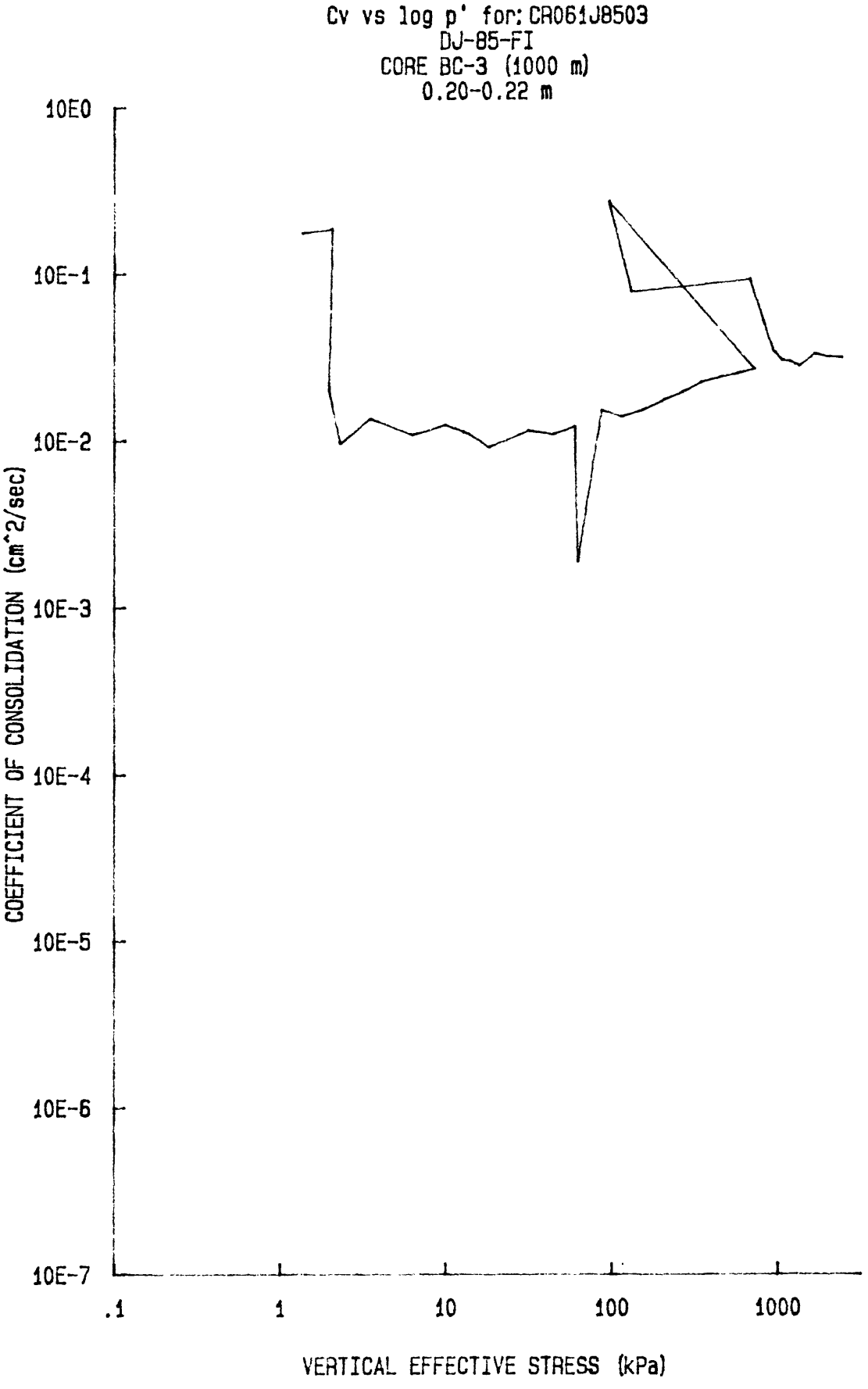
Cv vs log p' for: CR061J8503
DJ-85-FI
CORE BC-3 (1000 m)
0.20-0.22 m
10E0
10E-1
10E-2
10E-3
10E-4
10E-5
10E-6
10E-7
COEFFICIENT OF CONSOLIDATION (cm^2/sec)
.1
1
10
100
1000
VERTICAL EFFECTIVE STRESS (kPa)

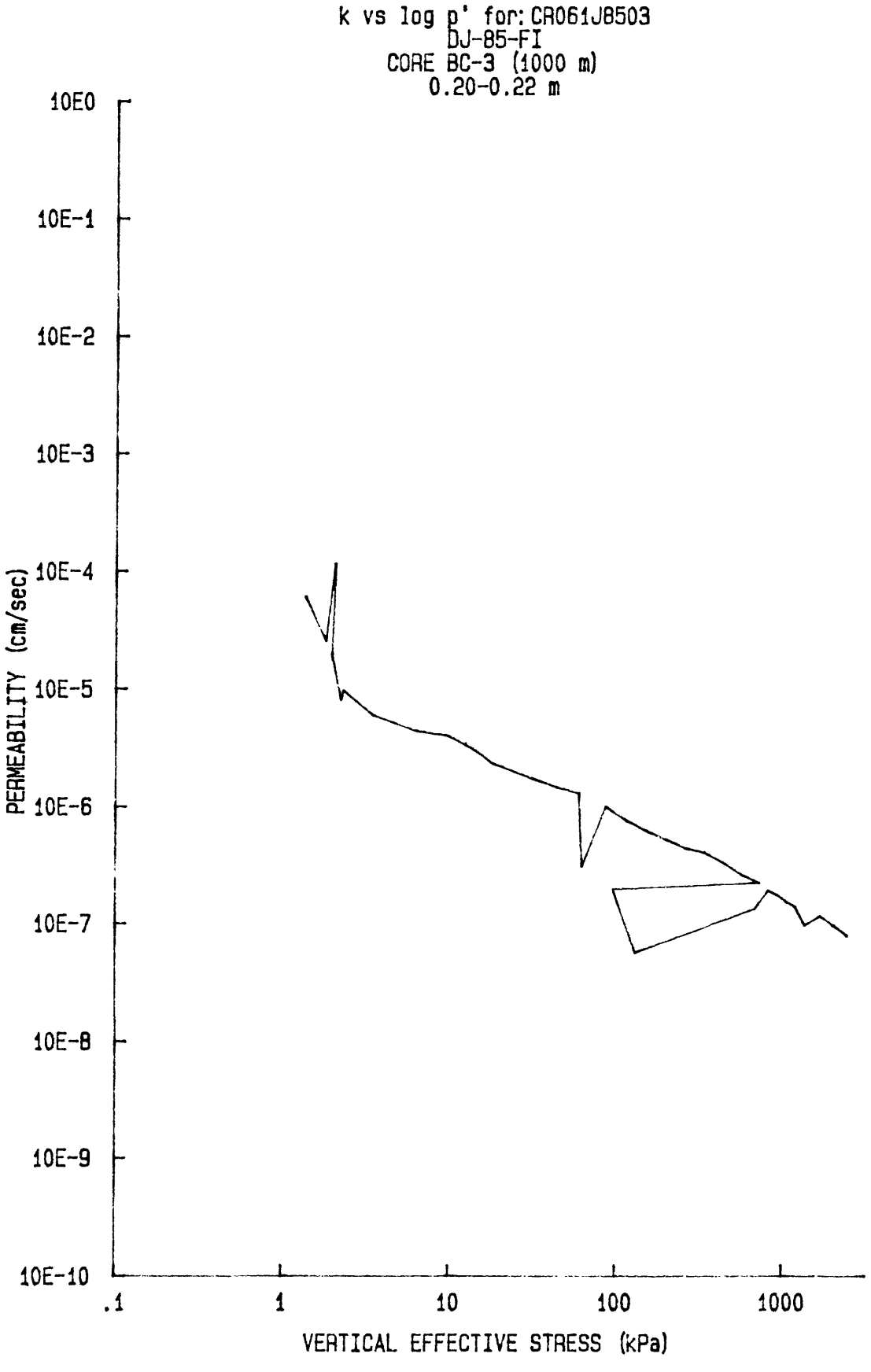
k vs log p' for: CR061J8503
DJ-85-FI
CORE BC-3 (1000 m)
0.20-0.22 m
10E0
10E-1
10E-2
10E-3
10E-4
10E-5
10E-6
10E-7
10E-8
10E-9
10E-10
PERMEABILITY (cm/sec)
.1
1
10
100
1000
VERTICAL EFFECTIVE STRESS (kPa)

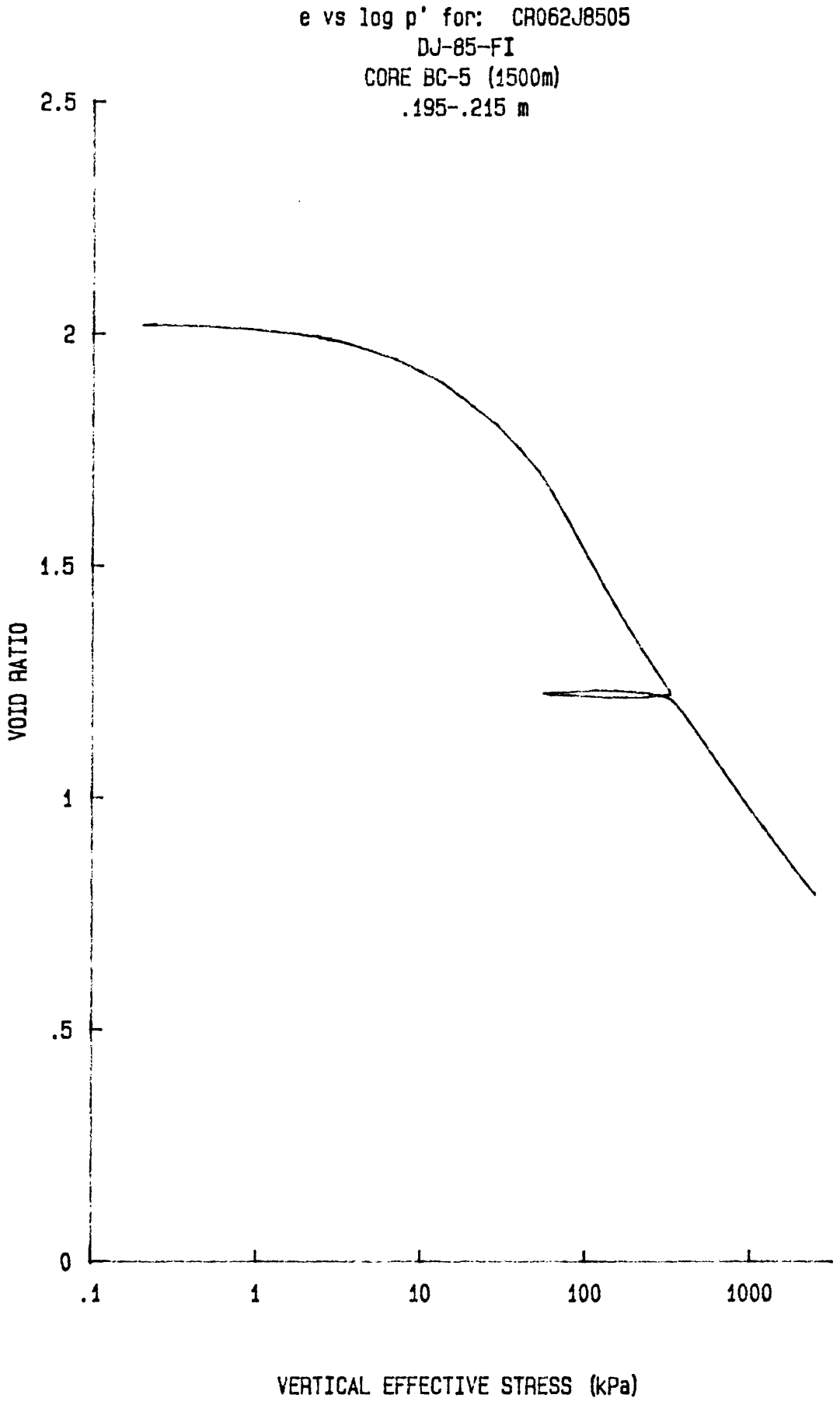
e vs log p' for: CR062J8505
DJ-85-FI
CORE BC-5 (1500m)
.195-.215 m
2.5
2
1.5
1
.5
0
VOID RATIO
.1
1
10
100
1000
VERTICAL EFFECTIVE STRESS (kPa)

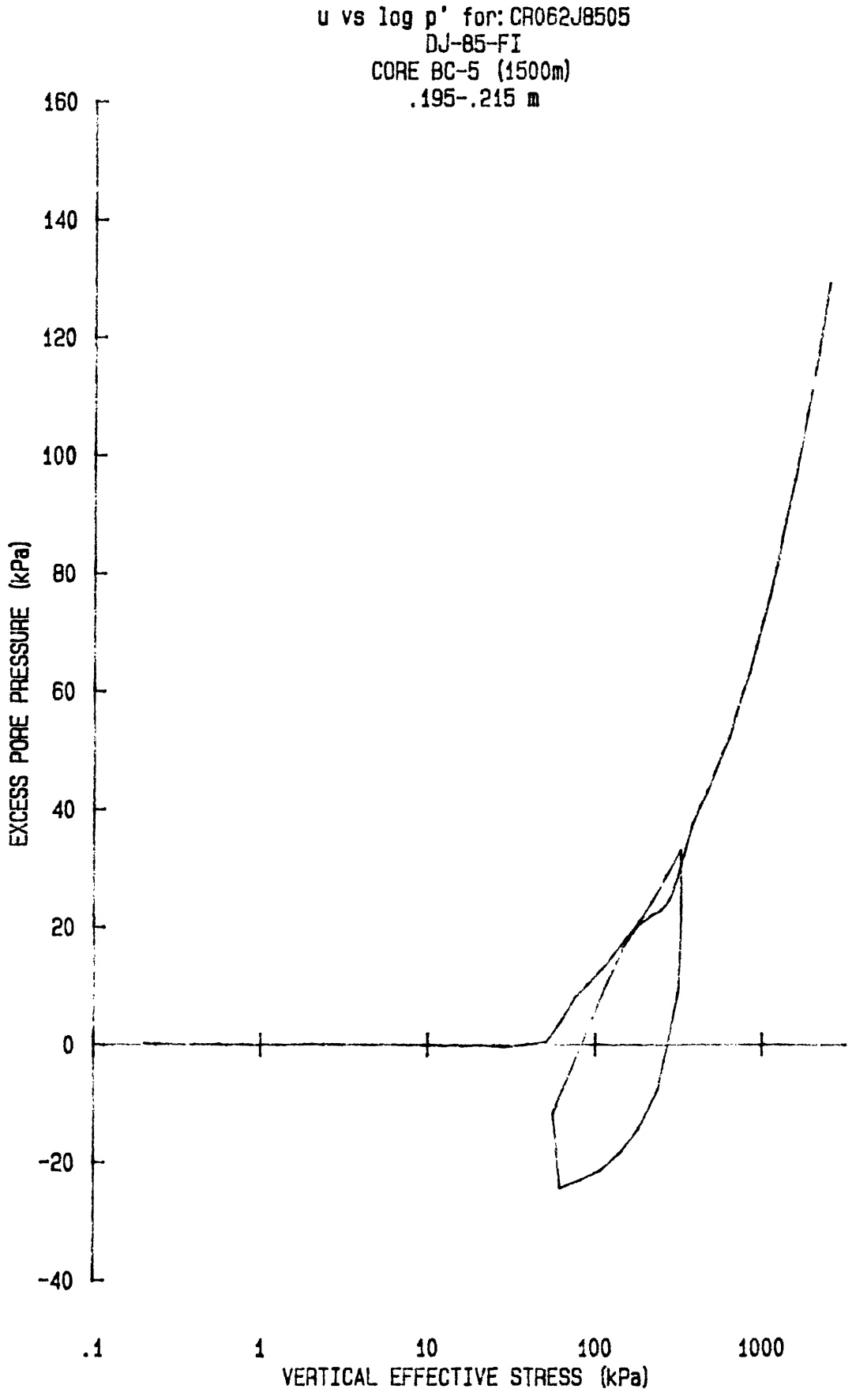
u vs log p' for: CR062J8505
DJ-85-FI
CORE BC-5 (1500m)
.195-.215 m
160
140
120
100
80
60
40
20
0
-20
-40
EXCESS PORE PRESSURE (kPa)
.1
1
10
100
1000
VERTICAL EFFECTIVE STRESS (kPa)

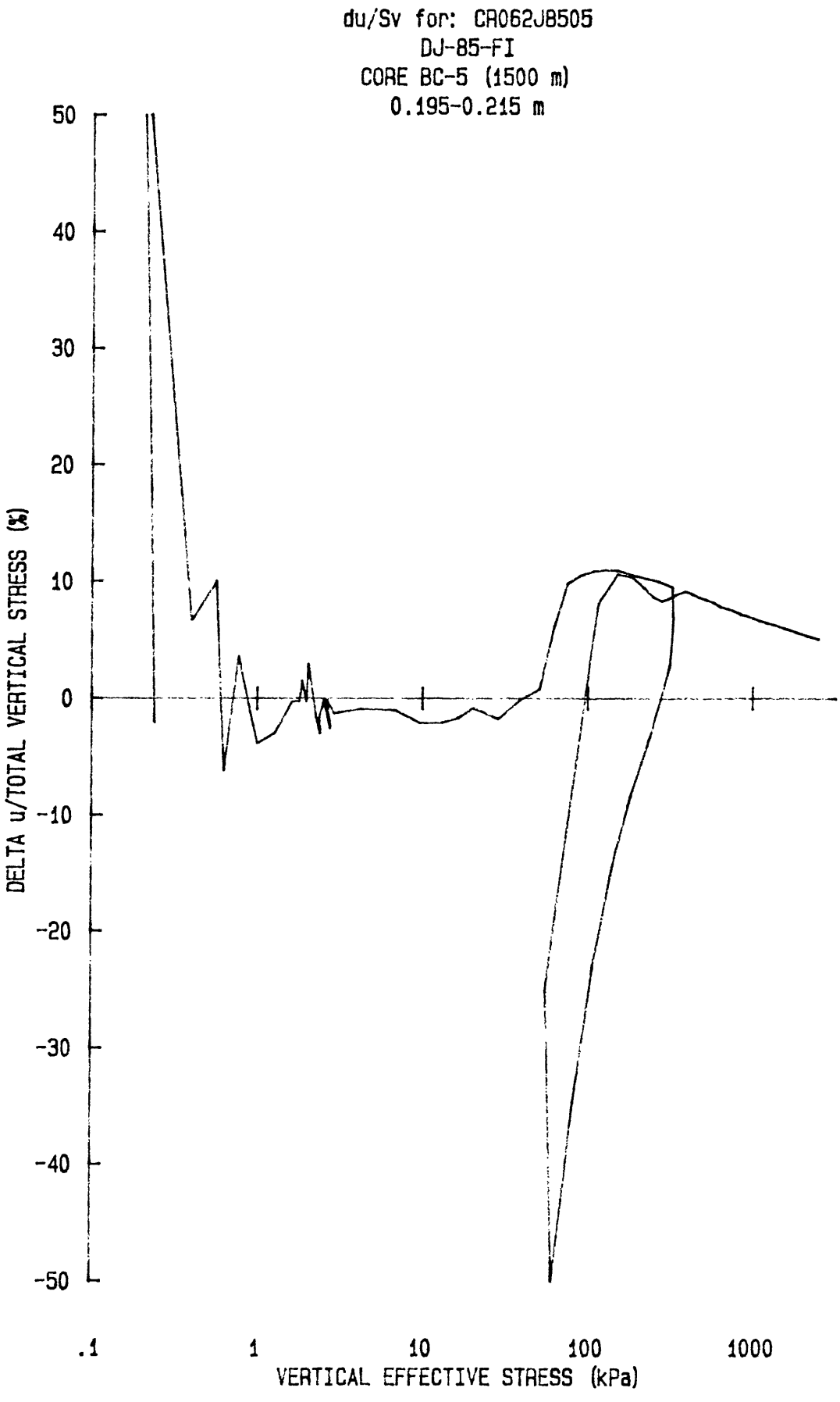
du/Sv for: CR062J8505
DJ-85-FI
CORE BC-5 (1500 m)
0.195-0.215 m
50
40
30
20
10
0
-10
-20
-30
-40
-50
DELTA u/TOTAL VERTICAL STRESS (%)
.1
1
10
100
1000
VERTICAL EFFECTIVE STRESS (kPa)

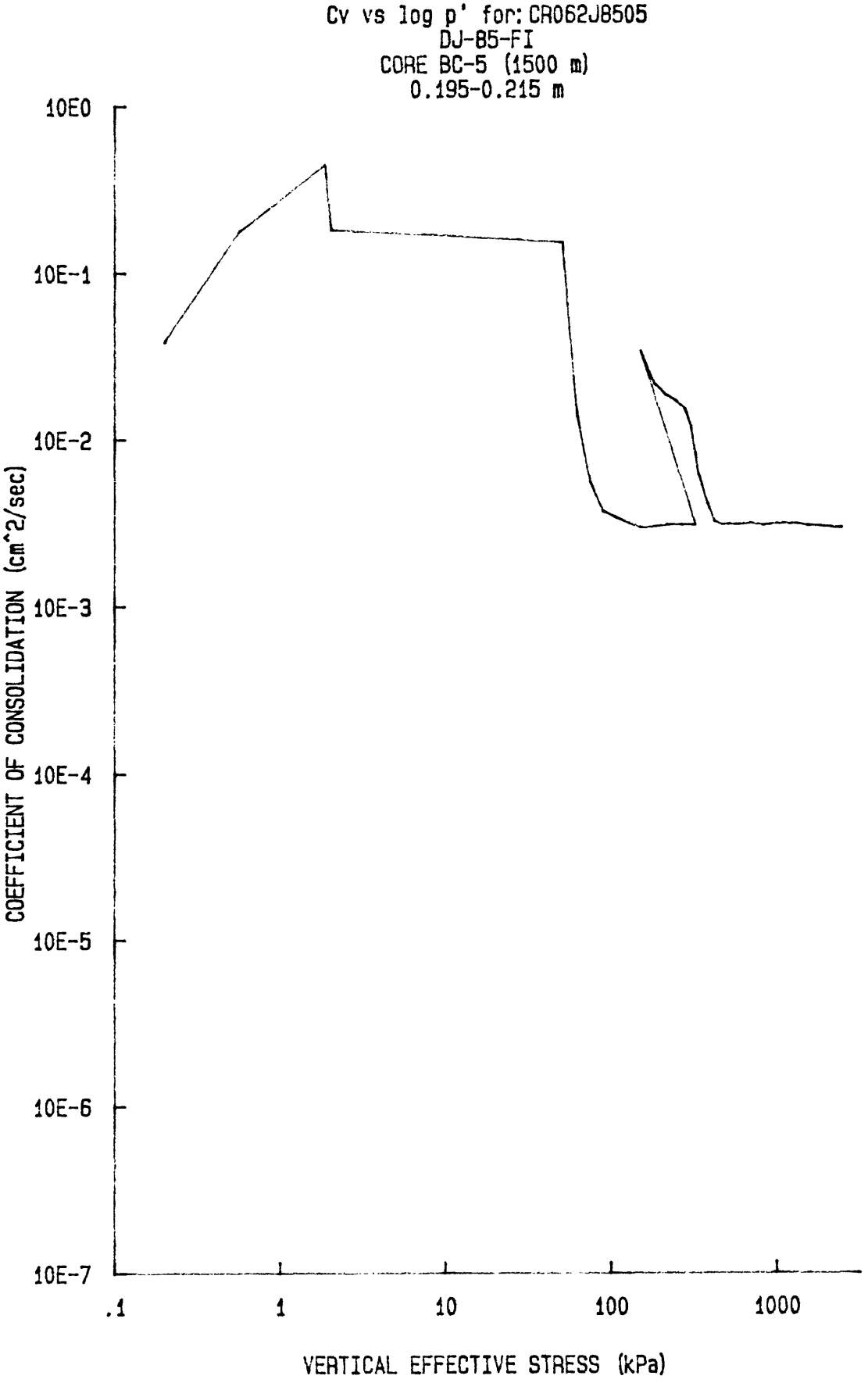
Cv vs log p' for: CR062J8505
DJ-85-FI
CORE BC-5 (1500 m)
0.195-0.215 m
10E0
10E-1
10E-2
10E-3
10E-4
10E-5
10E-6
10E-7
COEFFICIENT OF CONSOLIDATION (cm^2/sec)
.1
1
10
100
1000
VERTICAL EFFECTIVE STRESS (kPa)

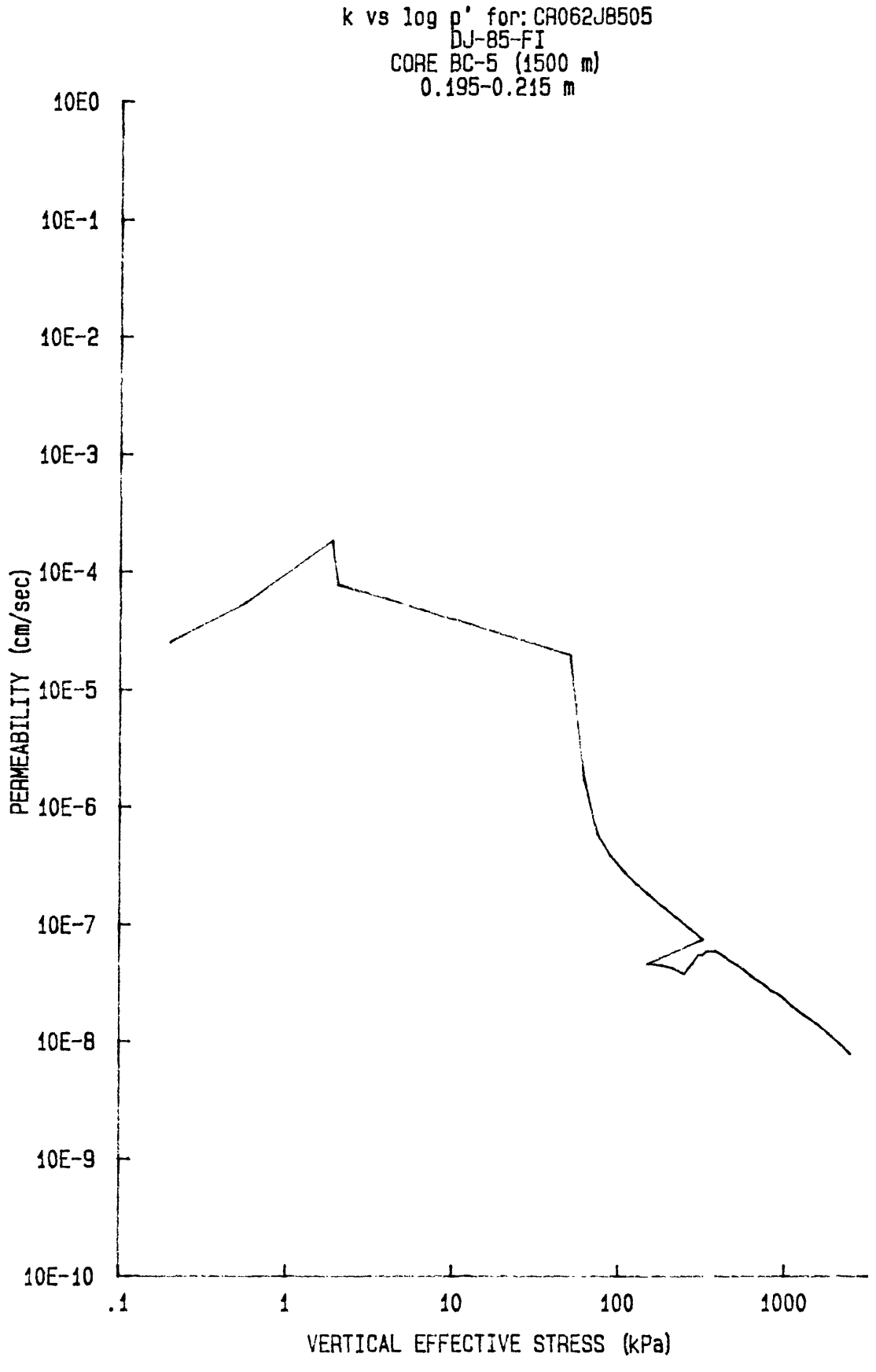
k vs log p' for: CR062J8505
DJ-85-FI
CORE BC-5 (1500 m)
0.195-0.215 m
10E0
10E-1
10E-2
10E-3
10E-4
10E-5
10E-6
10E-7
10E-8
10E-9
10E-10
PERMEABILITY (cm/sec)
.1
1
10
100
1000
VERTICAL EFFECTIVE STRESS (kPa)

APPENDIX B

Triaxial Compression Test Results

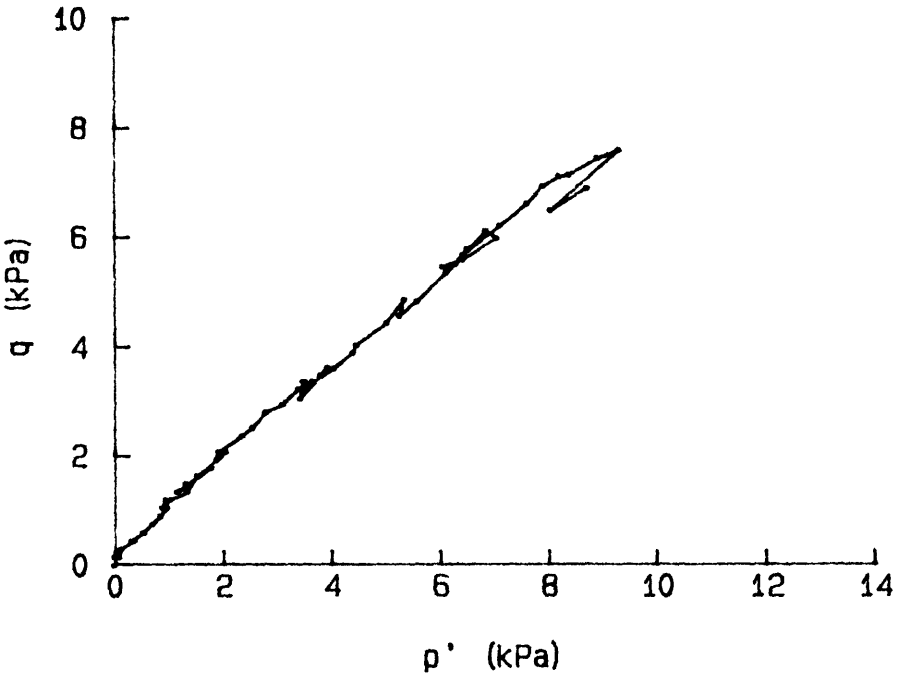

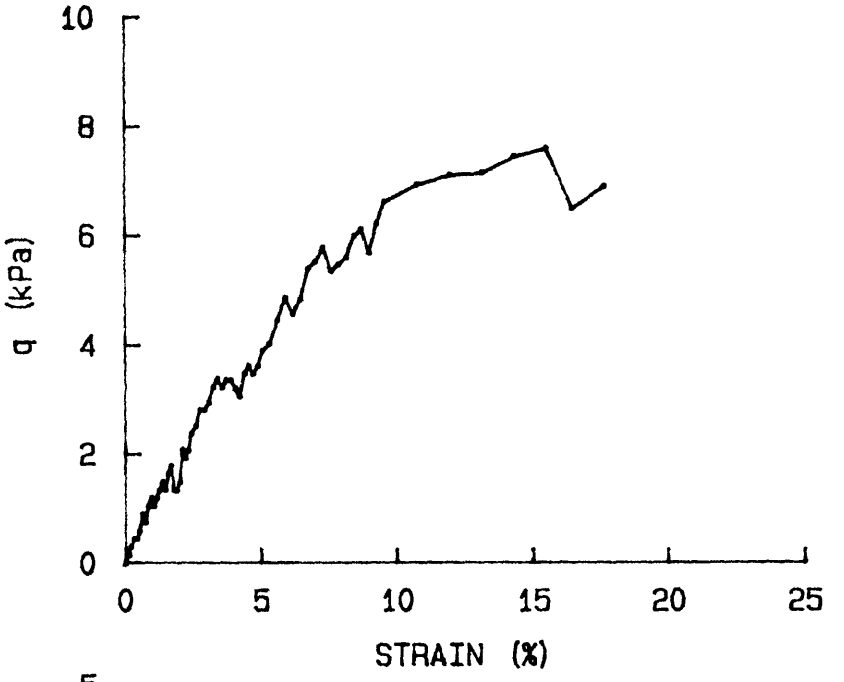

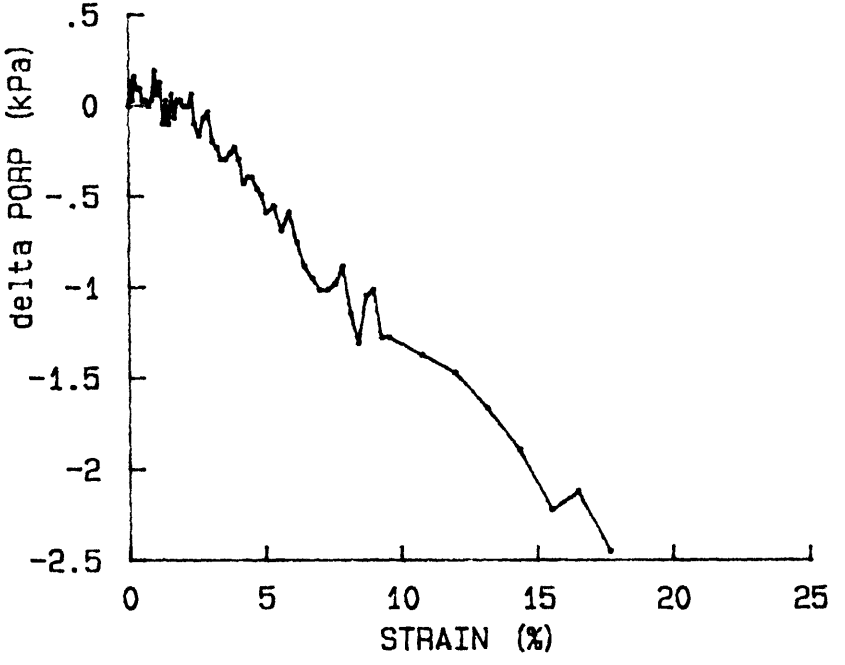

q vs p'
q vs AXIAL STRAIN
delta PORP vs AXIAL STRAIN

graphs for: TS008J8501
CRUISE: DJ-85-FI
CORE: BC-1 (500m)
SAMPLE INTERVAL: 0.105-0.175m

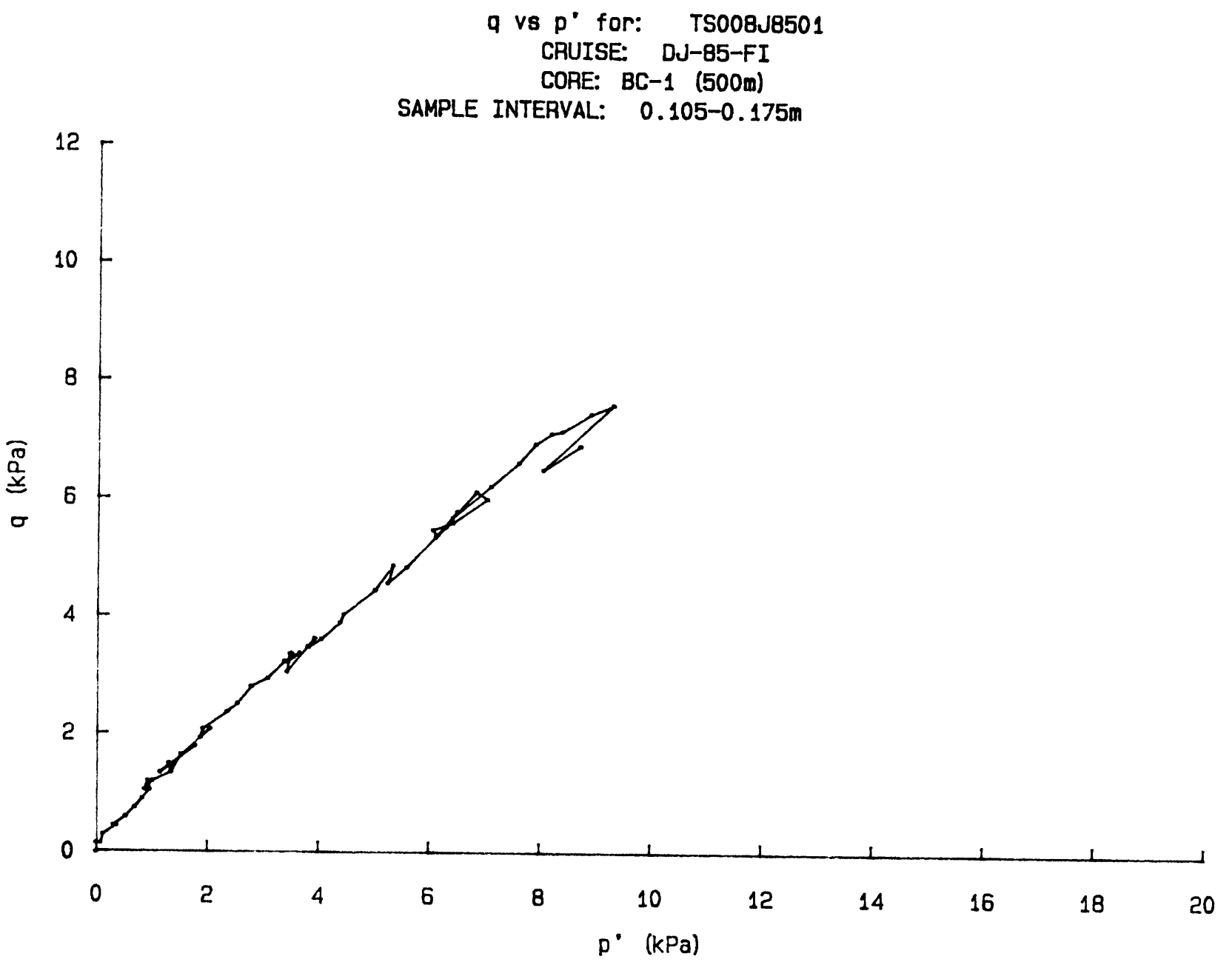
q vs p' for: TS008J8501
CRUISE: DJ-85-FI
CORE: BC-1 (500m)
SAMPLE INTERVAL: 0.105-0.175m
q (kPa)
p' (kPa)
0
2
4
6
8
10
12
14
16
18
20

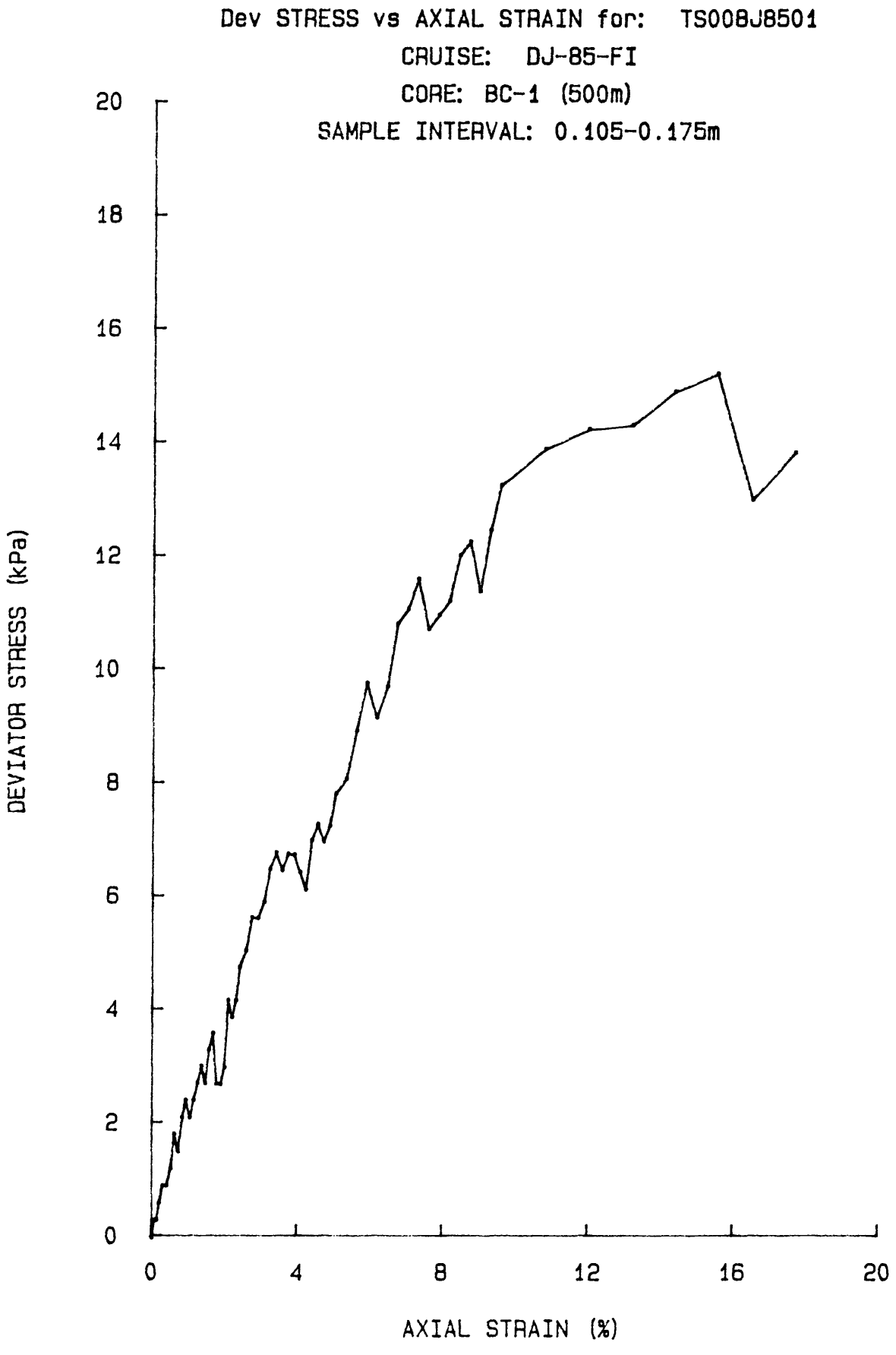
Dev STRESS vs AXIAL STRAIN for: TS008J8501
CRUISE: DJ-85-FI
CORE: BC-1 (500m)
SAMPLE INTERVAL: 0.105-0.175m
DEVIATOR STRESS (kPa)
0
2
4
6
8
10
12
14
16
18
20
0
4
8
12
16
20
AXIAL STRAIN (%)

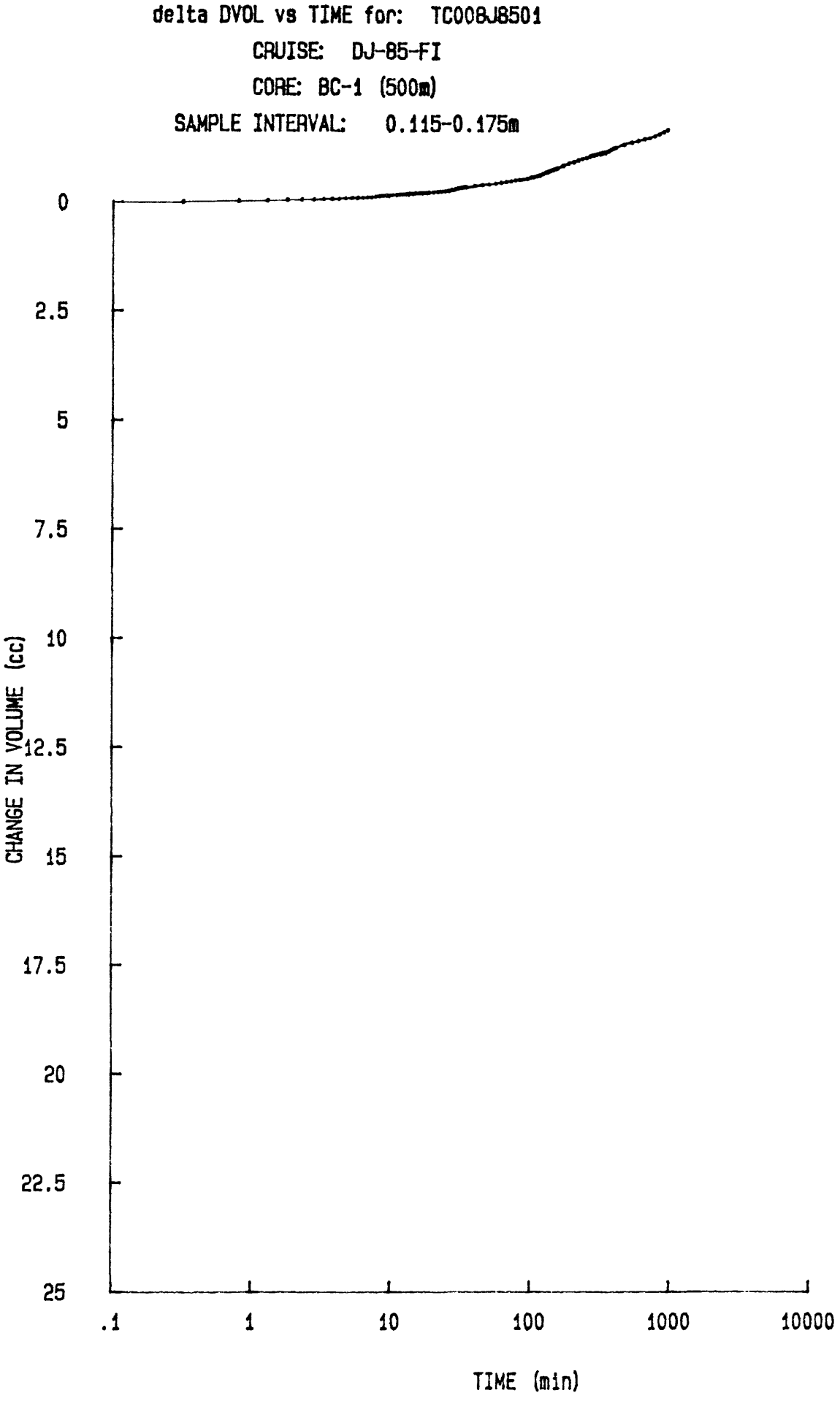
delta DVOL vs TIME for: TC008JB501
CRUISE: DJ-85-FI
CORE: BC-1 (500m)
SAMPLE INTERVAL: 0.115-0.175m
CHANGE IN VOLUME (cc)
0
2.5
5
7.5
10
12.5
15
17.5
20
22.5
25
.1
1
10
100
1000
10000
TIME (min)

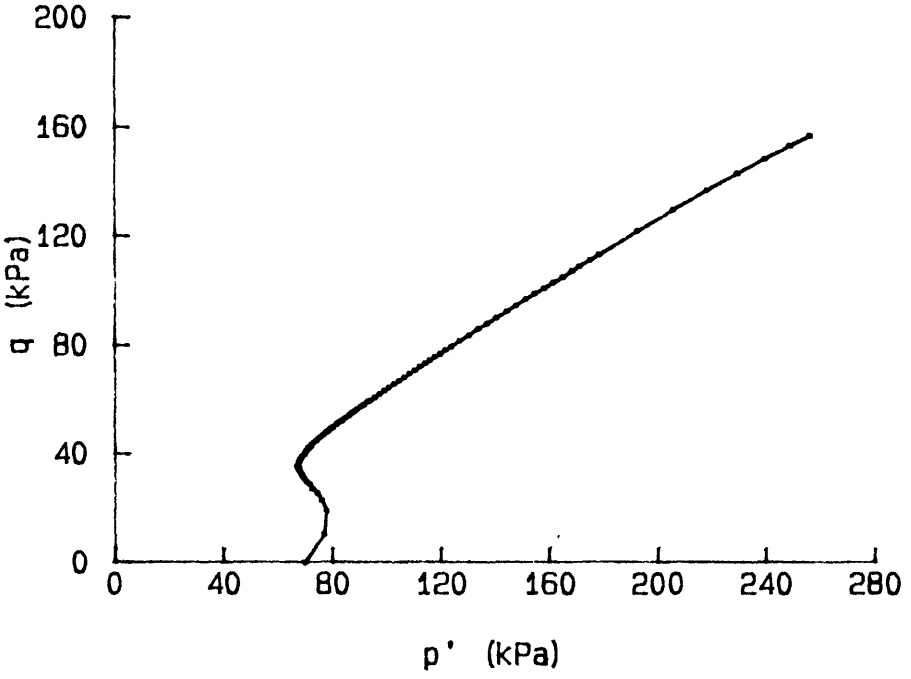

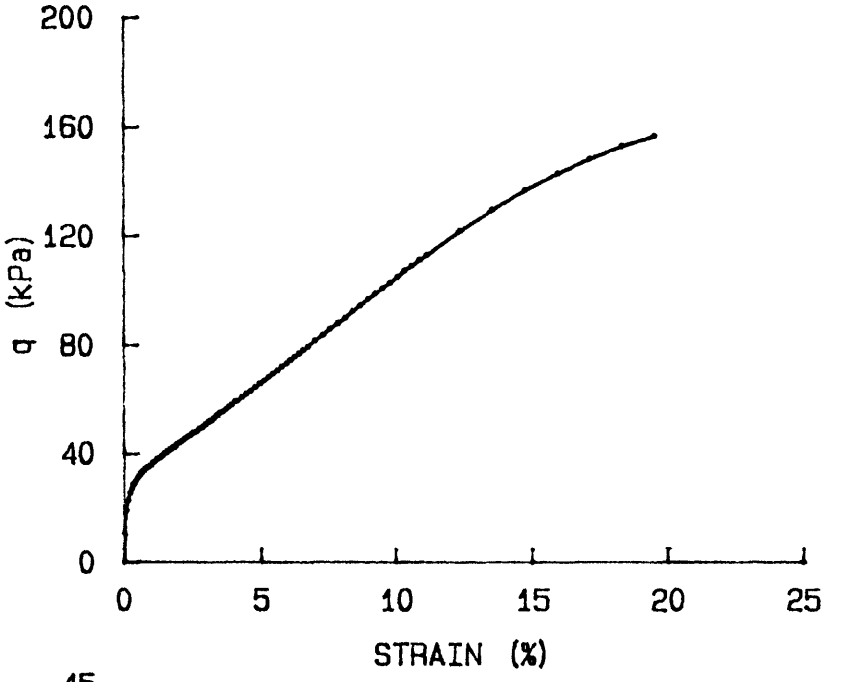

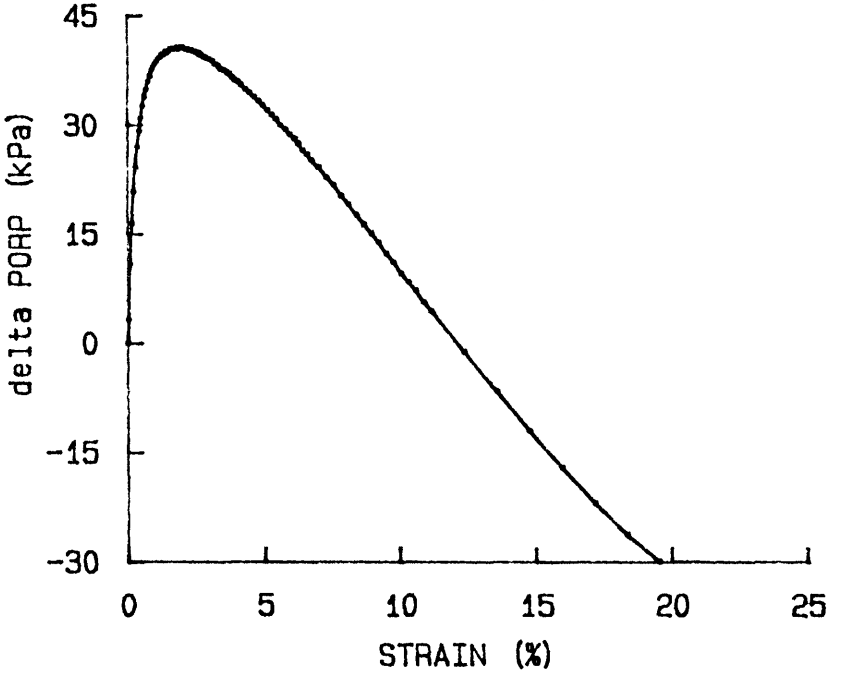

q vs p'
q vs AXIAL STRAIN
delta PORP vs AXIAL STRAIN

graphs for: TS007J8501
CRUISE: DJ-85-FI
CORE: BC-1 (500m)
SAMPLE INTERVAL: 0.105-0.175m

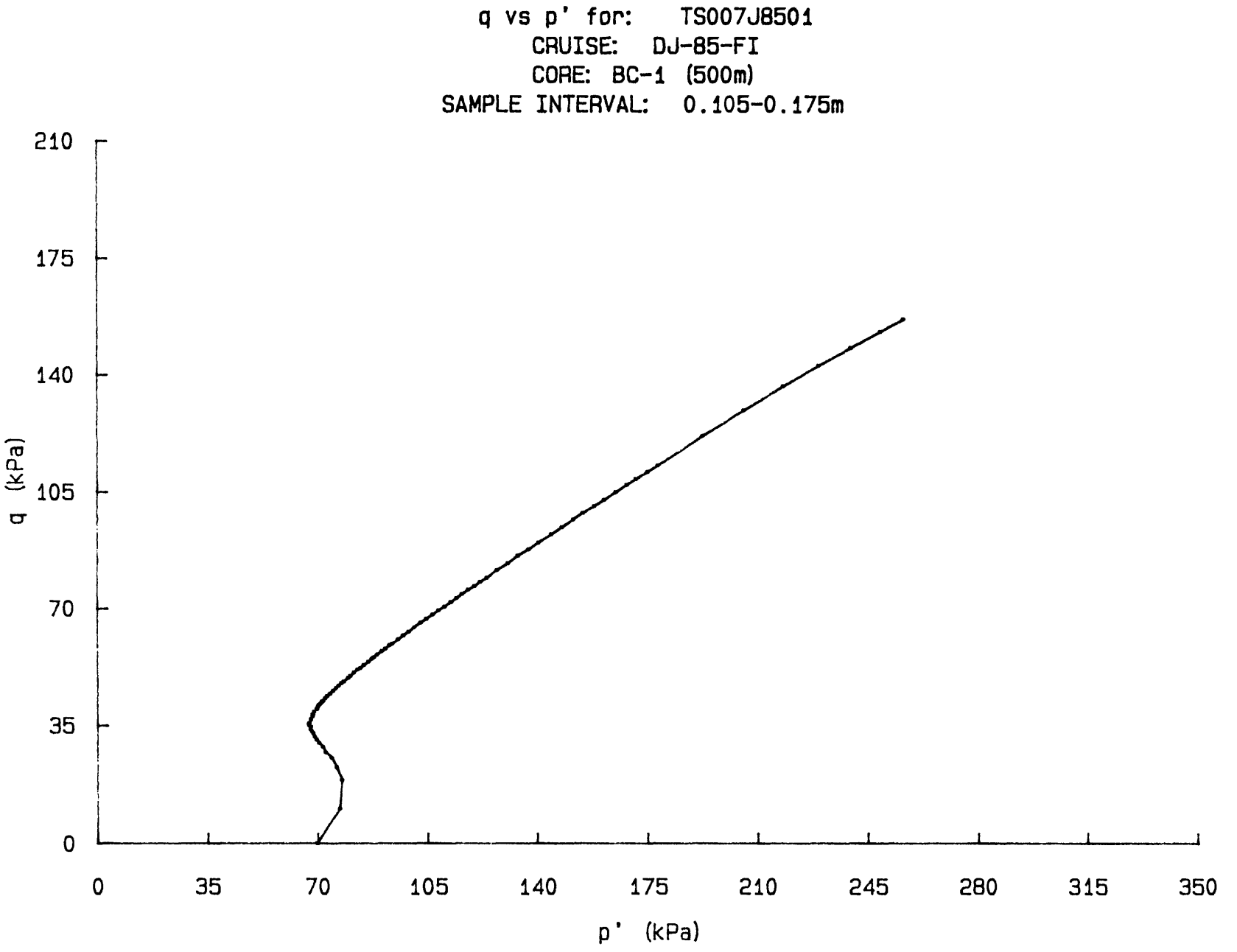
q vs p' for: TS007J8501
CRUISE: DJ-85-FI
CORE: BC-1 (500m)
SAMPLE INTERVAL: 0.105-0.175m
q (kPa)
p' (kPa)
0
35
70
105
140
175
210
245
280
315
350

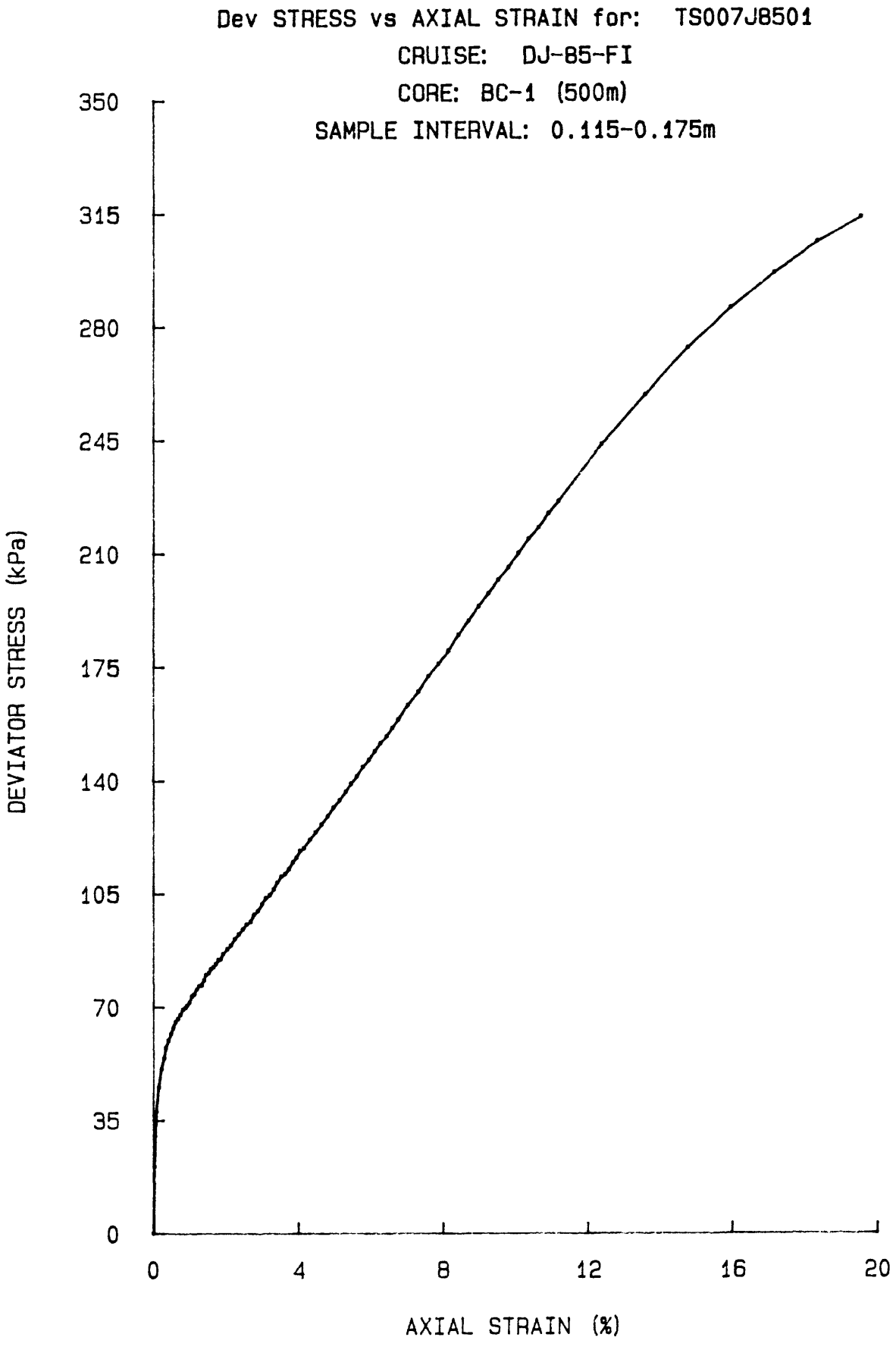
Dev STRESS vs AXIAL STRAIN for: TS007J8501
CRUISE: DJ-85-FI
CORE: BC-1 (500m)
SAMPLE INTERVAL: 0.115-0.175m
DEVIATOR STRESS (kPa)
350
315
280
245
210
175
140
105
70
35
0
0
4
8
12
16
20
AXIAL STRAIN (%)

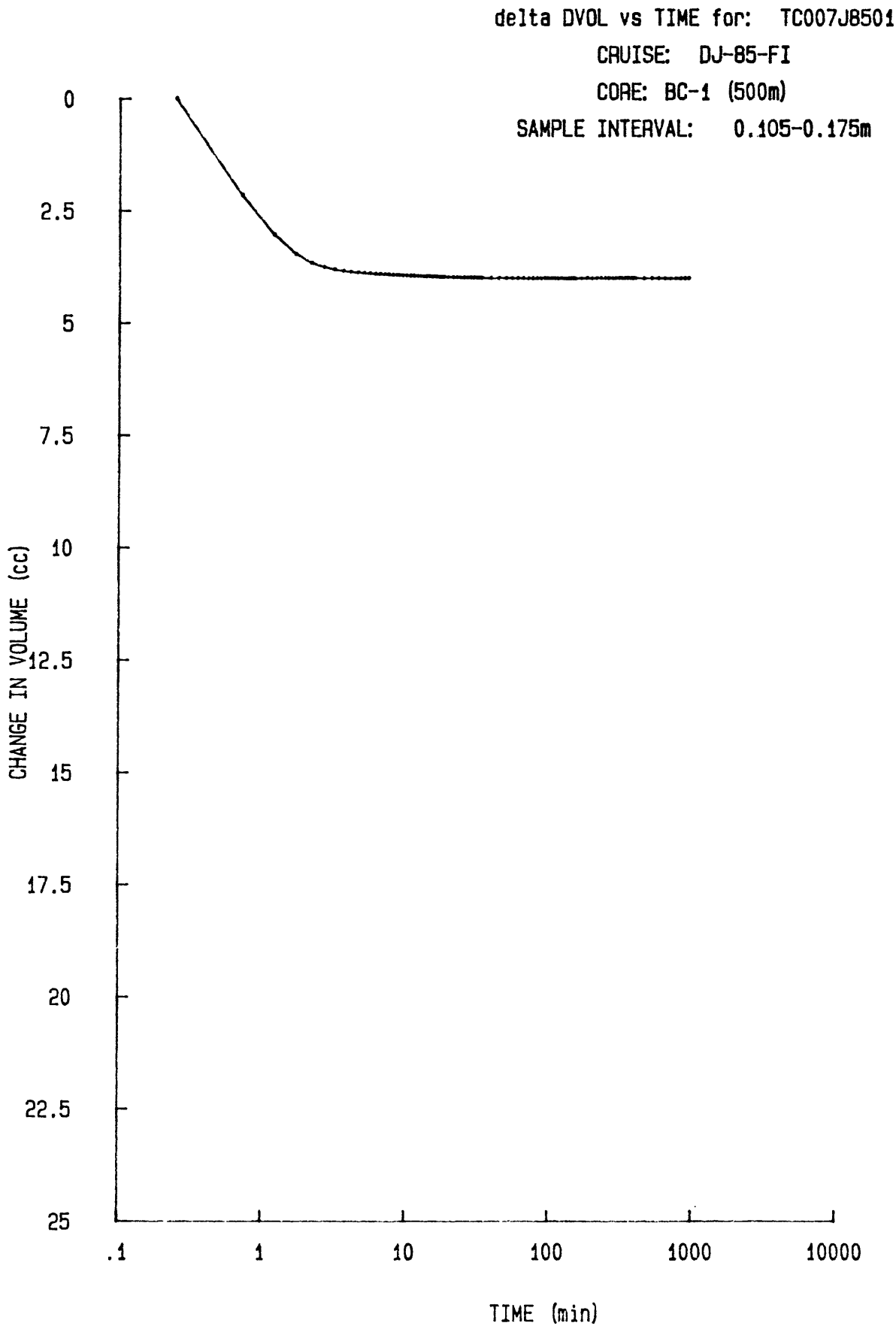
delta DVOL vs TIME for: TC007J8501
CRUISE: DJ-85-FI
CORE: BC-1 (500m)
SAMPLE INTERVAL: 0.105-0.175m
0
2.5
5
7.5
10
12.5
15
17.5
20
22.5
25
CHANGE IN VOLUME (cc)
.1
1
10
100
1000
10000
TIME (min)

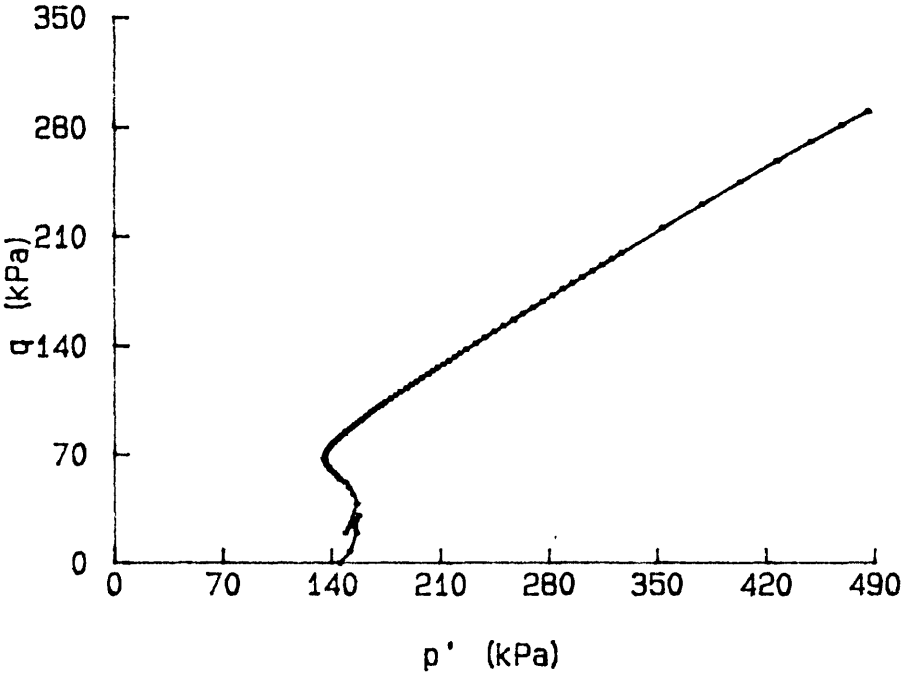

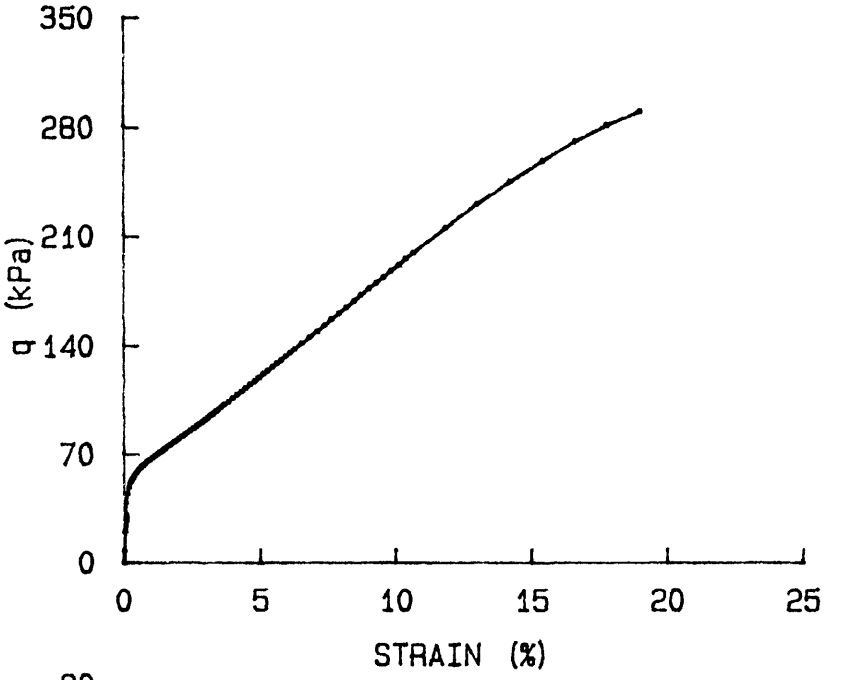

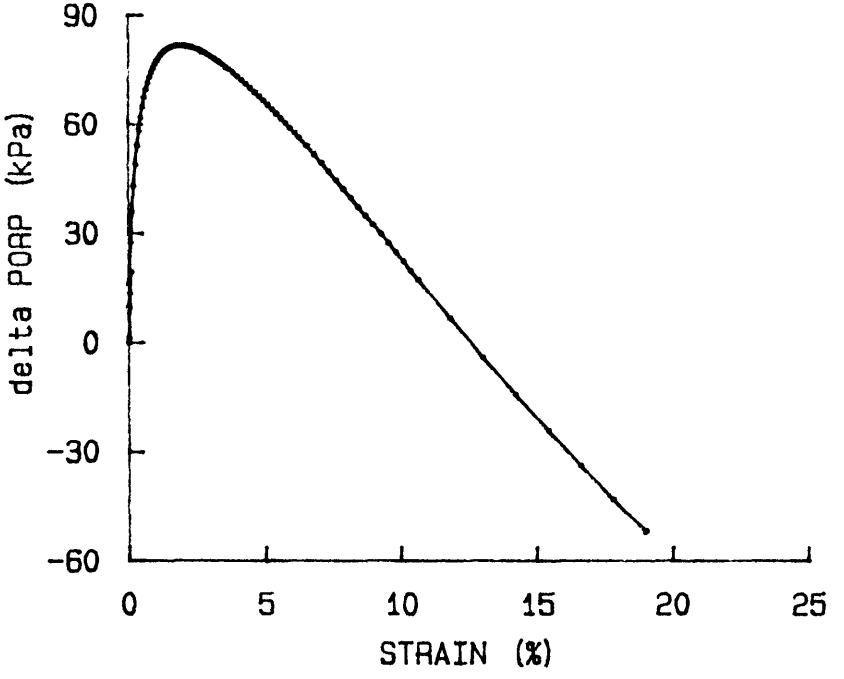

q vs p'
q vs AXIAL STRAIN
delta PORP vs AXIAL STRAIN

graphs for: TS006J8501
CRUISE: DJ-85-FI
CORE: BC-1 (500m)
SAMPLE INTERVAL: 0.025-0.095 m

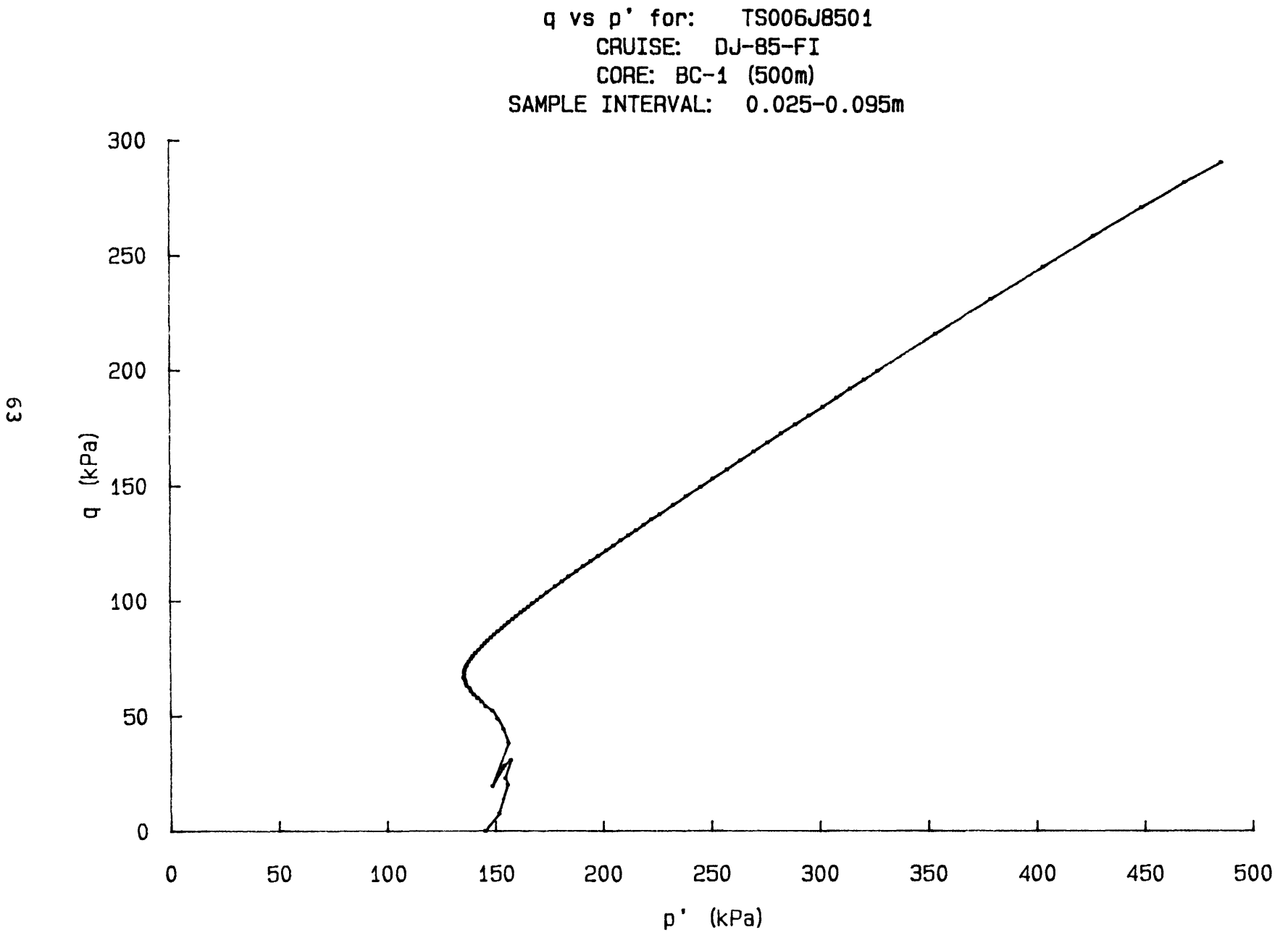
q vs p' for: TS006J8501
CRUISE: DJ-85-FI
CORE: BC-1 (500m)
SAMPLE INTERVAL: 0.025-0.095m
300
250
200
150
100
50
0
q (kPa)
0
50
100
150
200
250
300
350
400
450
500
p' (kPa)

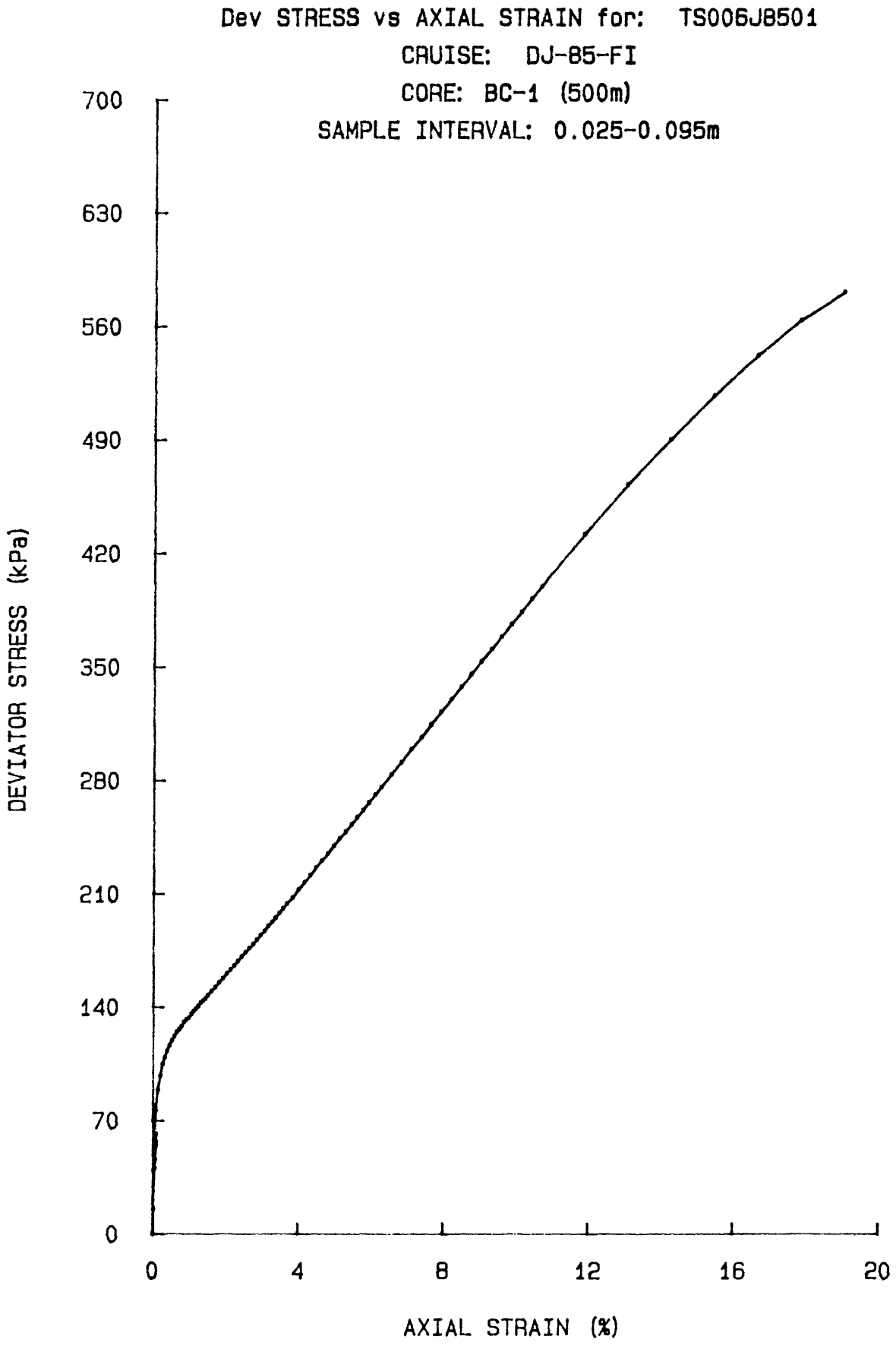
Dev STRESS vs AXIAL STRAIN for: TS006J8501
CRUISE: DJ-85-FI
CORE: BC-1 (500m)
SAMPLE INTERVAL: 0.025-0.095m
DEVIATOR STRESS (kPa)
700
630
560
490
420
350
280
210
140
70
0
0
4
8
12
16
20
AXIAL STRAIN (%)

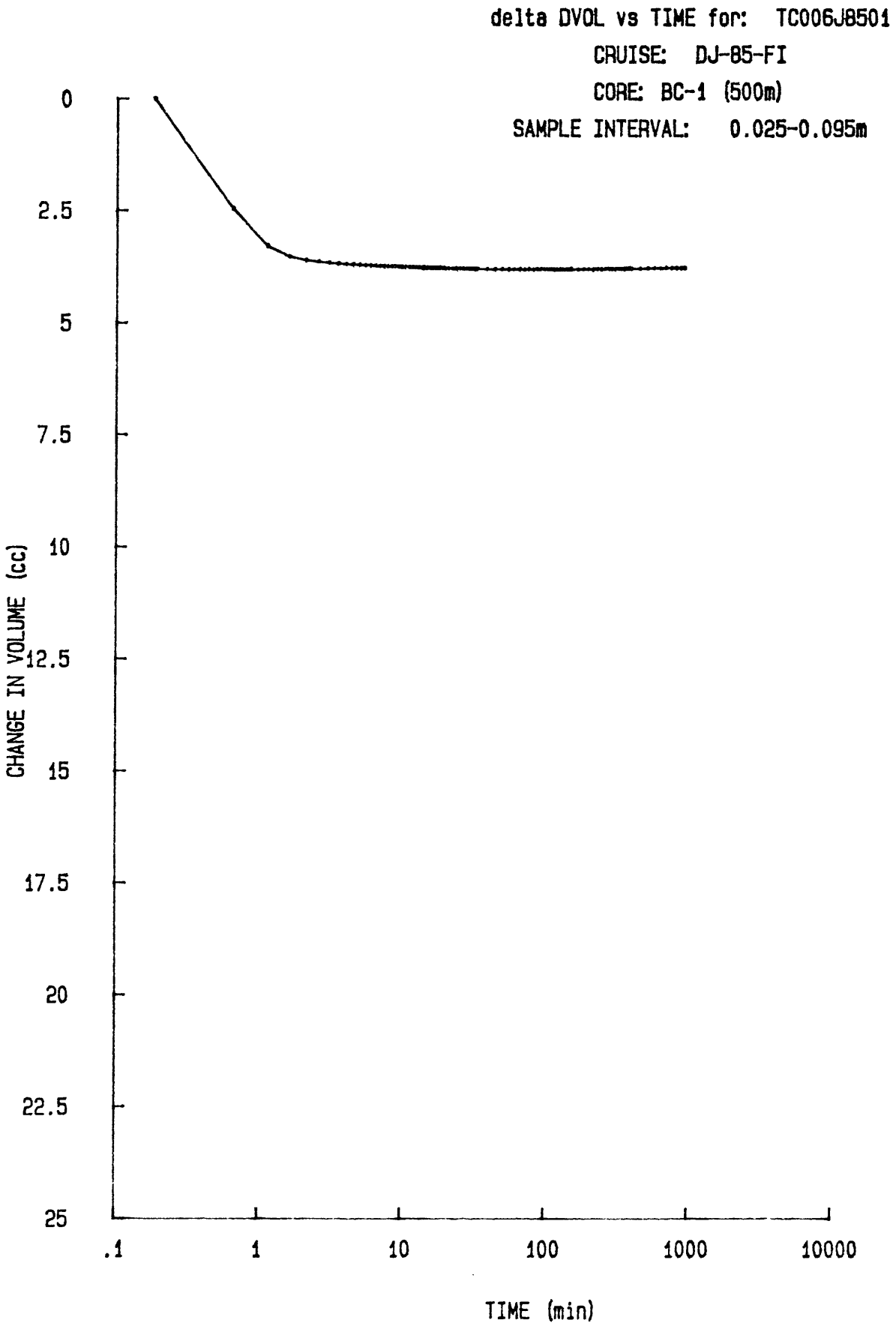
delta DVOL vs TIME for: TC006J8501
CRUISE: DJ-85-FI
CORE: BC-1 (500m)
SAMPLE INTERVAL: 0.025-0.095m
0
2.5
5
7.5
10
12.5
15
17.5
20
22.5
25
CHANGE IN VOLUME (cc)
.1
1
10
100
1000
10000
TIME (min)

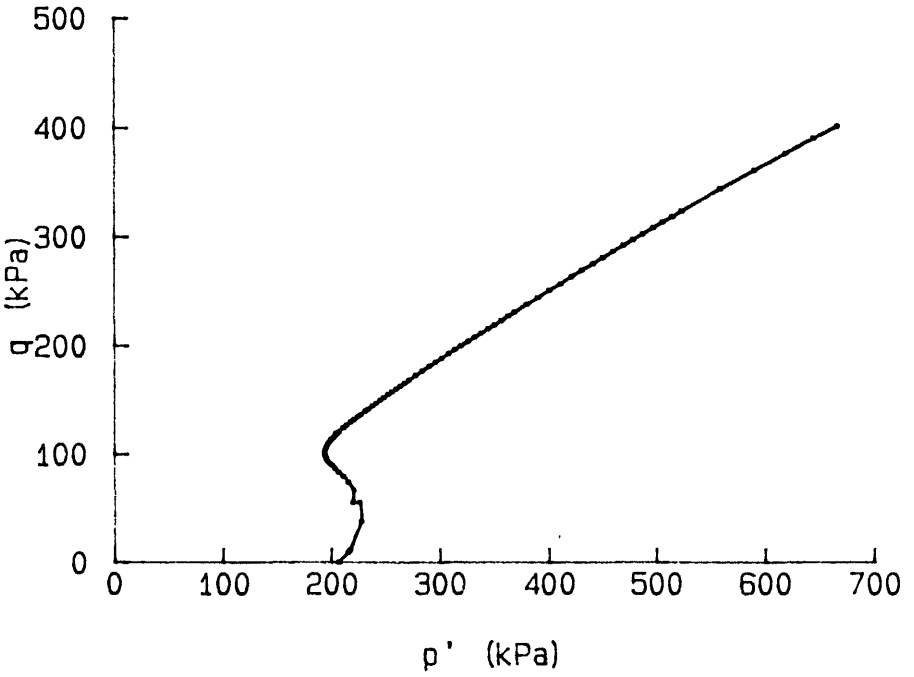

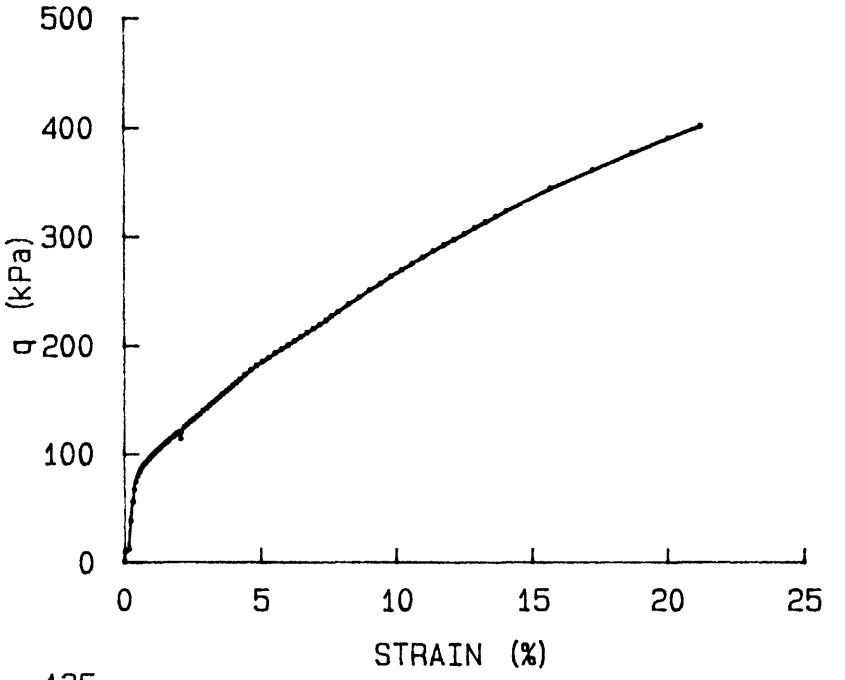

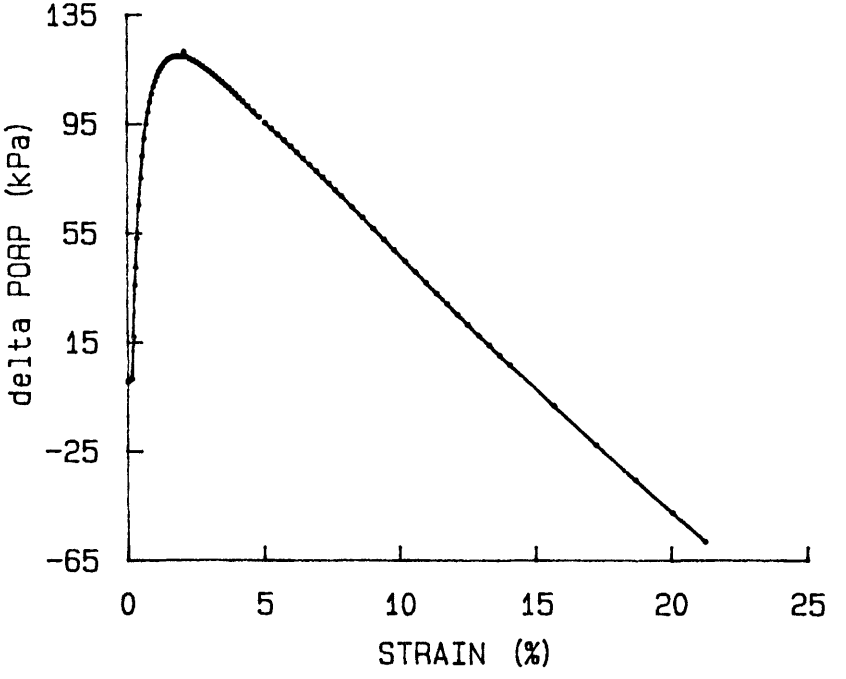

q vs p'
q vs AXIAL STRAIN
delta PORP vs AXIAL STRAIN

graphs for: TS005J8501
CRUISE: DJ-85-FI
CORE: BC-1 (500m)
SAMPLE INTERVAL: 0.025-0.095m

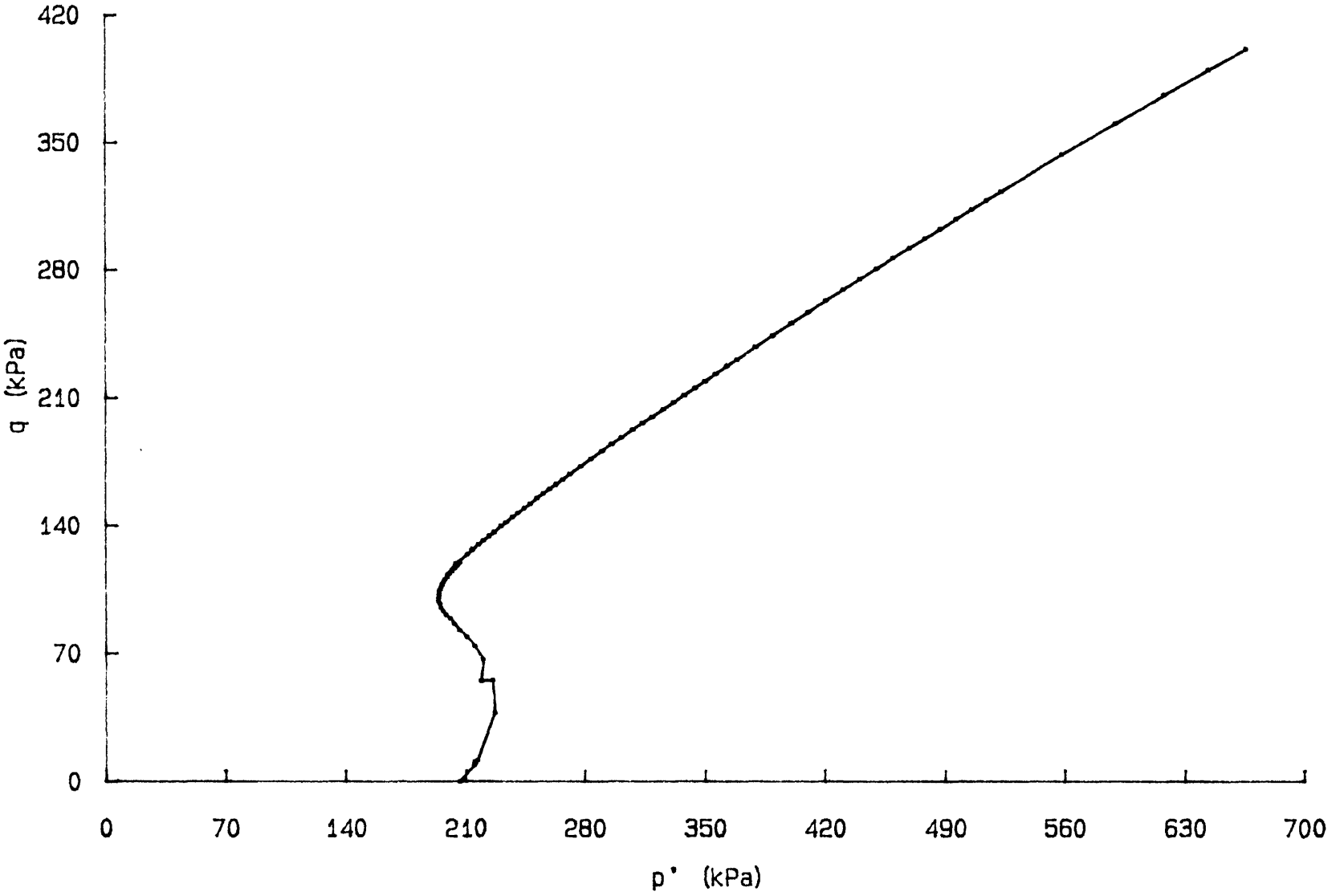
q vs p' for: TS005J8501
CRUISE: DJ-85-FI
CORE: BC-1 (500m)
SAMPLE INTERVAL: 0.025-0.095m
420
350
280
210
140
70
0
q (kPa)
0
70
140
210
280
350
420
490
560
630
700
p' (kPa)

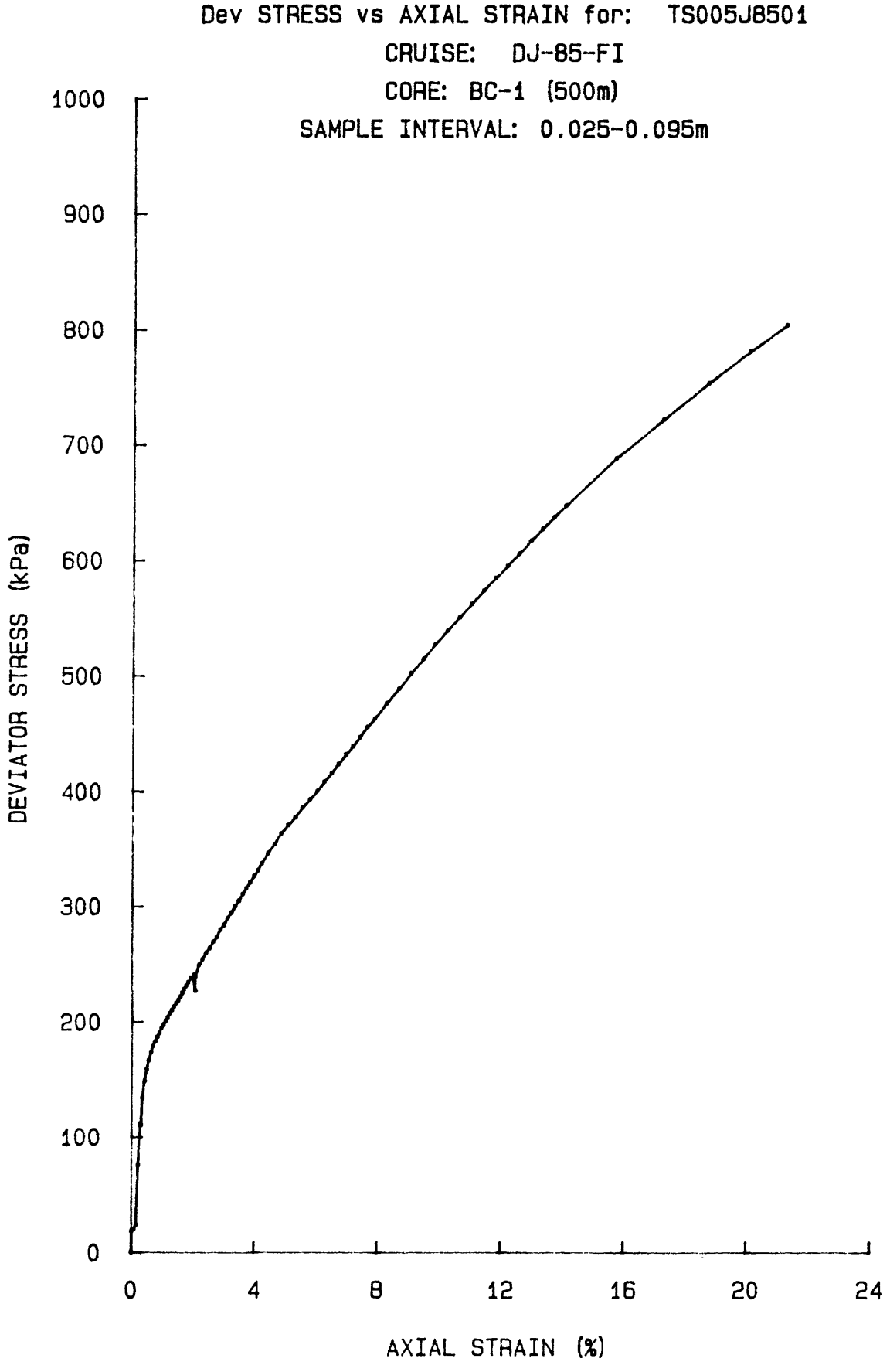
Dev STRESS vs AXIAL STRAIN for: TS005J8501
CRUISE: DJ-85-FI
CORE: BC-1 (500m)
SAMPLE INTERVAL: 0.025-0.095m
DEVIATOR STRESS (kPa)
1000
900
800
700
600
500
400
300
200
100
0
0
4
8
12
16
20
24
AXIAL STRAIN (%)

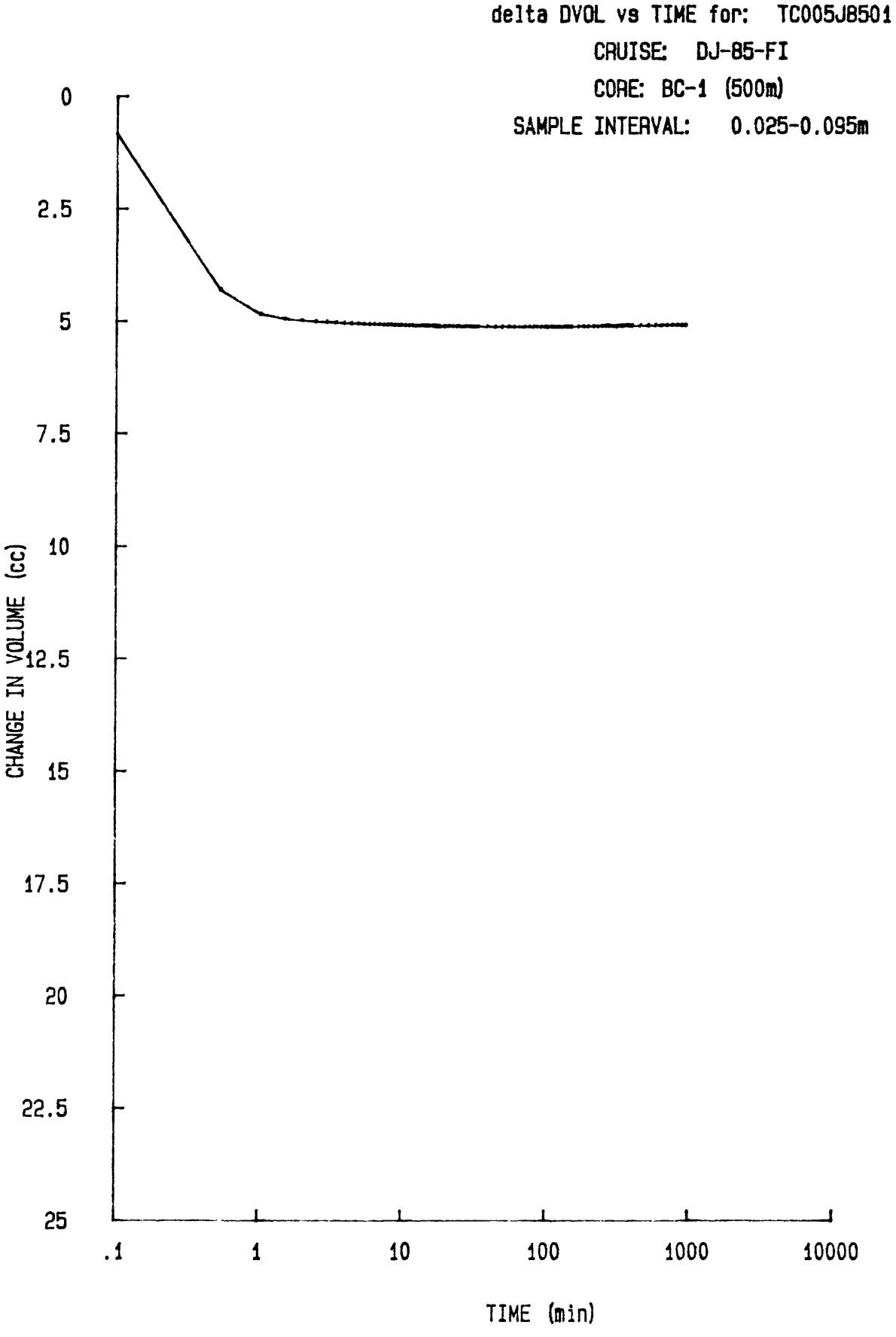
delta DVOL vs TIME for: TC005J8501
CRUISE: DJ-85-FI
CORE: BC-1 (500m)
SAMPLE INTERVAL: 0.025-0.095m
0
2.5
5
7.5
10
12.5
15
17.5
20
22.5
25
CHANGE IN VOLUME (cc)
.1
1
10
100
1000
10000
TIME (min)

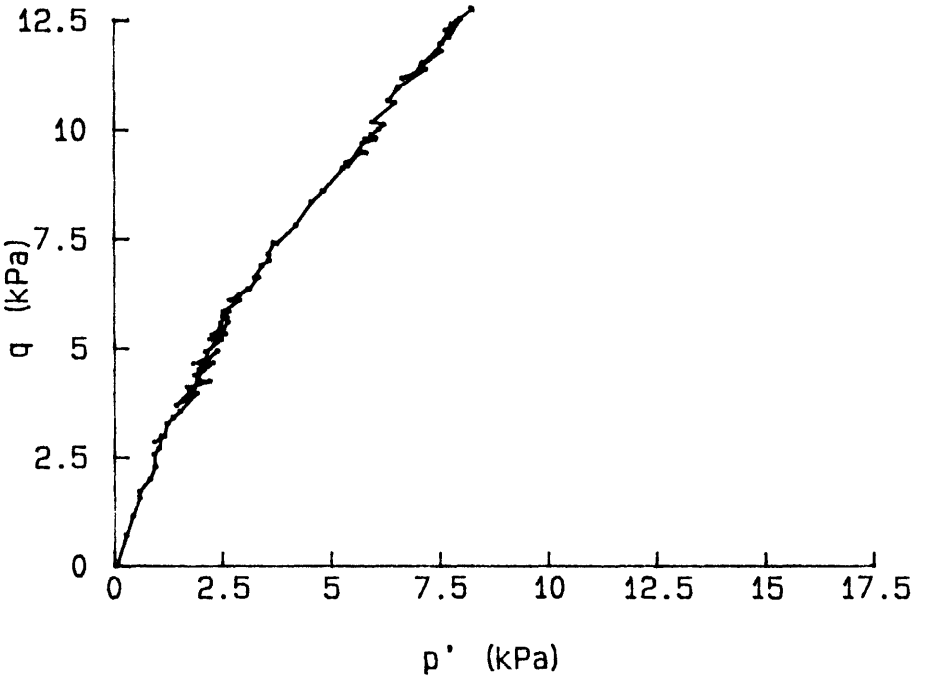

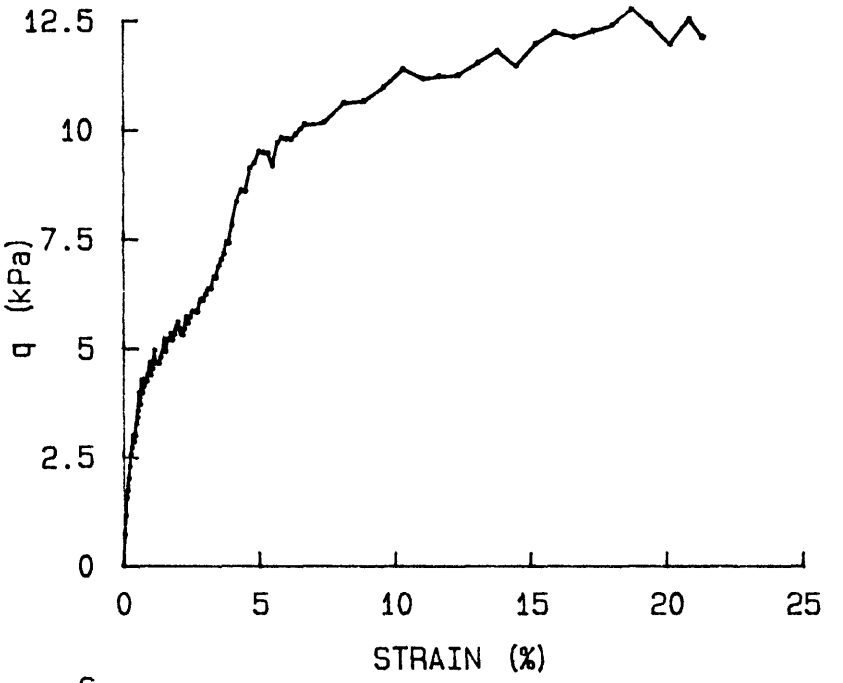

q vs p'
q vs AXIAL STRAIN
delta PORP vs AXIAL STRAIN

graphs for: TS004J8503
CRUISE: DJ-85-FI
CORE: BC-3 (1000m)
SAMPLE INTERVAL: 0.1075-0.185 m

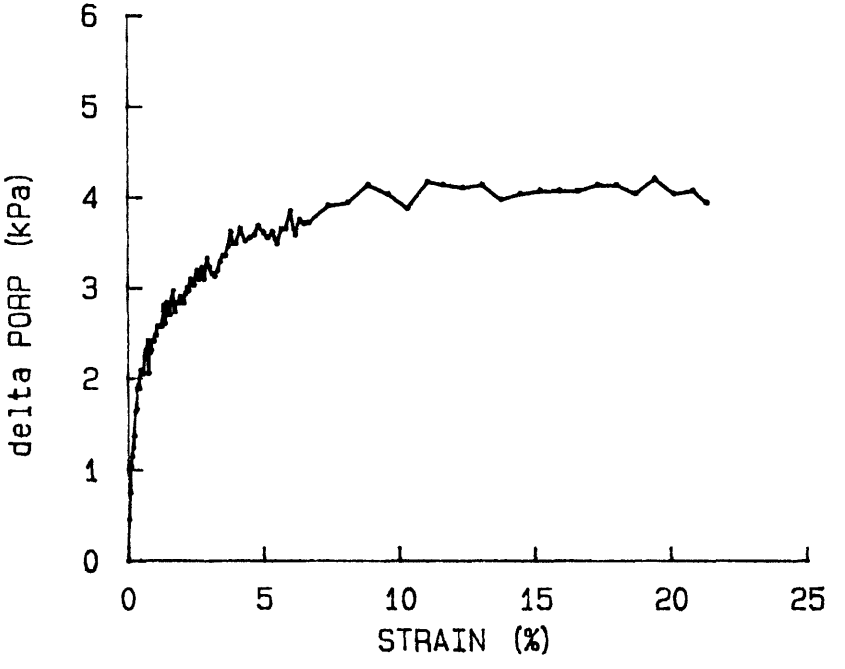

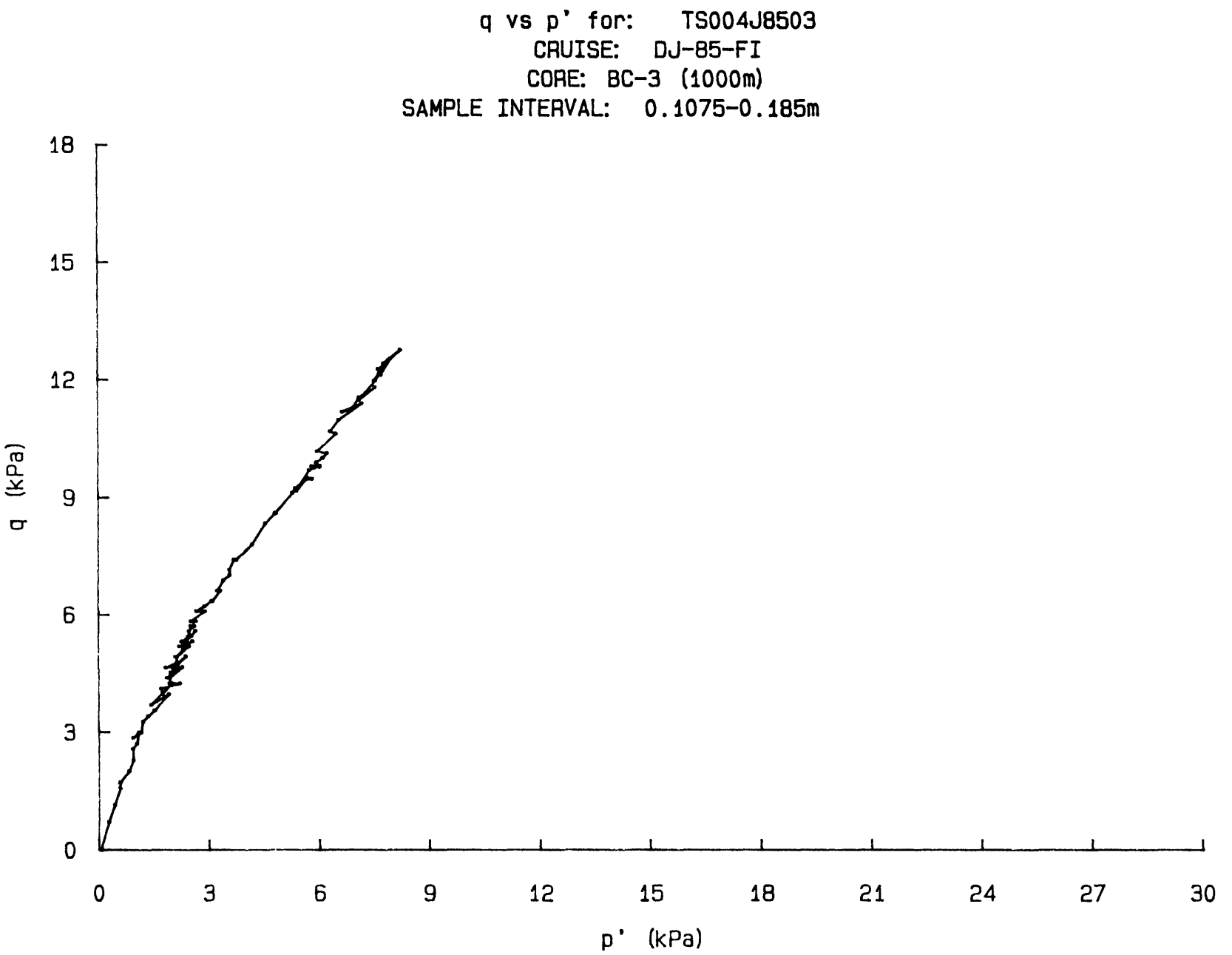
q vs p' for: TS004J8503
CRUISE: DJ-85-FI
CORE: BC-3 (1000m)
SAMPLE INTERVAL: 0.1075-0.185m
q (kPa)
p' (kPa)
0
3
6
9
12
15
18
21
24
27
30

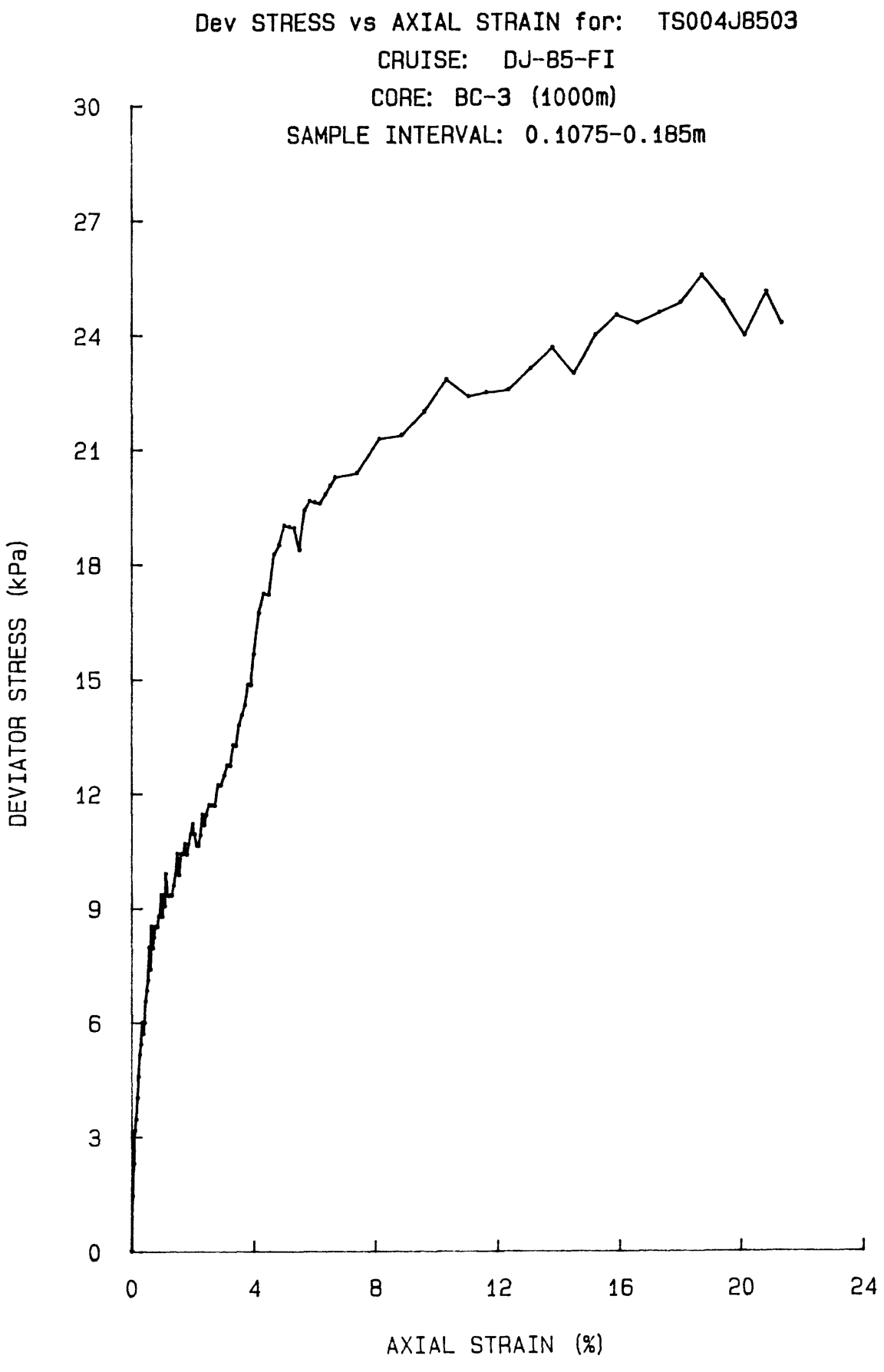
Dev STRESS vs AXIAL STRAIN for: TS004JB503
CRUISE: DJ-85-FI
CORE: BC-3 (1000m)
SAMPLE INTERVAL: 0.1075-0.185m
DEVIATOR STRESS (kPa)
30
27
24
21
18
15
12
9
6
3
0
0
4
8
12
16
20
24
AXIAL STRAIN (%)

delta DVOL vs TIME for: TC004J8503

CRUISE: DJ-85-FI

CORE: BC-3 (1000m)

SAMPLE INTERVAL: 0.1075-0.185m

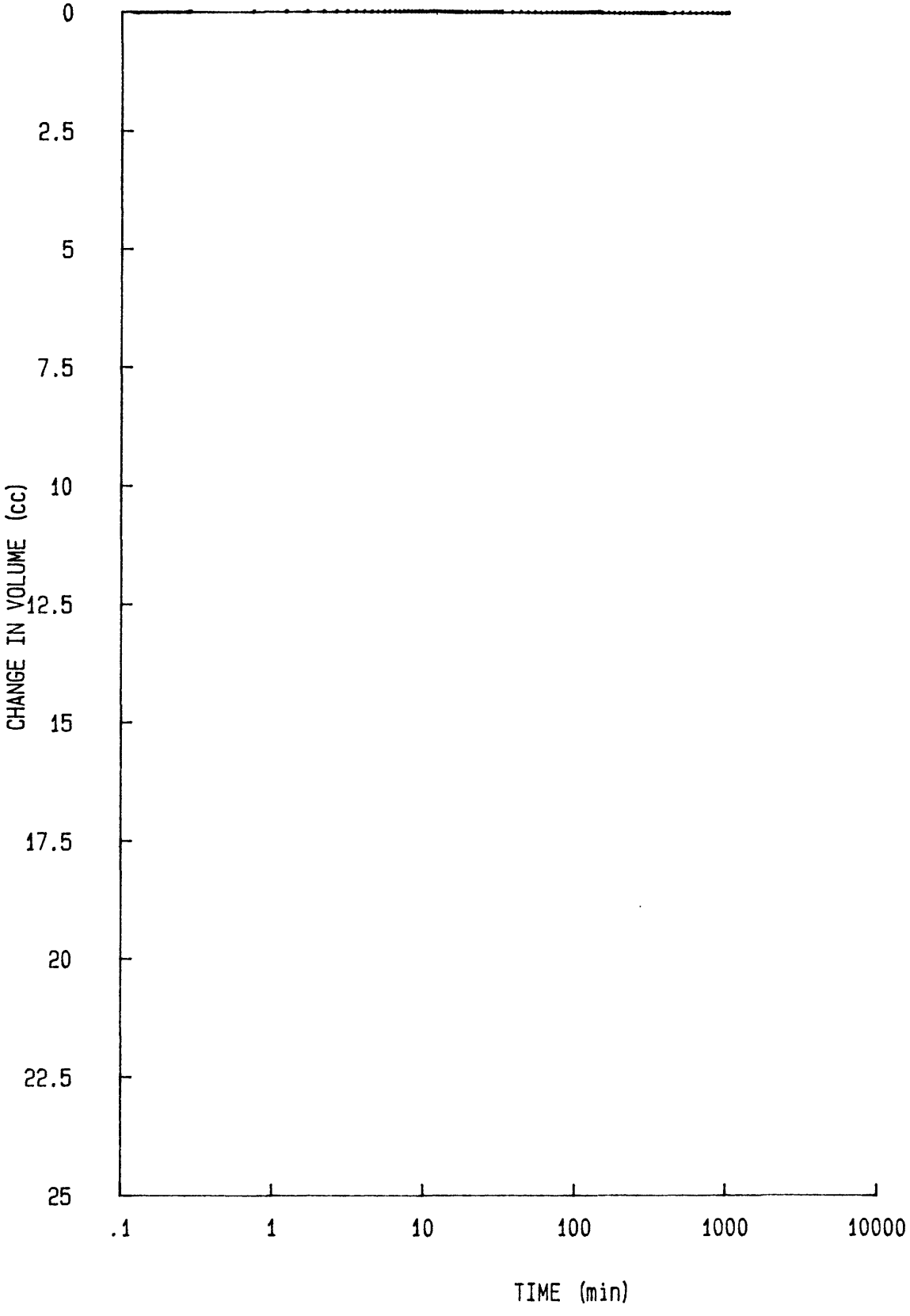

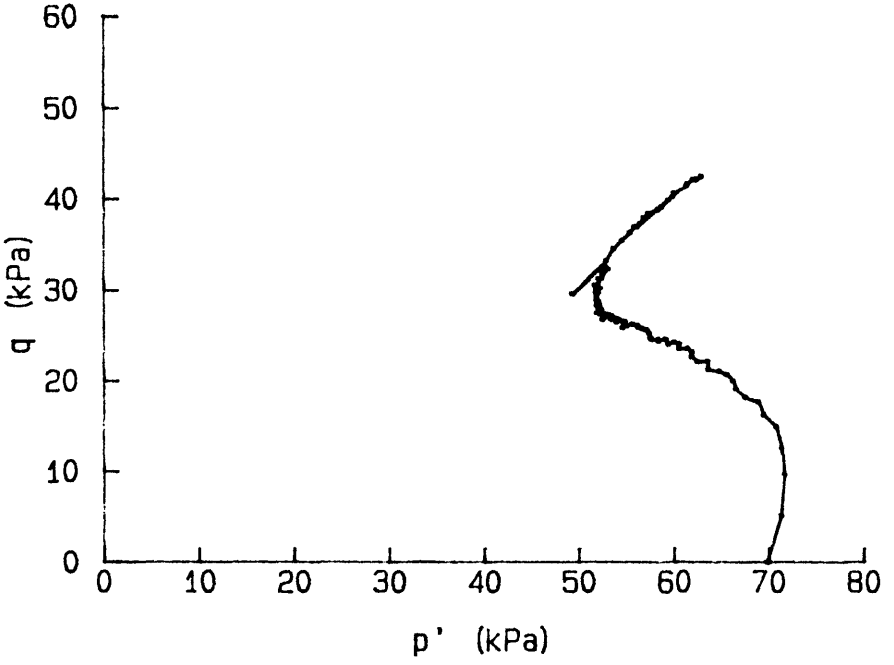

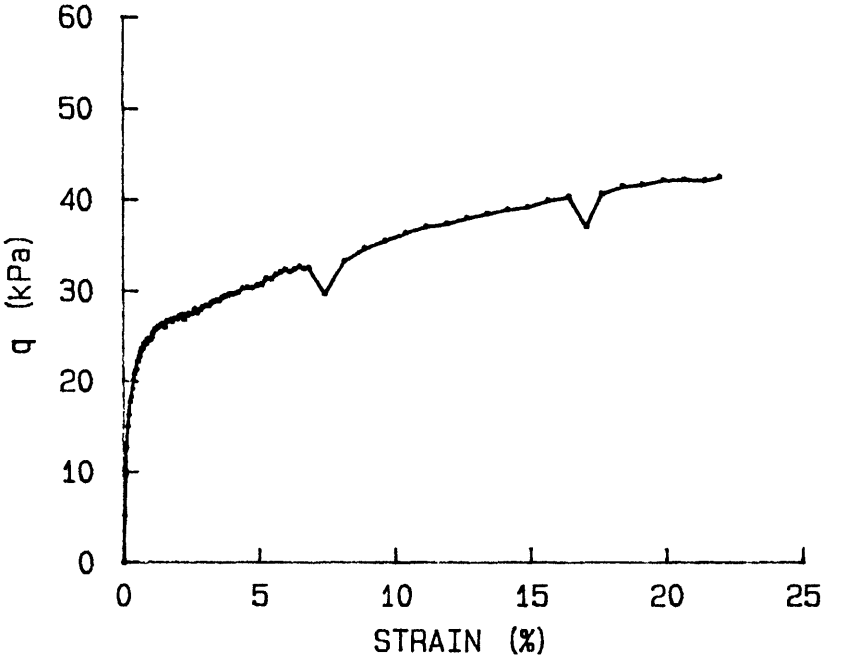

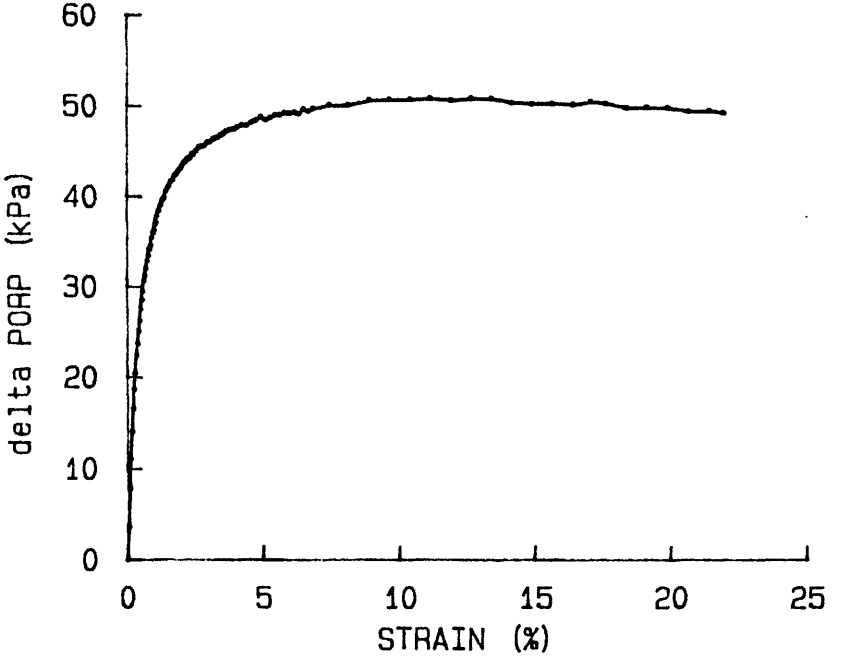

q vs p'
q vs AXIAL STRAIN
delta PORP vs AXIAL STRAIN

graphs for: TS003J8503
CRUISE: DJ-85-FI
CORE: BC-3 (1000m)
SAMPLE INTERVAL: 0.1075-0.185 m

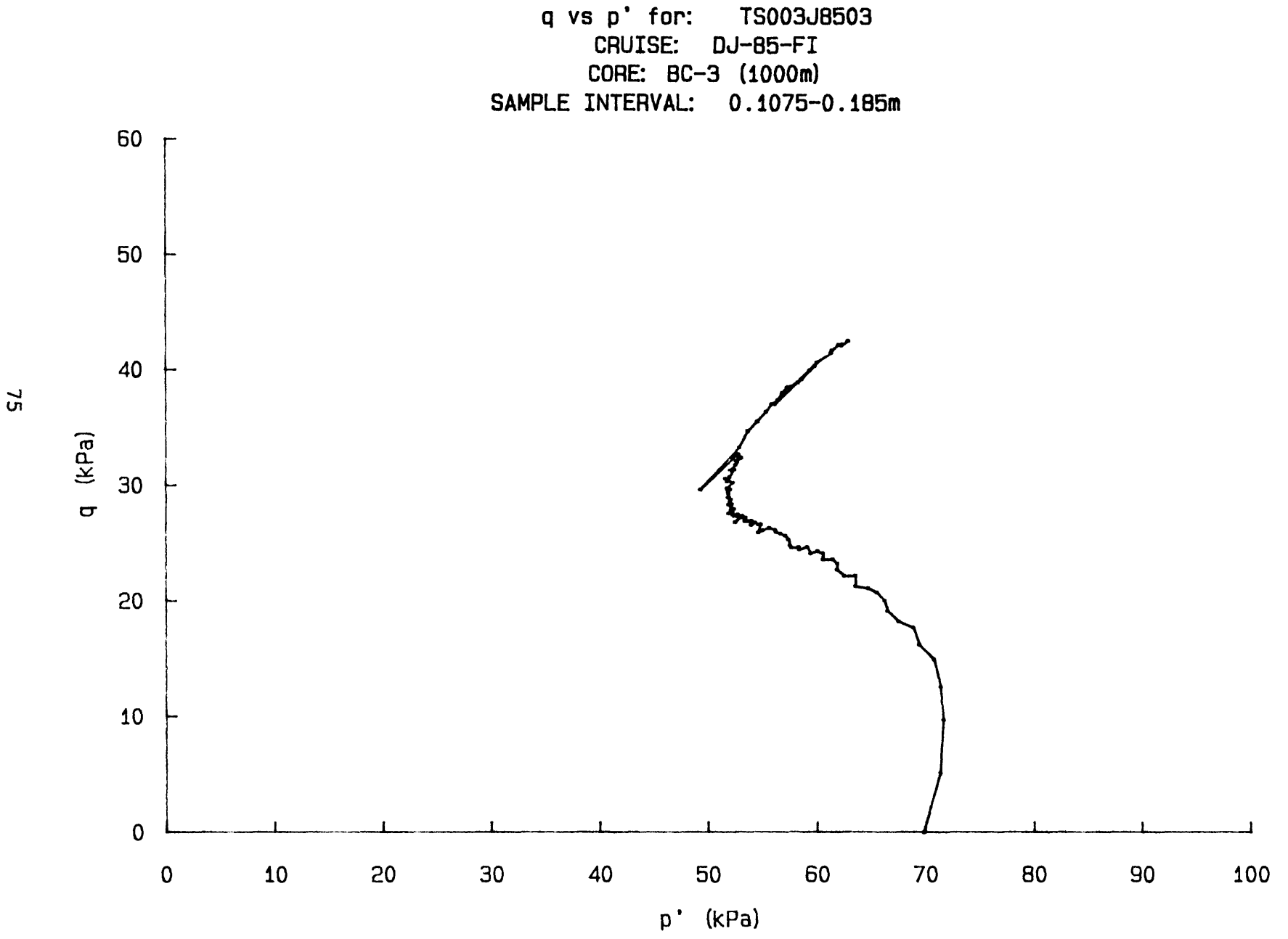
q vs p' for: TS003J8503
CRUISE: DJ-85-FI
CORE: BC-3 (1000m)
SAMPLE INTERVAL: 0.1075-0.185m
q (kPa)
p' (kPa)
0
10
20
30
40
50
60
70
80
90
100

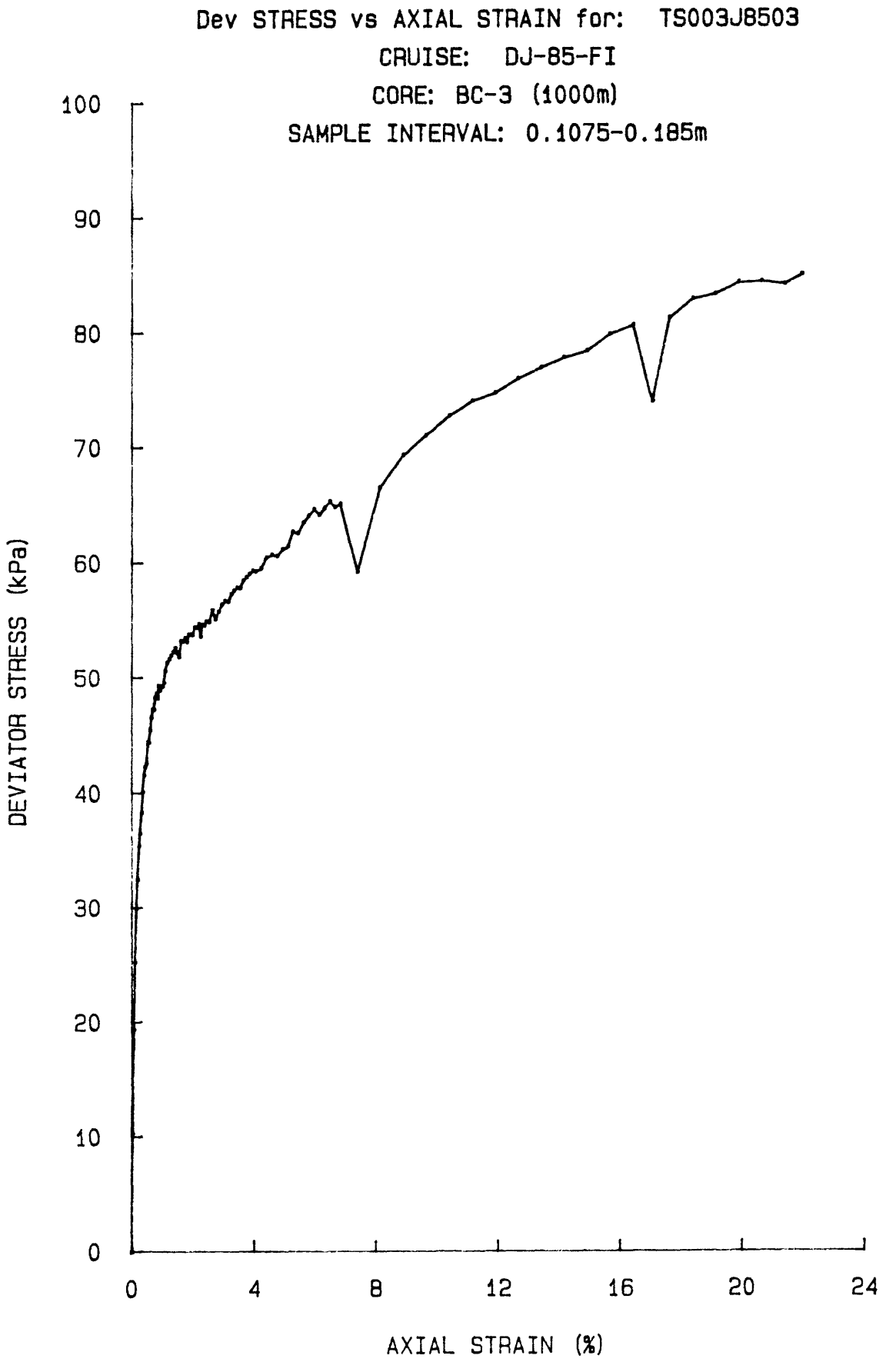
Dev STRESS vs AXIAL STRAIN for: TS003J8503
CRUISE: DJ-85-FI
CORE: BC-3 (1000m)
SAMPLE INTERVAL: 0.1075-0.185m
DEVIATOR STRESS (kPa)
100
90
80
70
60
50
40
30
20
10
0
0
4
8
12
16
20
24
AXIAL STRAIN (%)

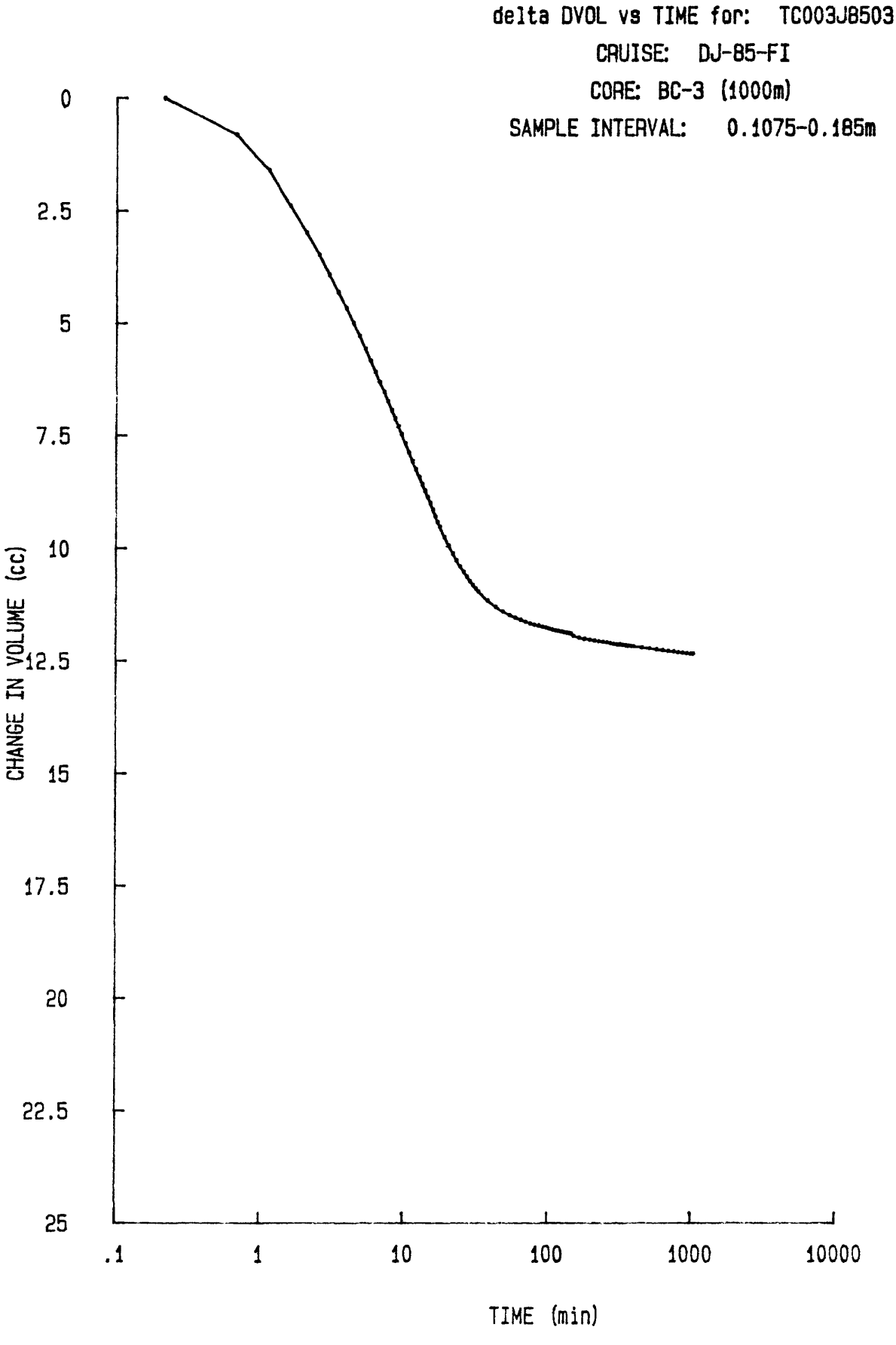
delta DVOL vs TIME for: TC003J8503
CRUISE: DJ-85-FI
CORE: BC-3 (1000m)
SAMPLE INTERVAL: 0.1075-0.185m
0
2.5
5
7.5
10
12.5
15
17.5
20
22.5
25
CHANGE IN VOLUME (cc)
.1
1
10
100
1000
10000
TIME (min)

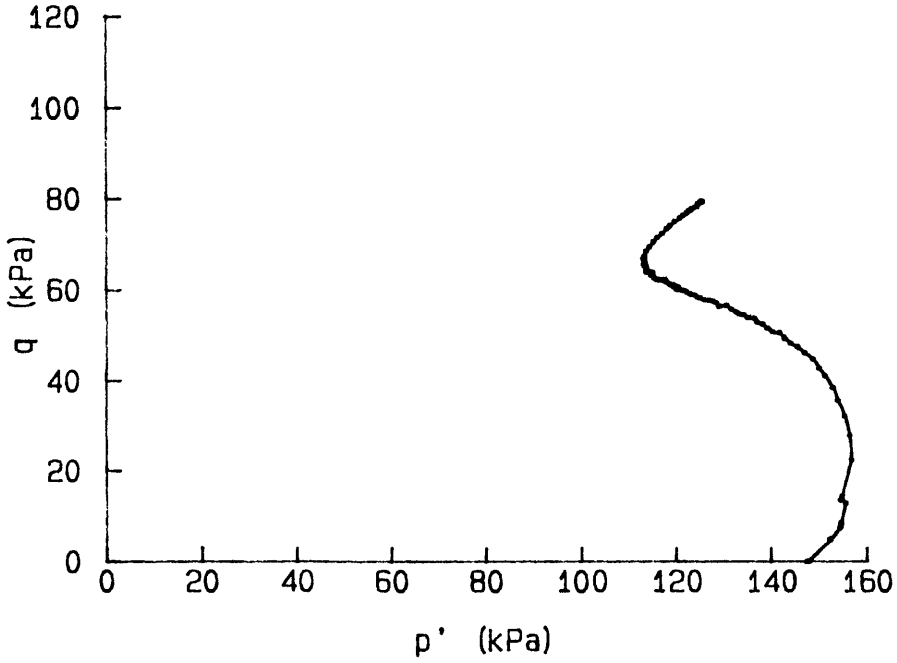

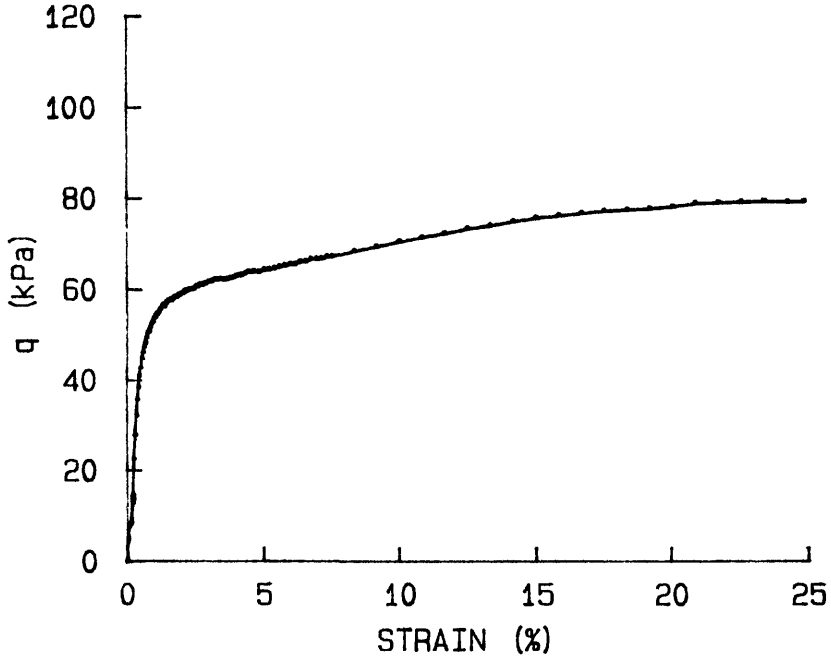

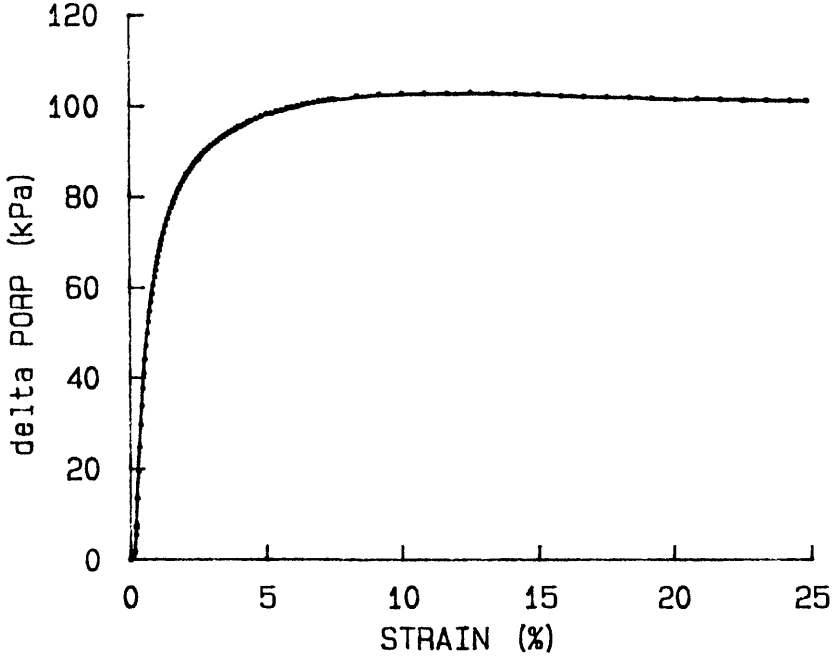

q vs p'
q vs AXIAL STRAIN
delta PORP vs AXIAL STRAIN

graphs for: TS002J8503
CRUISE: DJ-85-FI
CORE: BC-3 (1000m)
SAMPLE INTERVAL: 0.035-0.1075 m

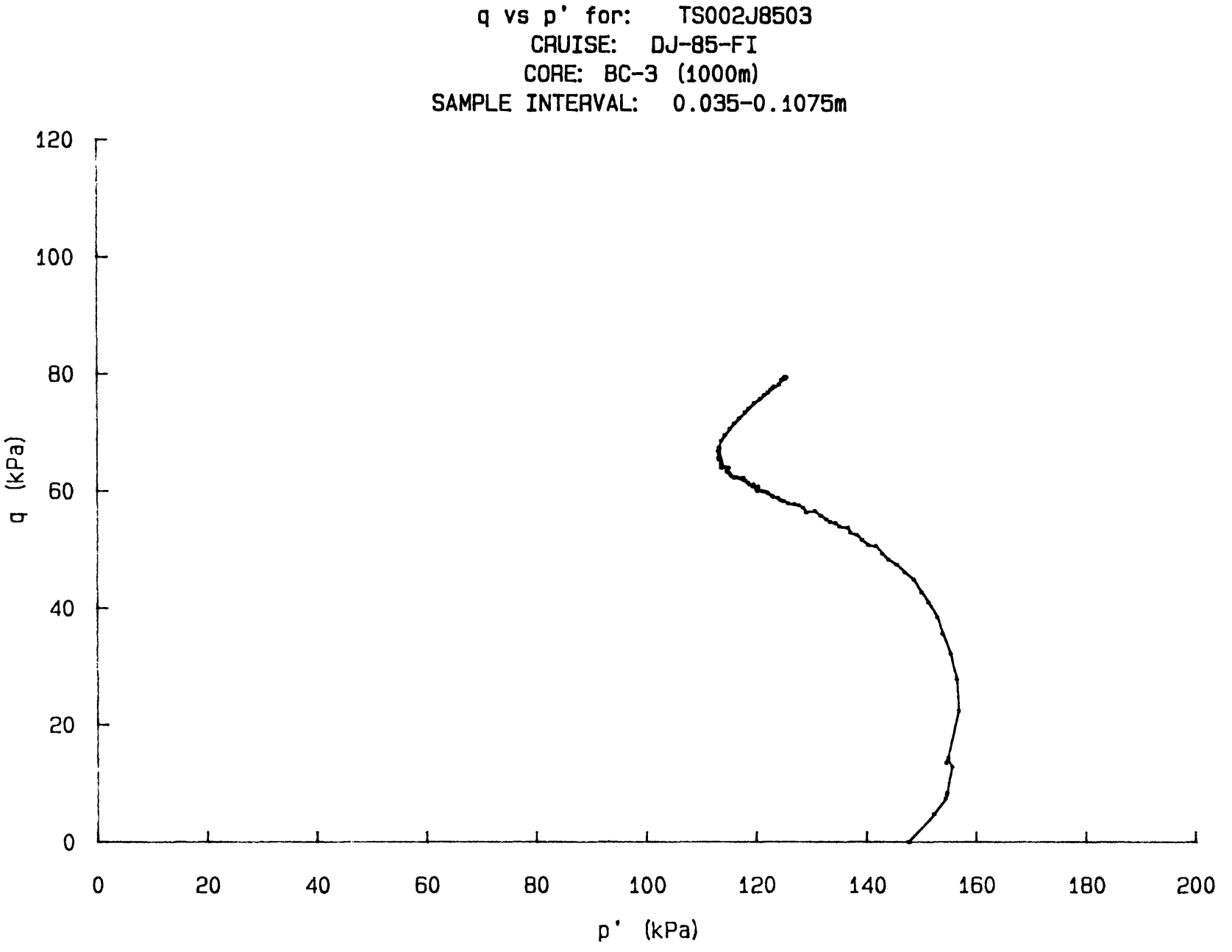
q vs p' for: TS002J8503
CRUISE: DJ-85-FI
CORE: BC-3 (1000m)
SAMPLE INTERVAL: 0.035-0.1075m
120
100
80
60
40
20
0
q (kPa)
0
20
40
60
80
100
120
140
160
180
200
p' (kPa)

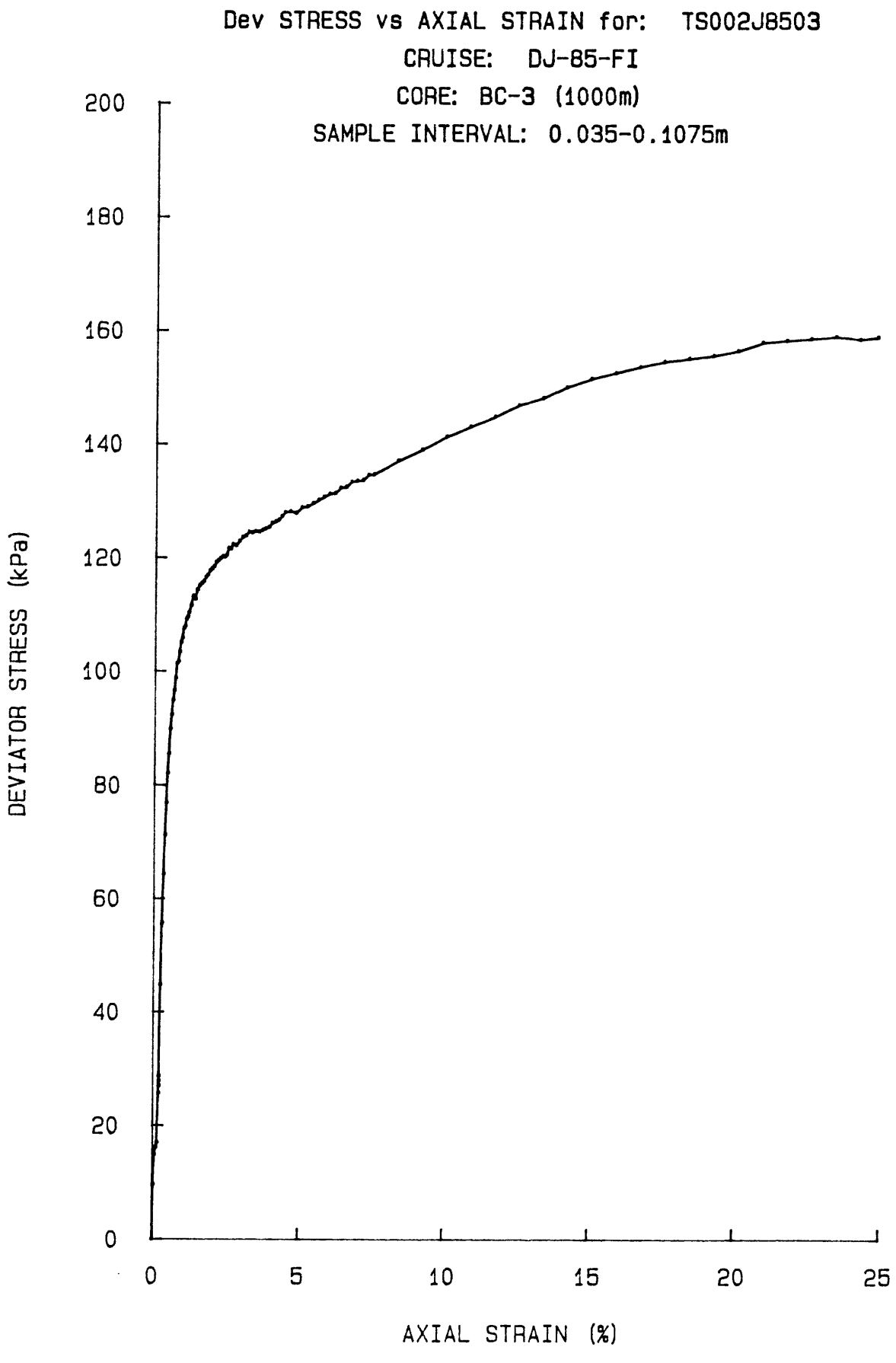
Dev STRESS vs AXIAL STRAIN for: TS002J8503
CRUISE: DJ-85-FI
CORE: BC-3 (1000m)
SAMPLE INTERVAL: 0.035-0.1075m
DEVIATOR STRESS (kPa)
200
180
160
140
120
100
80
60
40
20
0
0
5
10
15
20
25
AXIAL STRAIN (%)

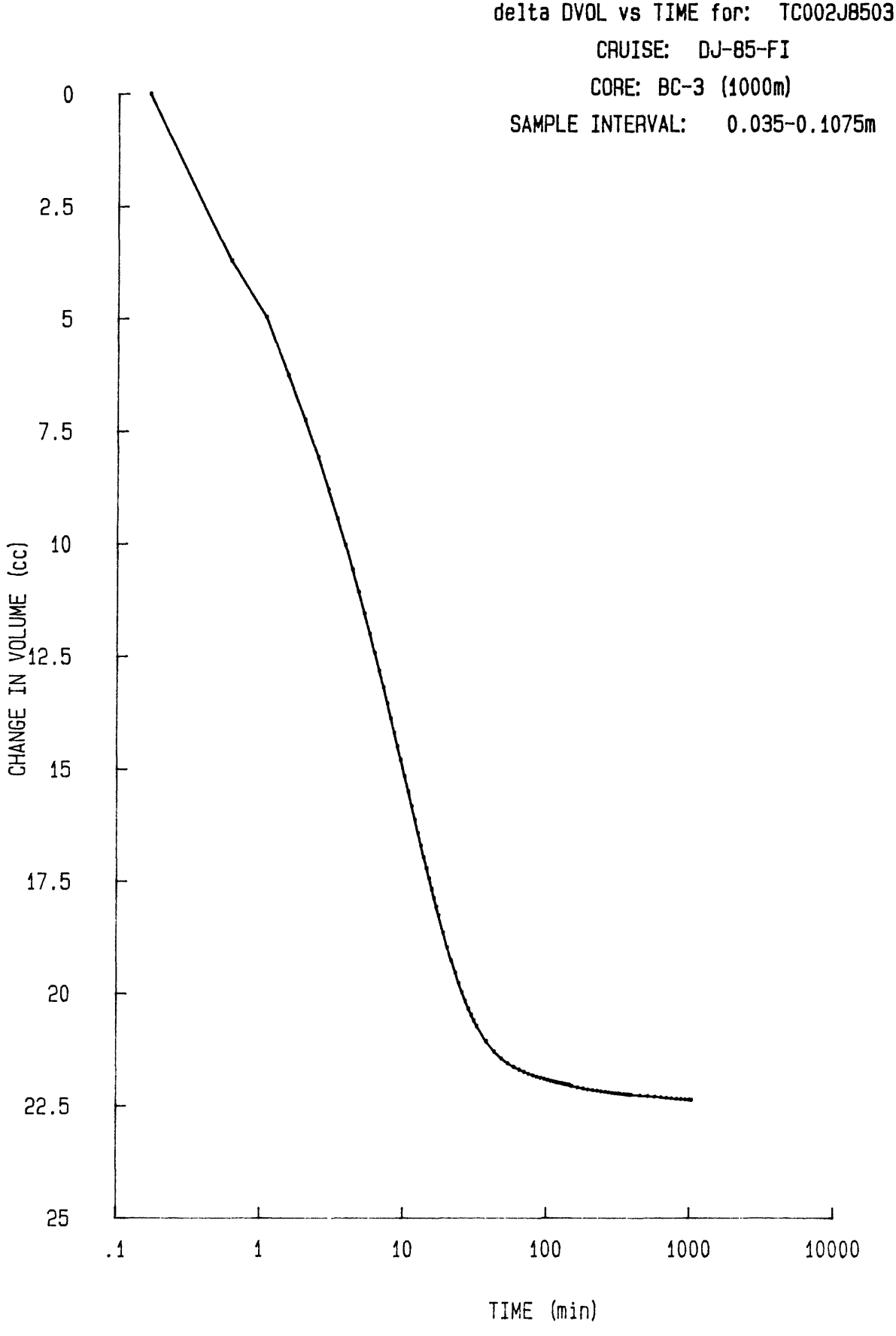
delta DVOL vs TIME for: TC002J8503
CRUISE: DJ-85-FI
CORE: BC-3 (1000m)
SAMPLE INTERVAL: 0.035-0.1075m
CHANGE IN VOLUME (cc)
0
2.5
5
7.5
10
12.5
15
17.5
20
22.5
25
.1
1
10
100
1000
10000
TIME (min)

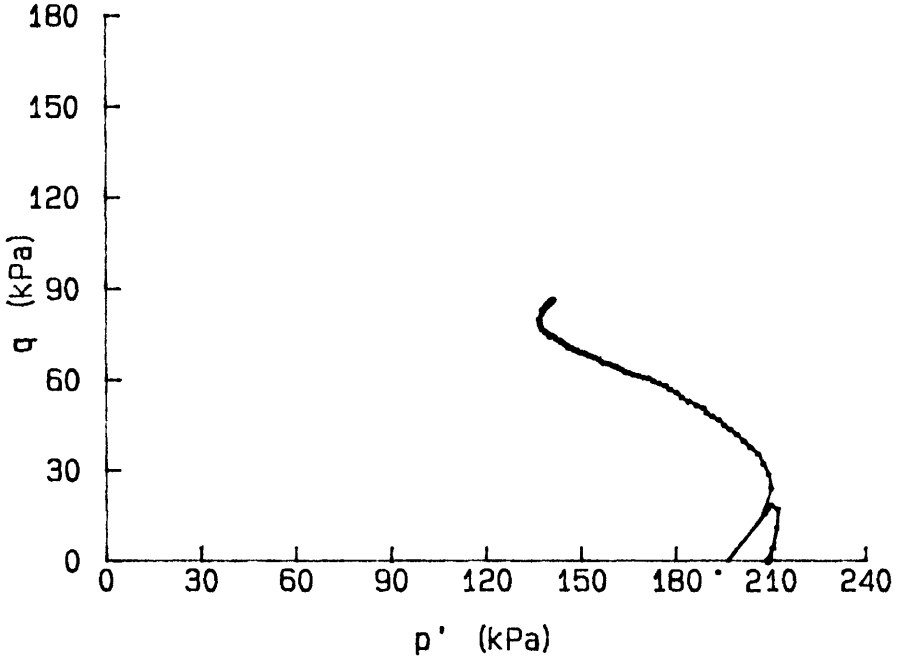

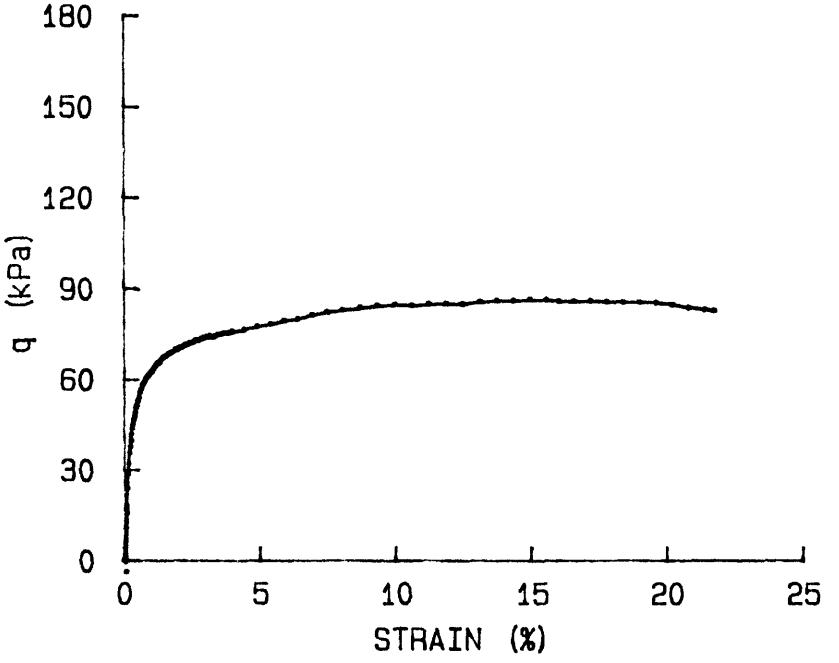

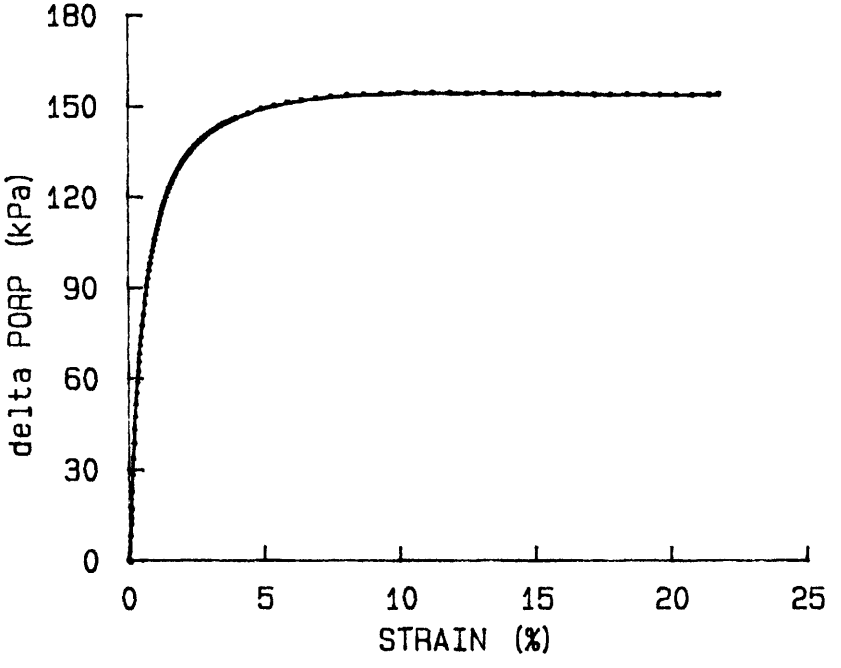

q vs p'
q vs AXIAL STRAIN
delta PORP vs AXIAL STRAIN

graphs for: TS001J8503
CRUISE: DJ-85-FI
CORE: BC-3 (1000m)
SAMPLE INTERVAL: 0.035-0.1075 m

q vs p' for: TS001J8503
CRUISE: DJ-85-FI
CORE: BC-3 (1000m)
SAMPLE INTERVAL: 0.035-0.1075m

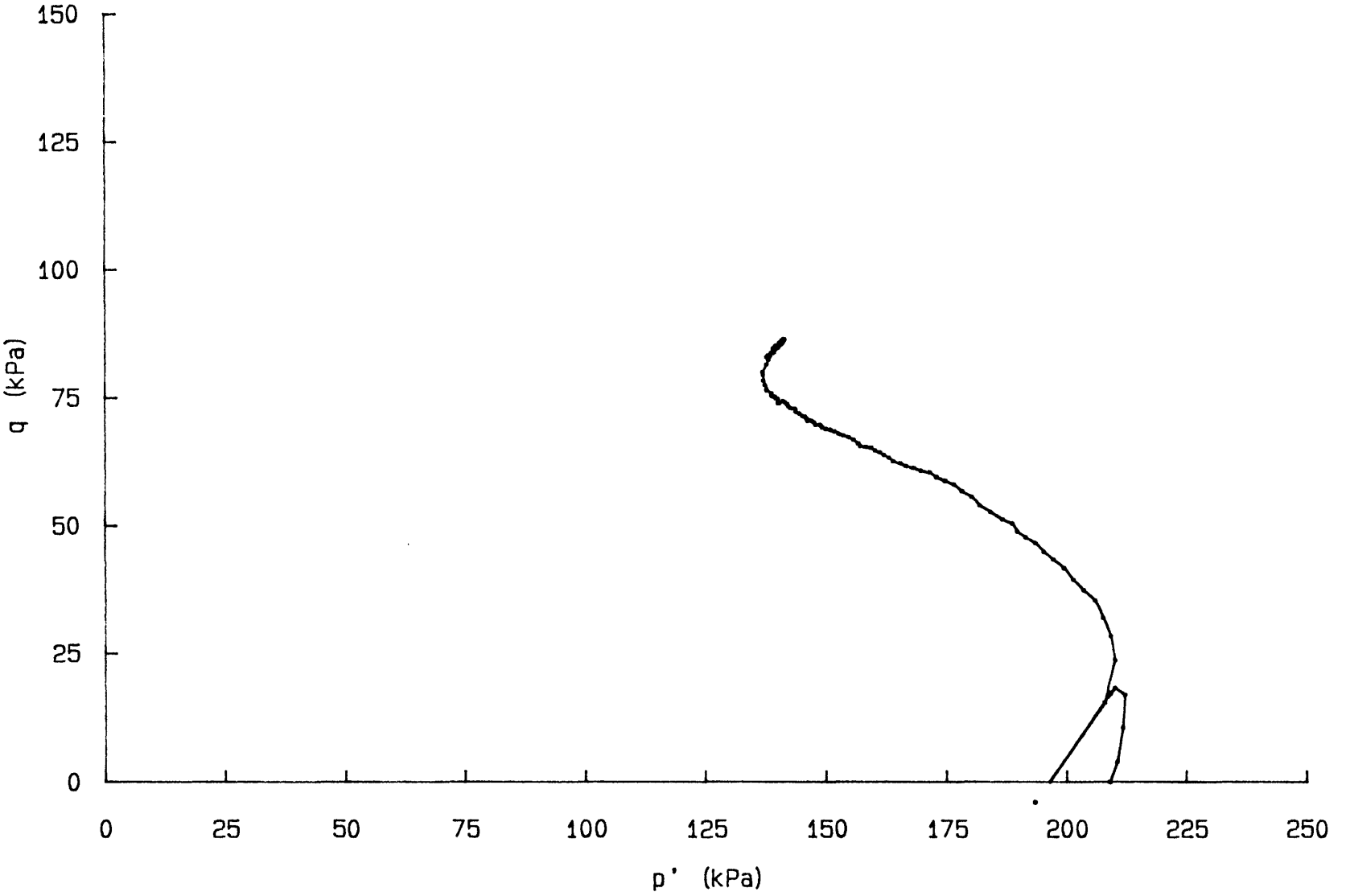

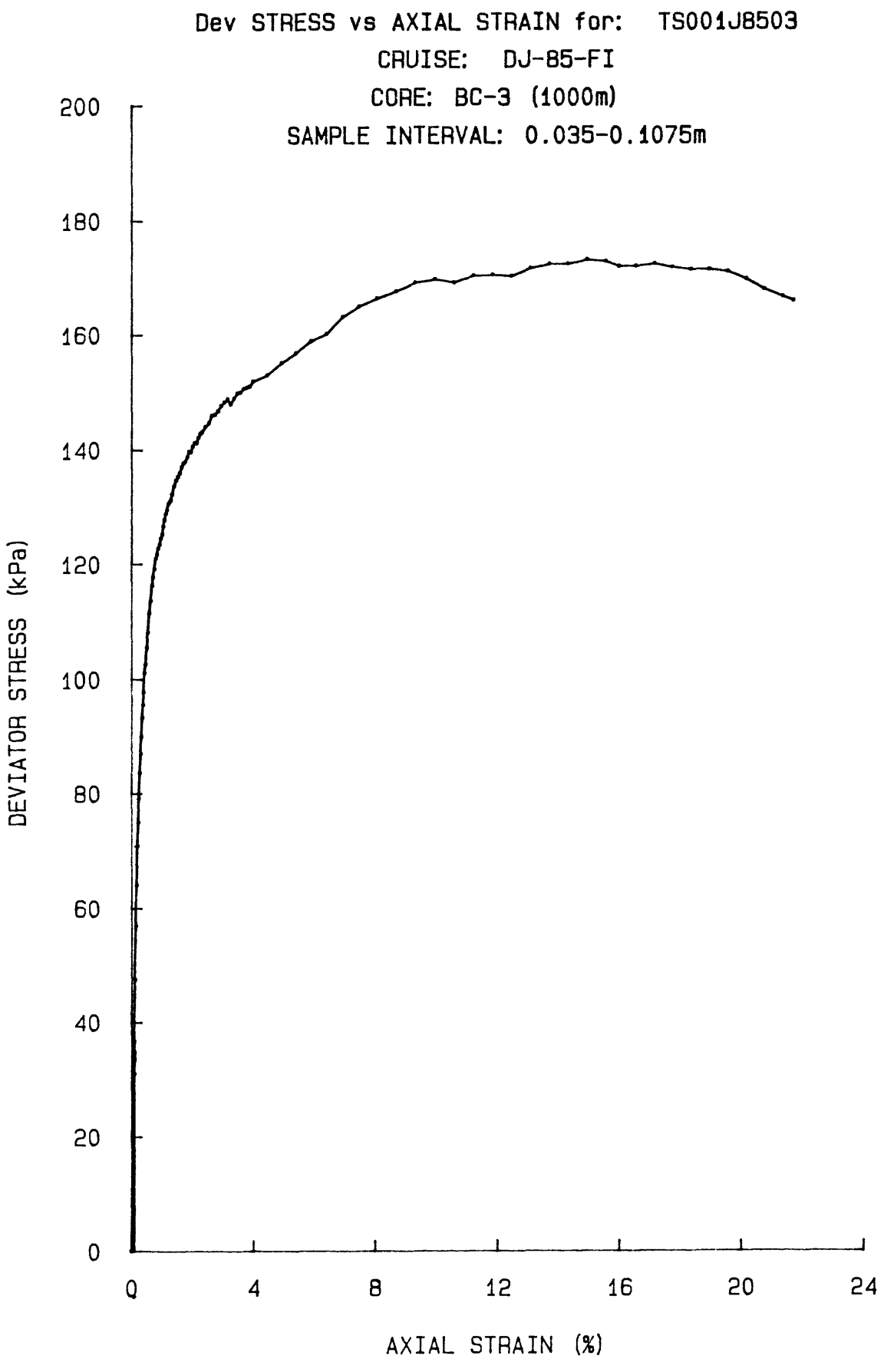
Dev STRESS vs AXIAL STRAIN for: TS001J8503
CRUISE: DJ-85-FI
CORE: BC-3 (1000m)
SAMPLE INTERVAL: 0.035-0.1075m
DEVIATOR STRESS (kPa)
200
180
160
140
120
100
80
60
40
20
0
0
4
8
12
16
20
24
AXIAL STRAIN (%)

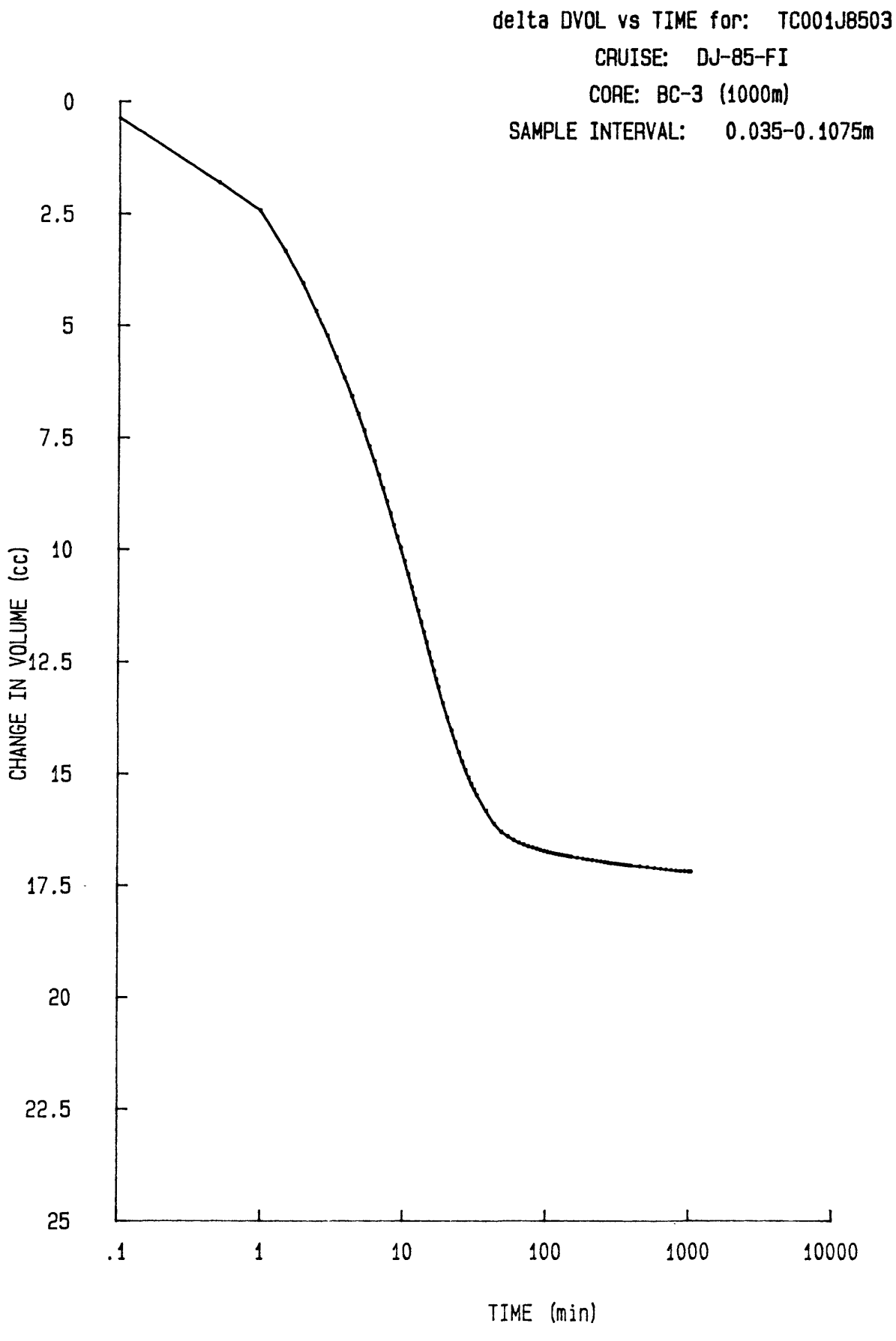
delta DVOL vs TIME for: TC001J8503
CRUISE: DJ-85-FI
CORE: BC-3 (1000m)
SAMPLE INTERVAL: 0.035-0.1075m
CHANGE IN VOLUME (cc)
0
2.5
5
7.5
10
12.5
15
17.5
20
22.5
25
.1
1
10
100
1000
10000
TIME (min)

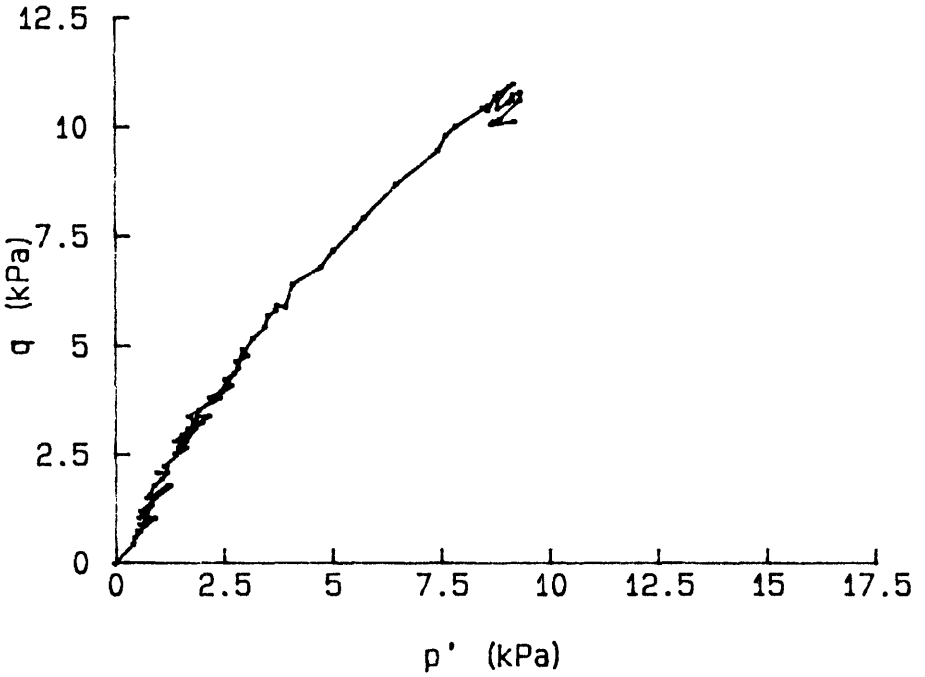

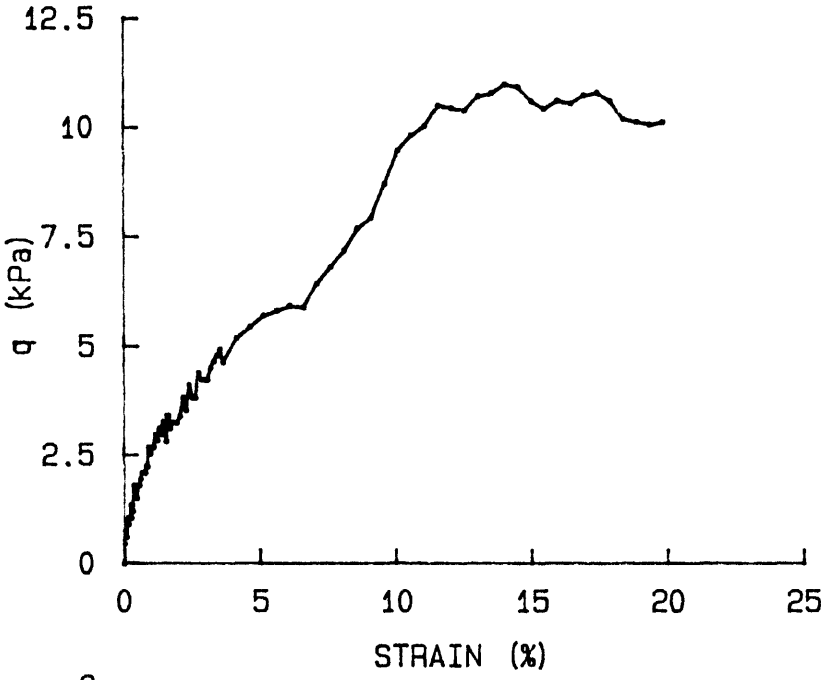

q vs p'
q vs AXIAL STRAIN
delta PORP vs AXIAL STRAIN

graphs for: TS012J8505
CRUISE: DJ-85-FI
CORE: BC-5 (1500m)
SAMPLE INTERVAL: 0.11-0.18 m

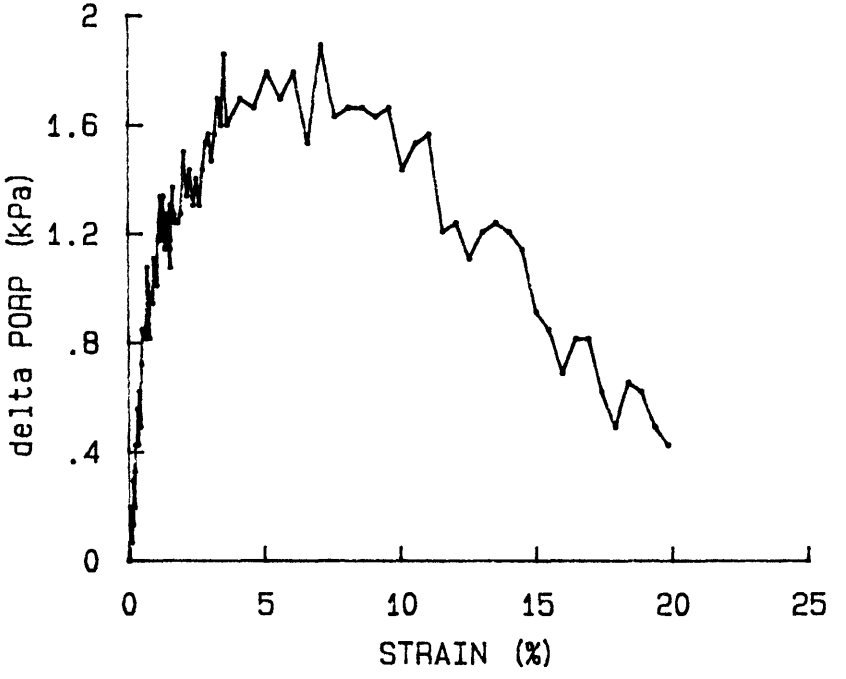

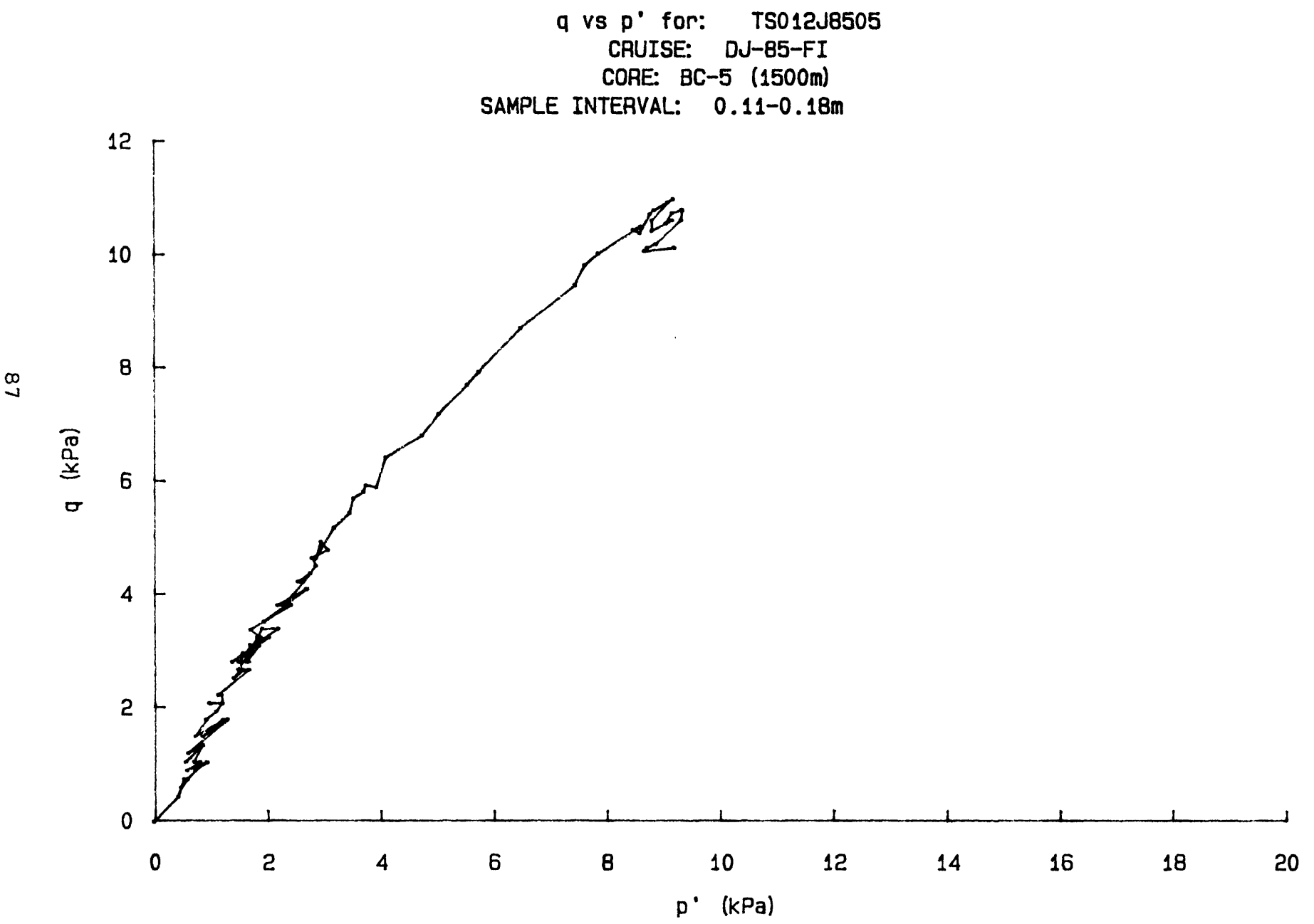
q vs p' for: TS012J8505
CRUISE: DJ-85-FI
CORE: BC-5 (1500m)
SAMPLE INTERVAL: 0.11-0.18m
q (kPa)
p' (kPa)
0
2
4
6
8
10
12
14
16
18
20

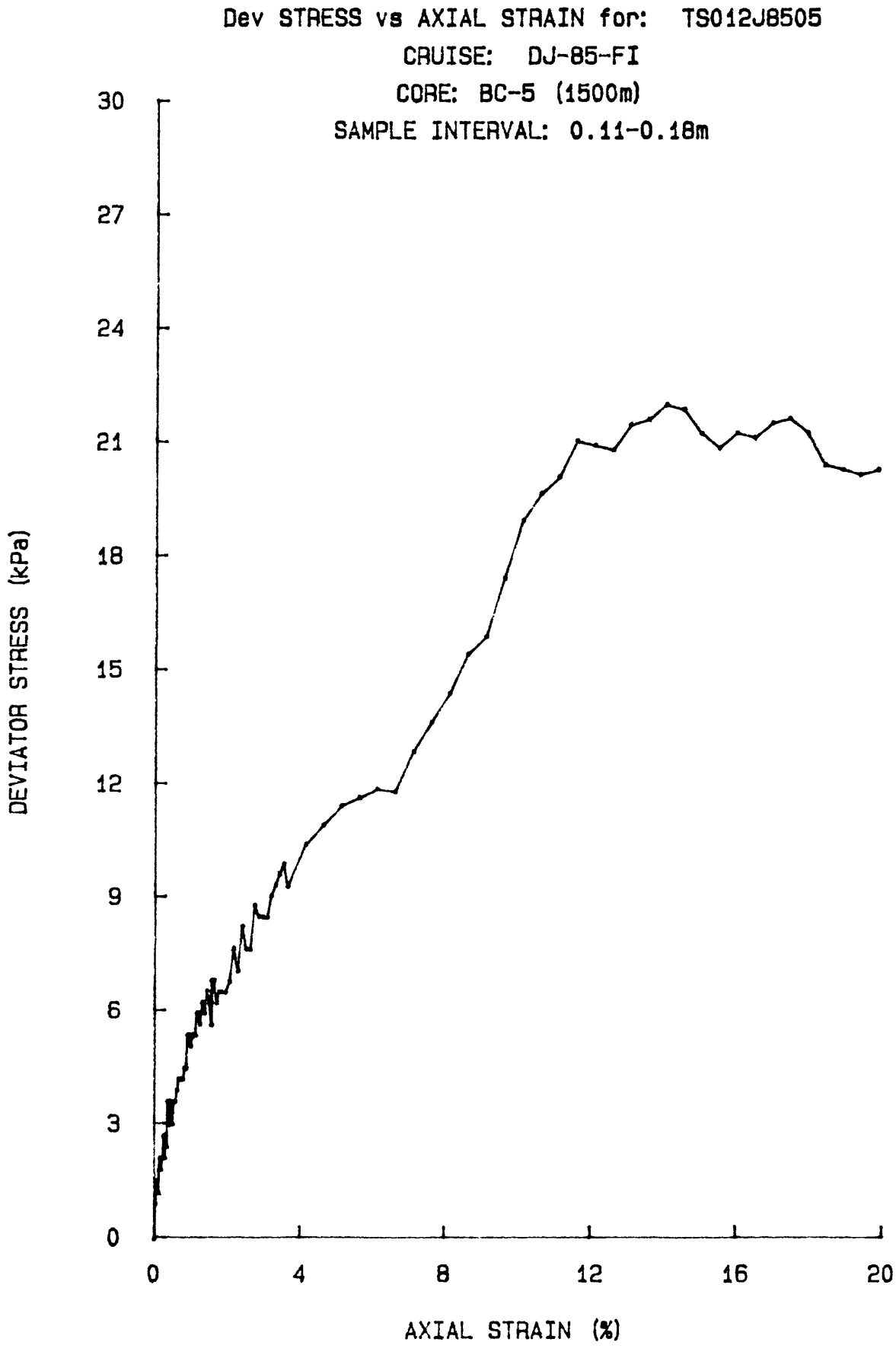
Dev STRESS vs AXIAL STRAIN for: TS012J8505
CRUISE: DJ-85-FI
CORE: BC-5 (1500m)
SAMPLE INTERVAL: 0.11-0.18m
DEVIATOR STRESS (kPa)
30
27
24
21
18
15
12
9
6
3
0
0
4
8
12
16
20
AXIAL STRAIN (%)

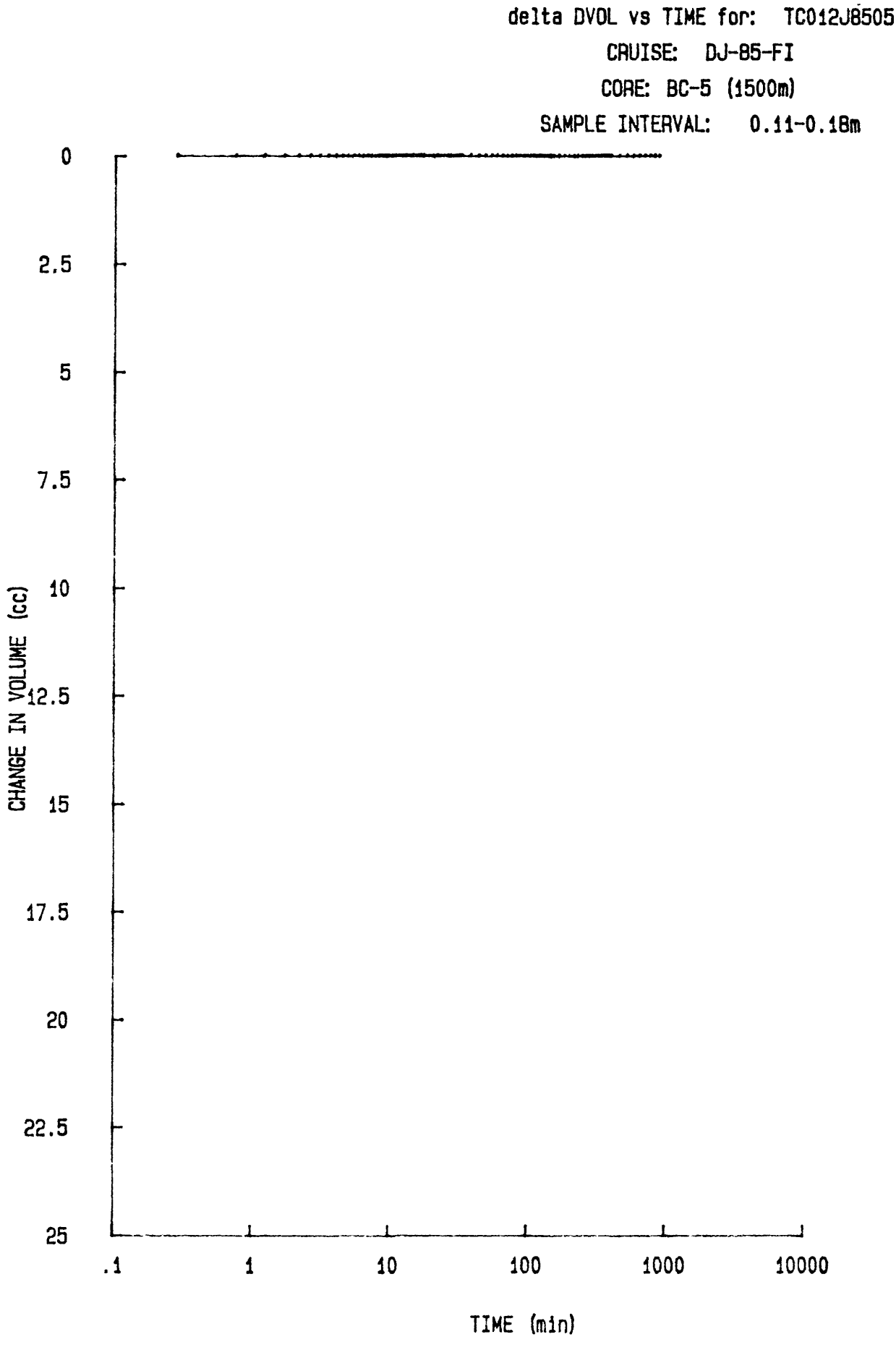
delta DVOL vs TIME for: TC012J8505
CRUISE: DJ-85-FI
CORE: BC-5 (1500m)
SAMPLE INTERVAL: 0.11-0.18m
0
2.5
5
7.5
10
12.5
15
17.5
20
22.5
25
CHANGE IN VOLUME (cc)
.1
1
10
100
1000
10000
TIME (min)

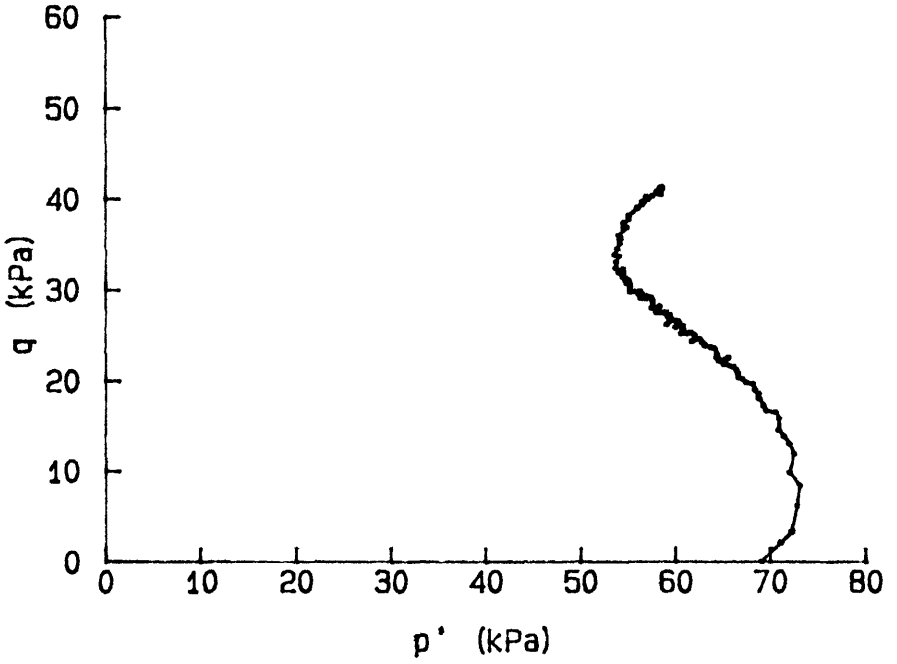

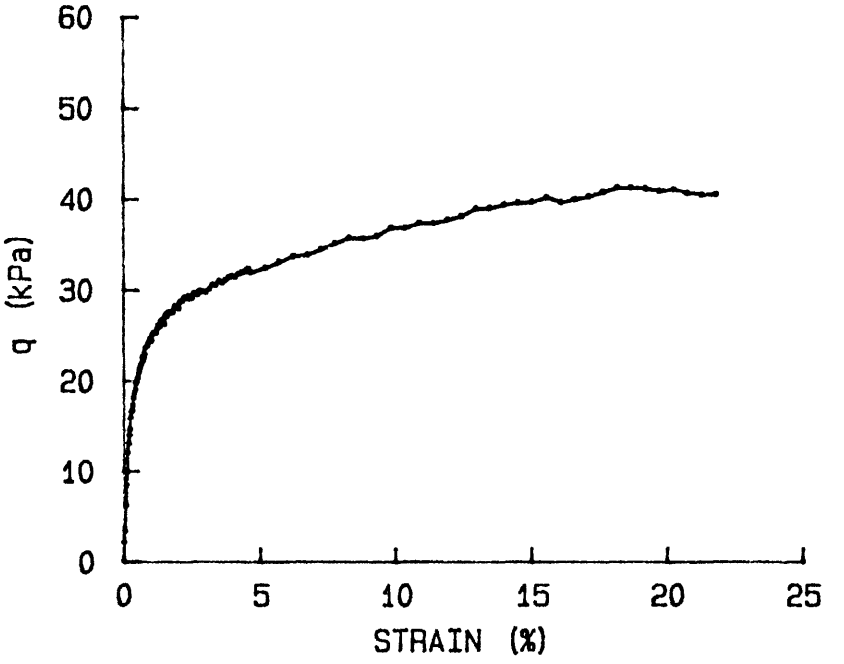

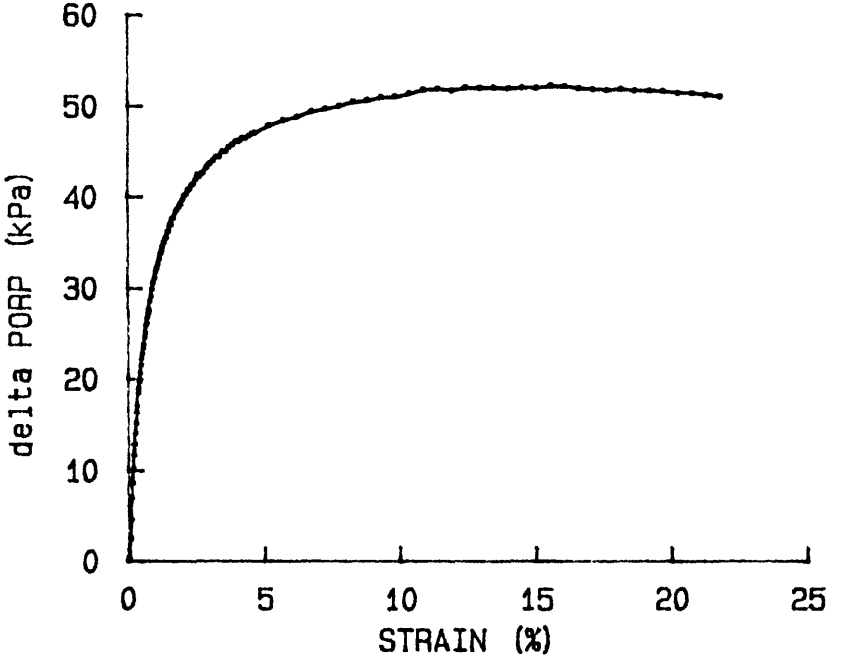

q vs p'
q vs AXIAL STRAIN
delta PORP vs AXIAL STRAIN

graphs for: TS011J8505
CRUISE: DJ-85-FI
CORE: BC-5 (1500m)
SAMPLE INTERVAL: 0.11-0.18 m

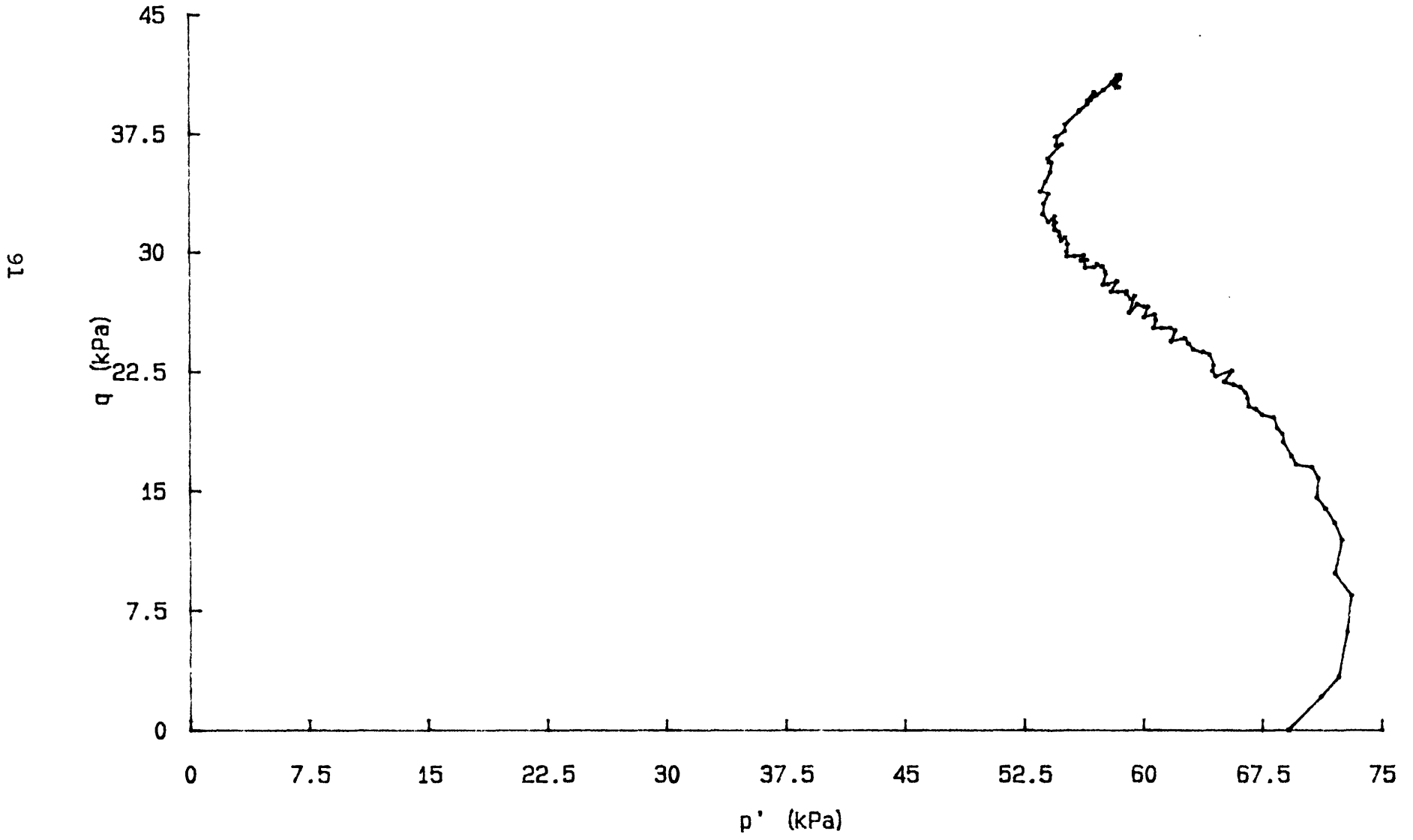
q vs p' for: TS011J8505
CRUISE: DJ-85-FI
CORE: BC-5 (1500m)
SAMPLE INTERVAL: 0.11-0.18m
45
37.5
30
22.5
15
7.5
0
q (kPa)
0
7.5
15
22.5
30
37.5
45
52.5
60
67.5
75
p' (kPa)

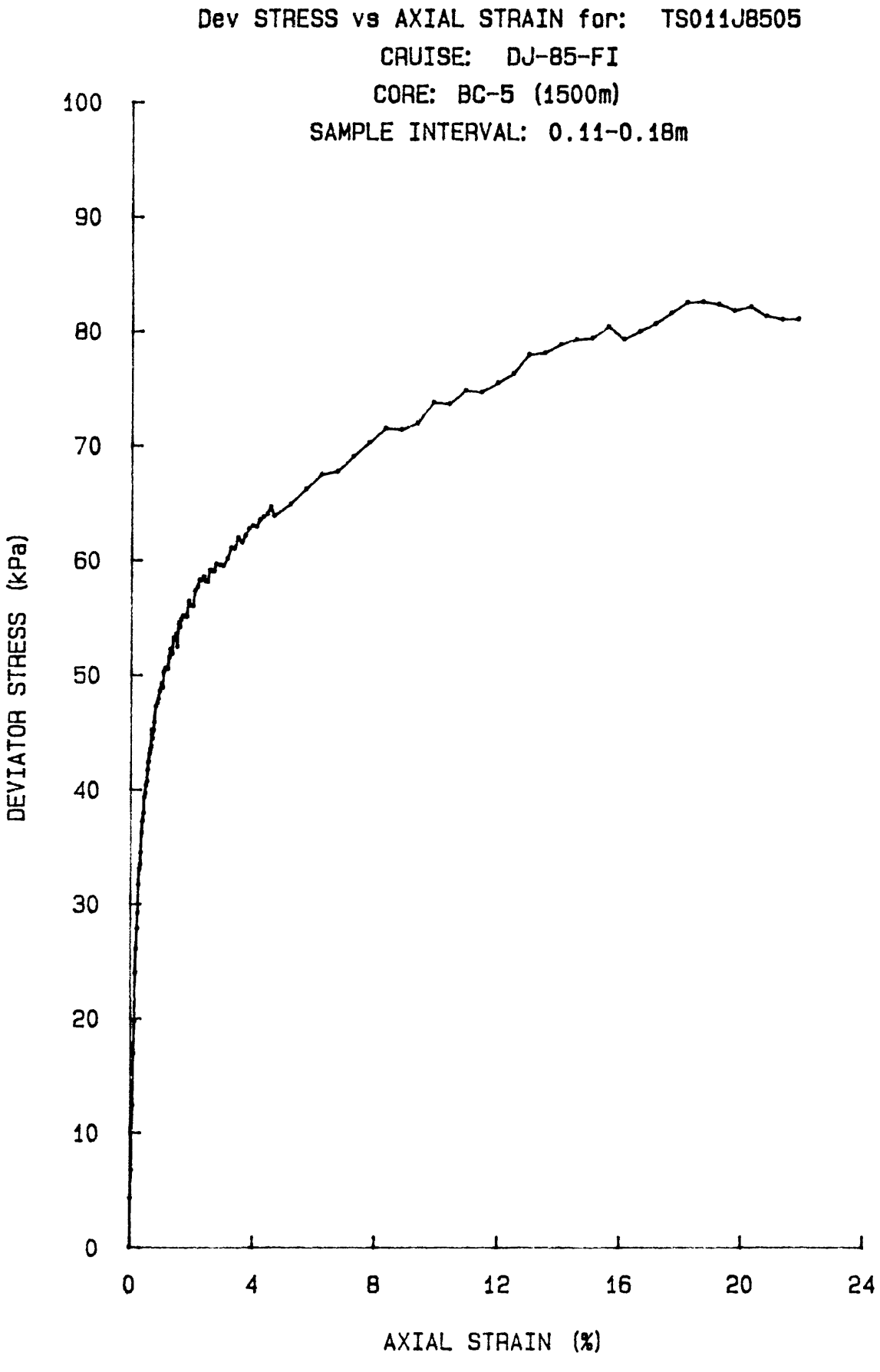
Dev STRESS vs AXIAL STRAIN for: TS011J8505
CRUISE: DJ-85-FI
CORE: BC-5 (1500m)
SAMPLE INTERVAL: 0.11-0.18m
DEVIATOR STRESS (kPa)
100
90
80
70
60
50
40
30
20
10
0
0
4
8
12
16
20
24
AXIAL STRAIN (%)

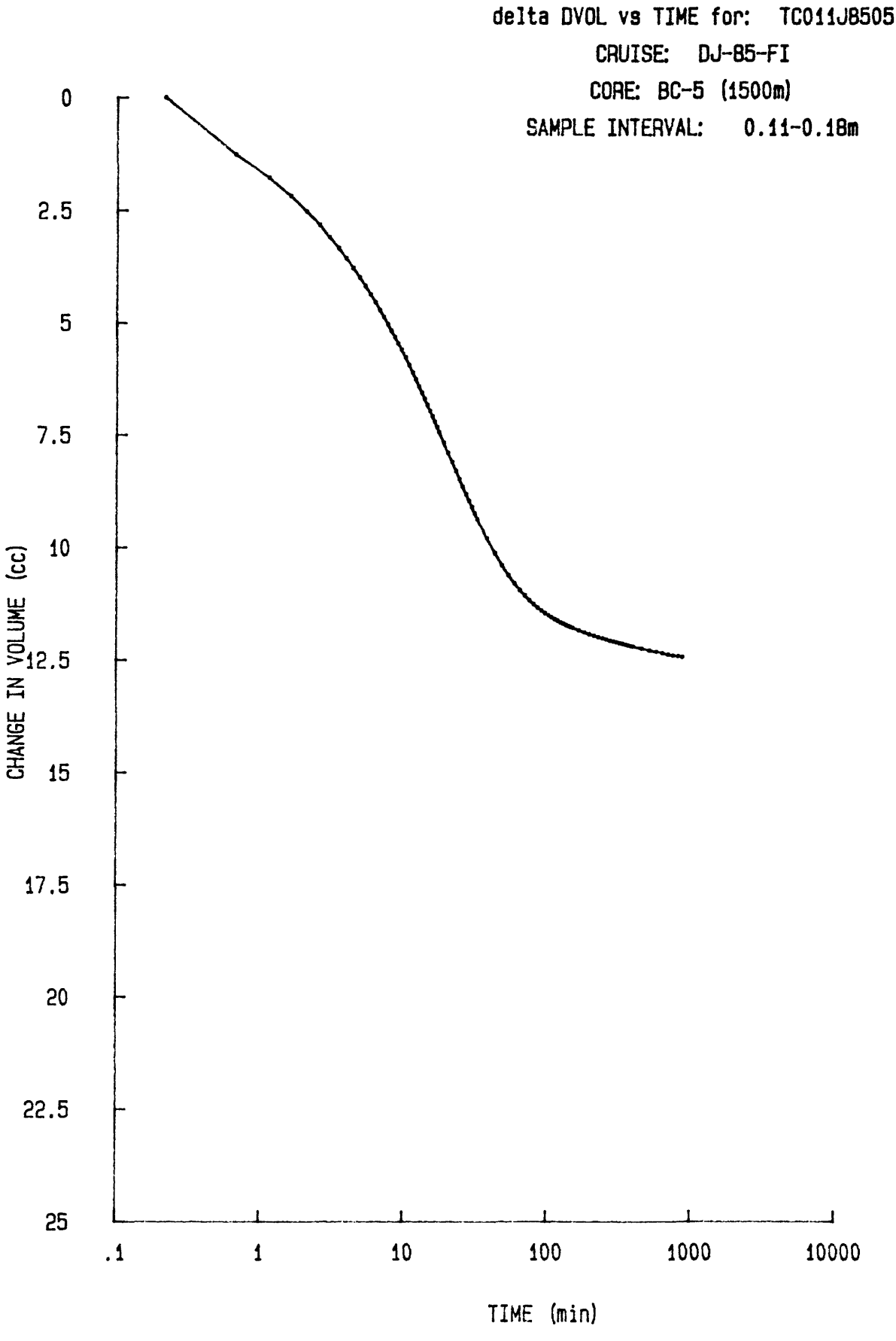
delta DVOL vs TIME for: TC011JB505
CRUISE: DJ-85-FI
CORE: BC-5 (1500m)
SAMPLE INTERVAL: 0.11-0.18m
CHANGE IN VOLUME (cc)
0
2.5
5
7.5
10
12.5
15
17.5
20
22.5
25
.1
1
10
100
1000
10000
TIME (min)

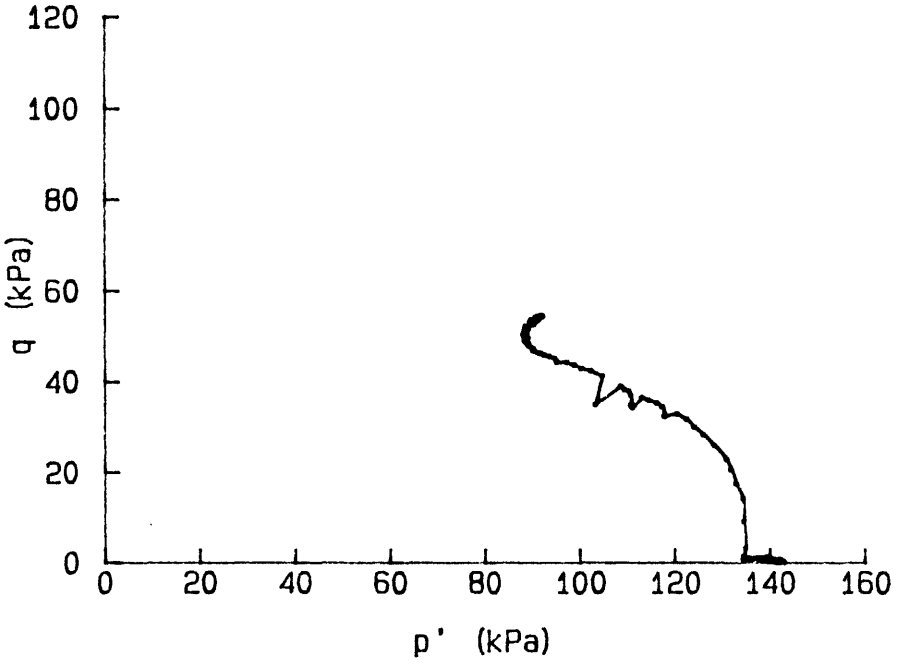

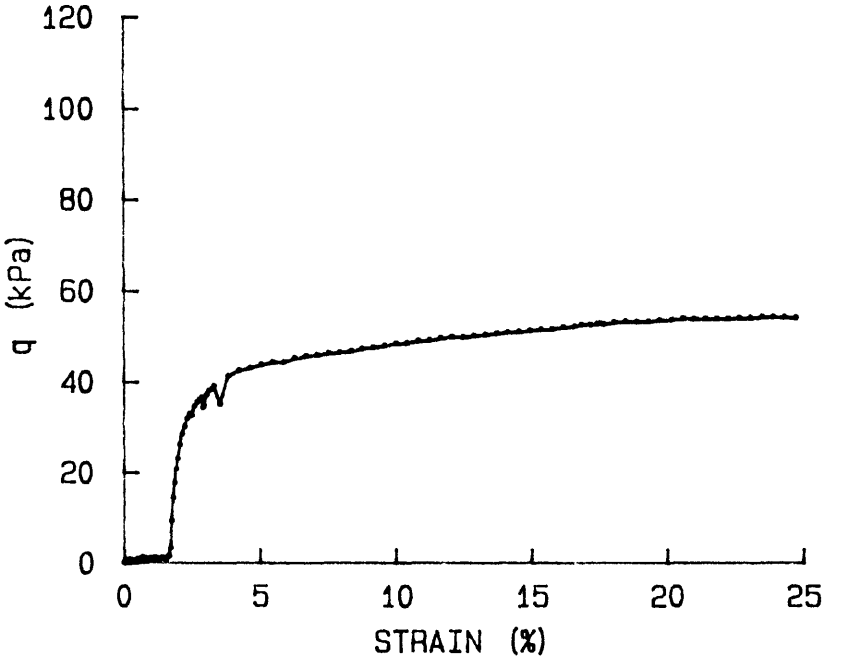

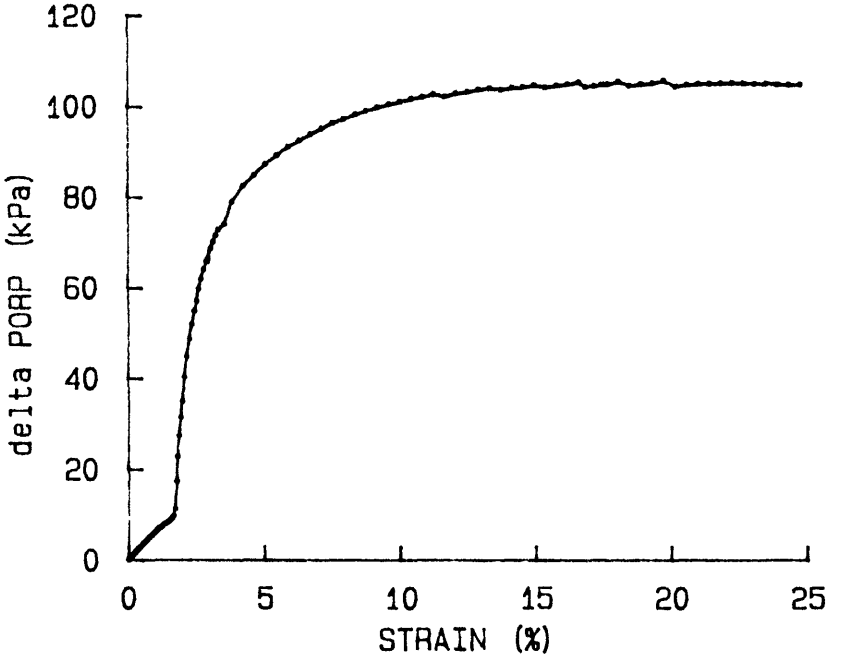

q vs p'
q vs AXIAL STRAIN
delta PORP vs AXIAL STRAIN

graphs for: TS010J8505
CRUISE: DJ-85-FI
CORE: BC-5 (1500m)
SAMPLE INTERVAL: 0.03-0.10 m

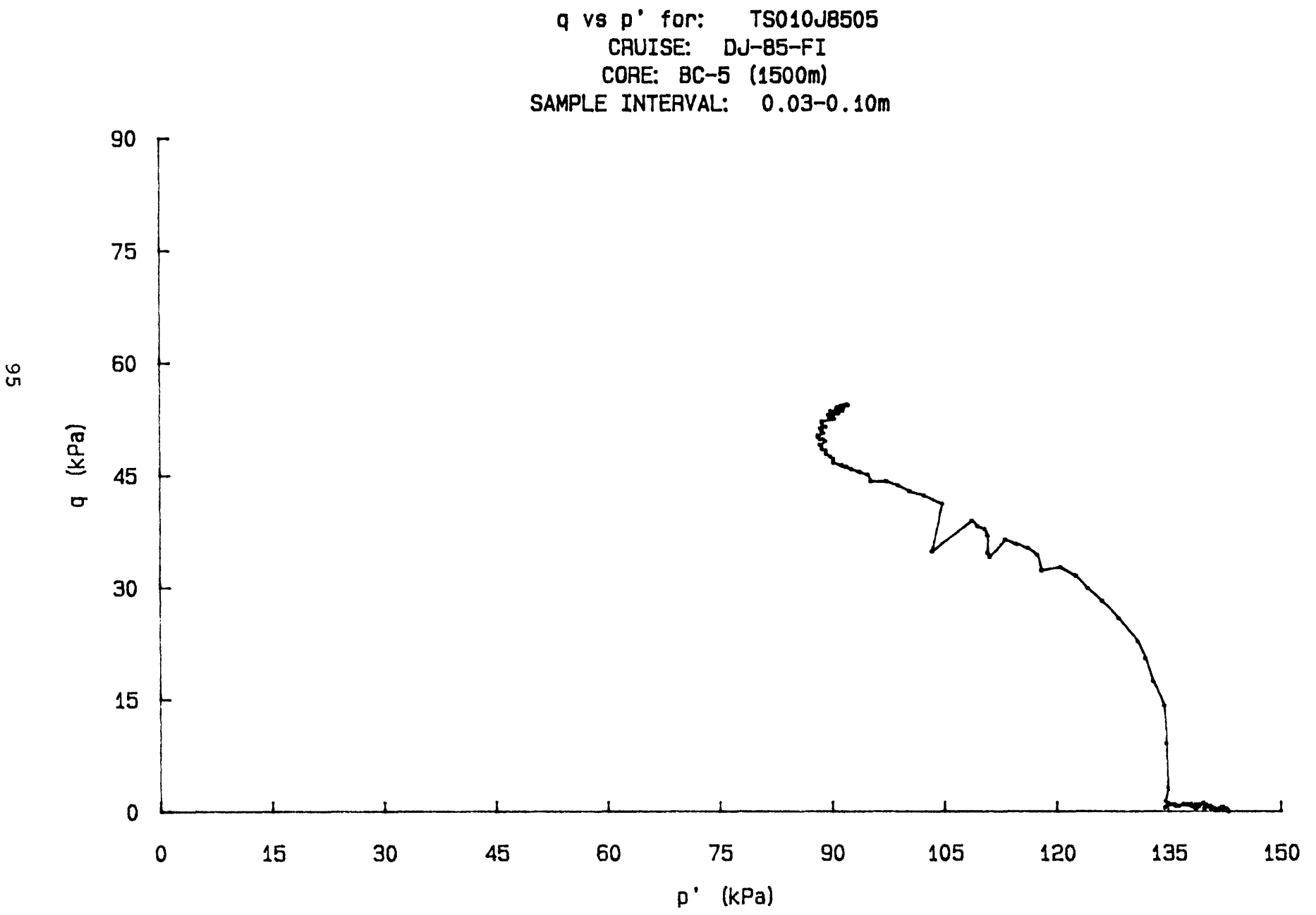
q vs p' for: TS010J8505
CRUISE: DJ-85-FI
CORE: BC-5 (1500m)
SAMPLE INTERVAL: 0.03-0.10m
q (kPa)
p' (kPa)
0
15
30
45
60
75
90
105
120
135
150

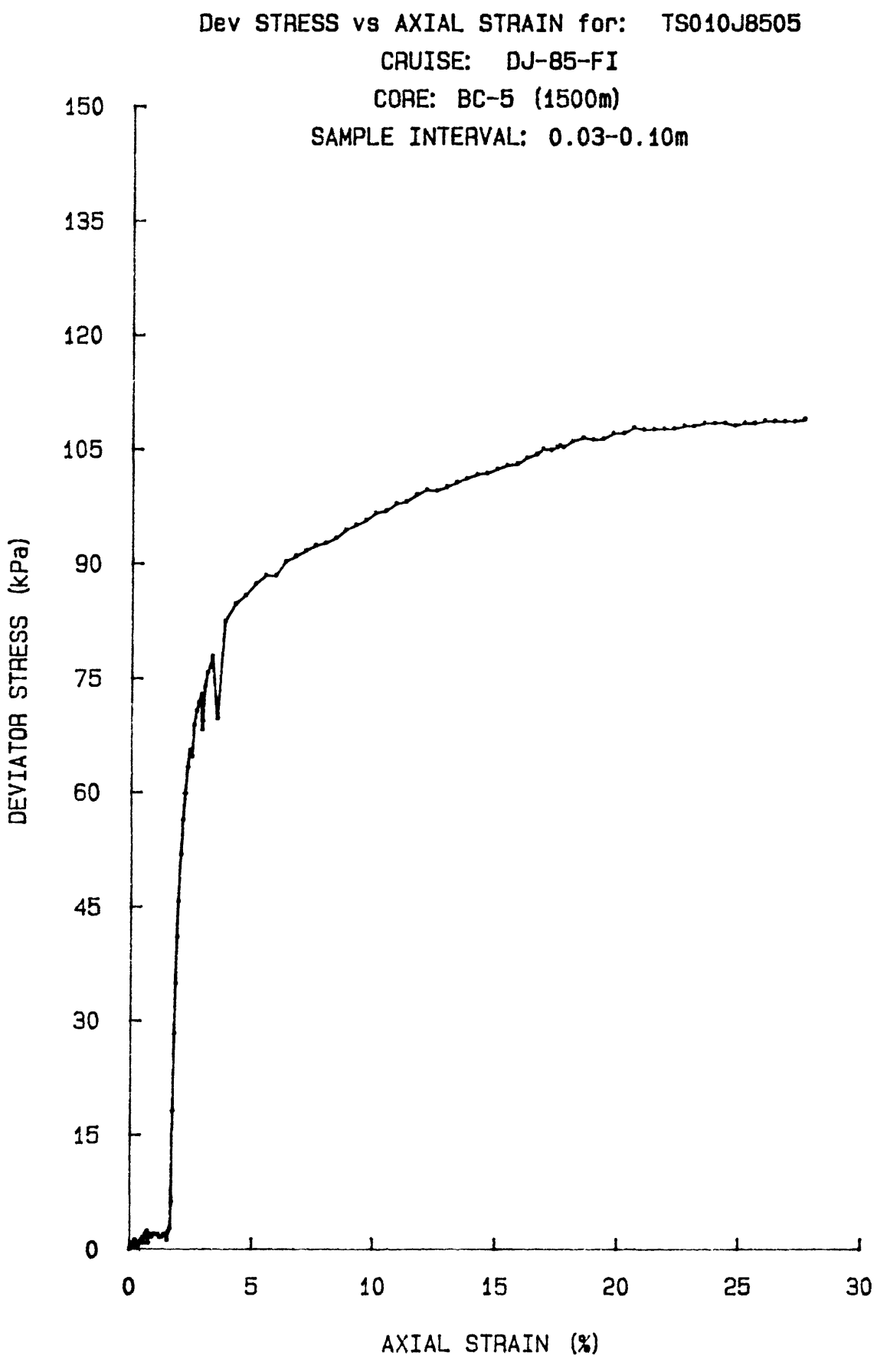
Dev STRESS vs AXIAL STRAIN for: TS010J8505
CRUISE: DJ-85-FI
CORE: BC-5 (1500m)
SAMPLE INTERVAL: 0.03-0.10m
DEVIATOR STRESS (kPa)
150
135
120
105
90
75
60
45
30
15
0
0
5
10
15
20
25
30
AXIAL STRAIN (%)

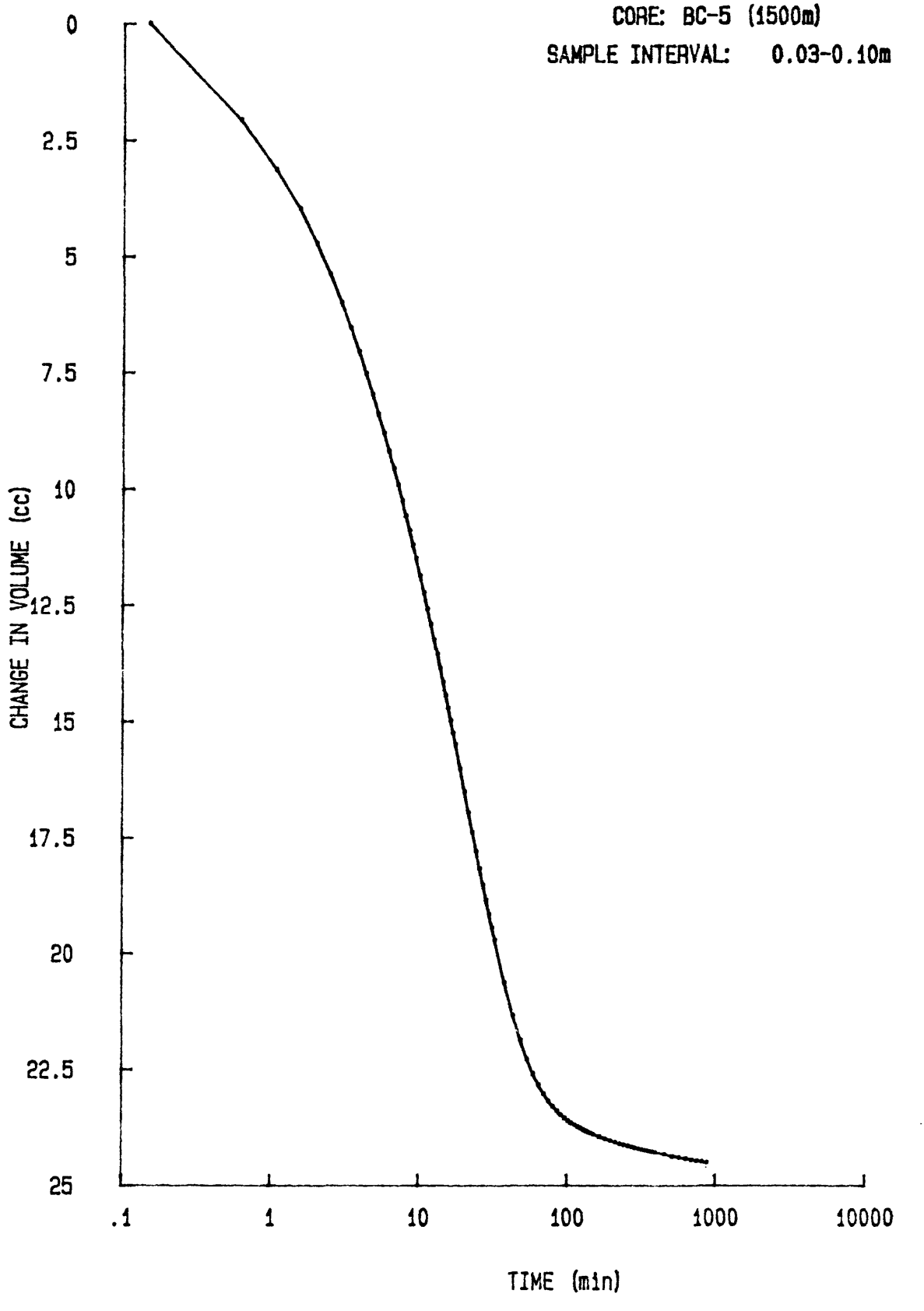
delta DVOL vs TIME for: TC010J8602
CRUISE: DJ-85-FI
CORE: BC-5 (1500m)
SAMPLE INTERVAL: 0.03-0.10m
CHANGE IN VOLUME (cc)
0
2.5
5
7.5
10
12.5
15
17.5
20
22.5
25
.1
1
10
100
1000
10000
TIME (min)

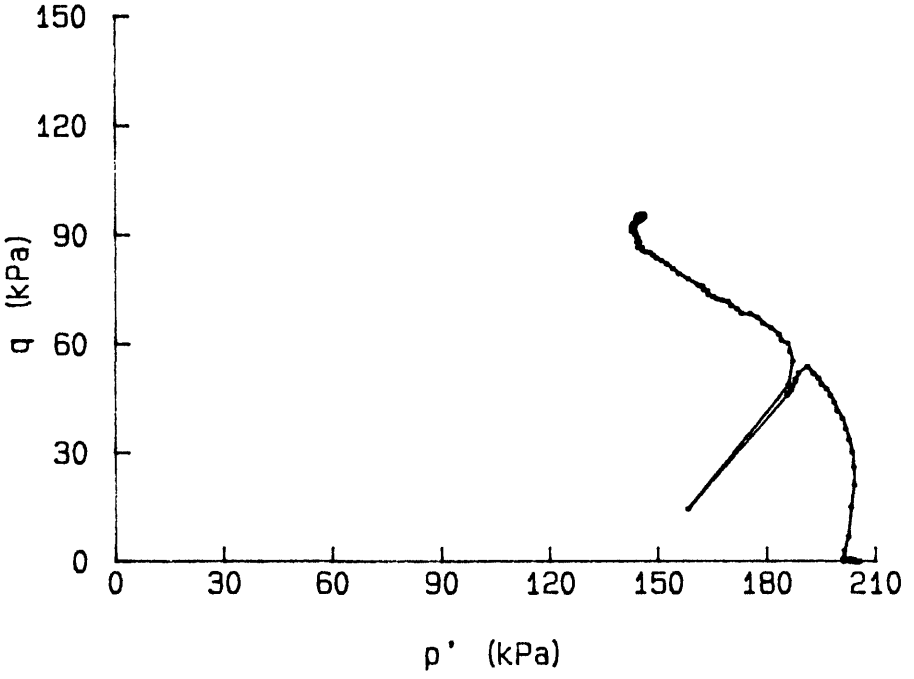

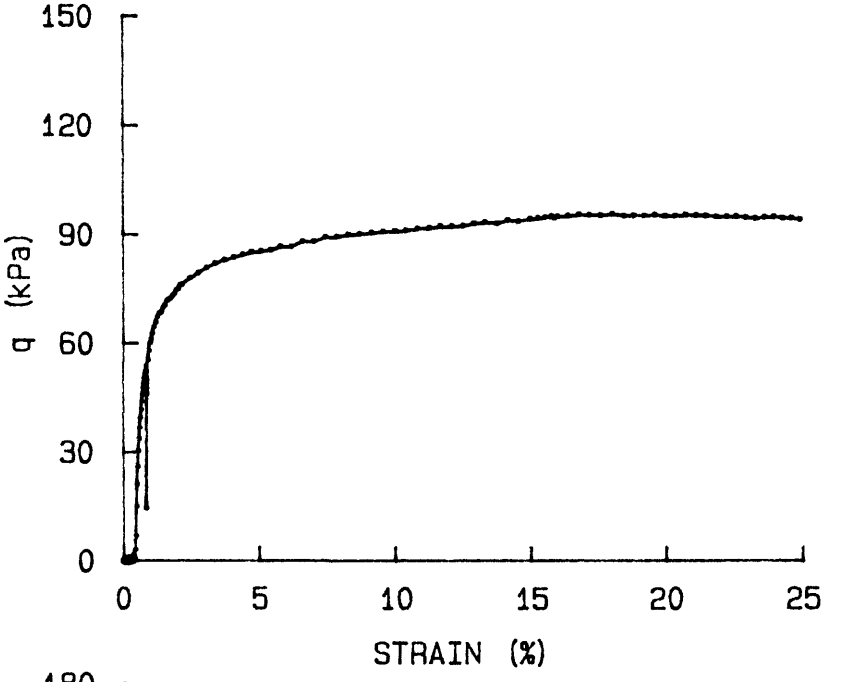

q vs p'
q vs AXIAL STRAIN
delta PORP vs AXIAL STRAIN

graphs for: TS009J8505
CRUISE: DJ-85-FI
CORE: BC-5 (1500m)
SAMPLE INTERVAL: 0.03-0.10 m

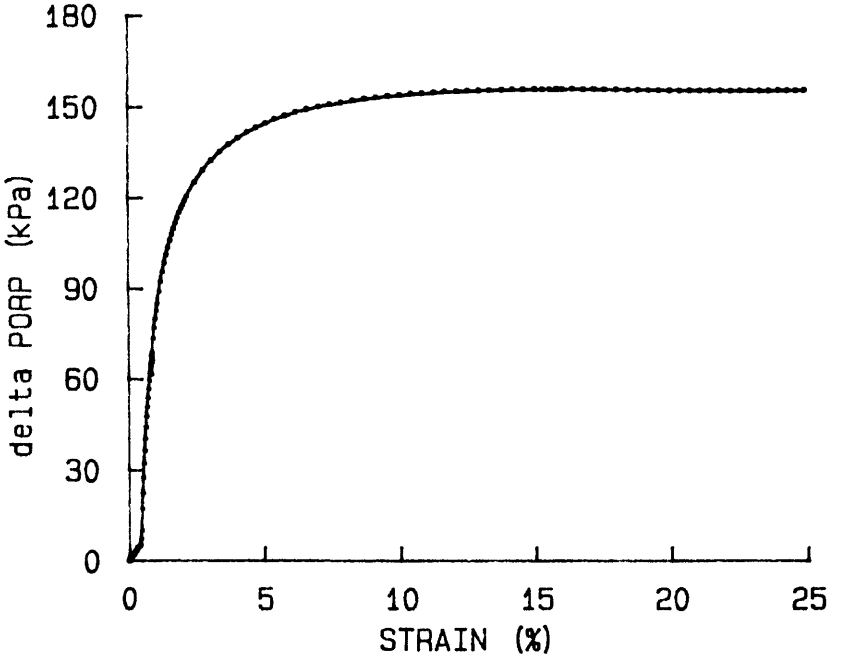

q vs p' for: TS009J8505
CRUISE: DJ-85-FI
CORE: BC-5 (1500m)
SAMPLE INTERVAL: 0.03-0.10m

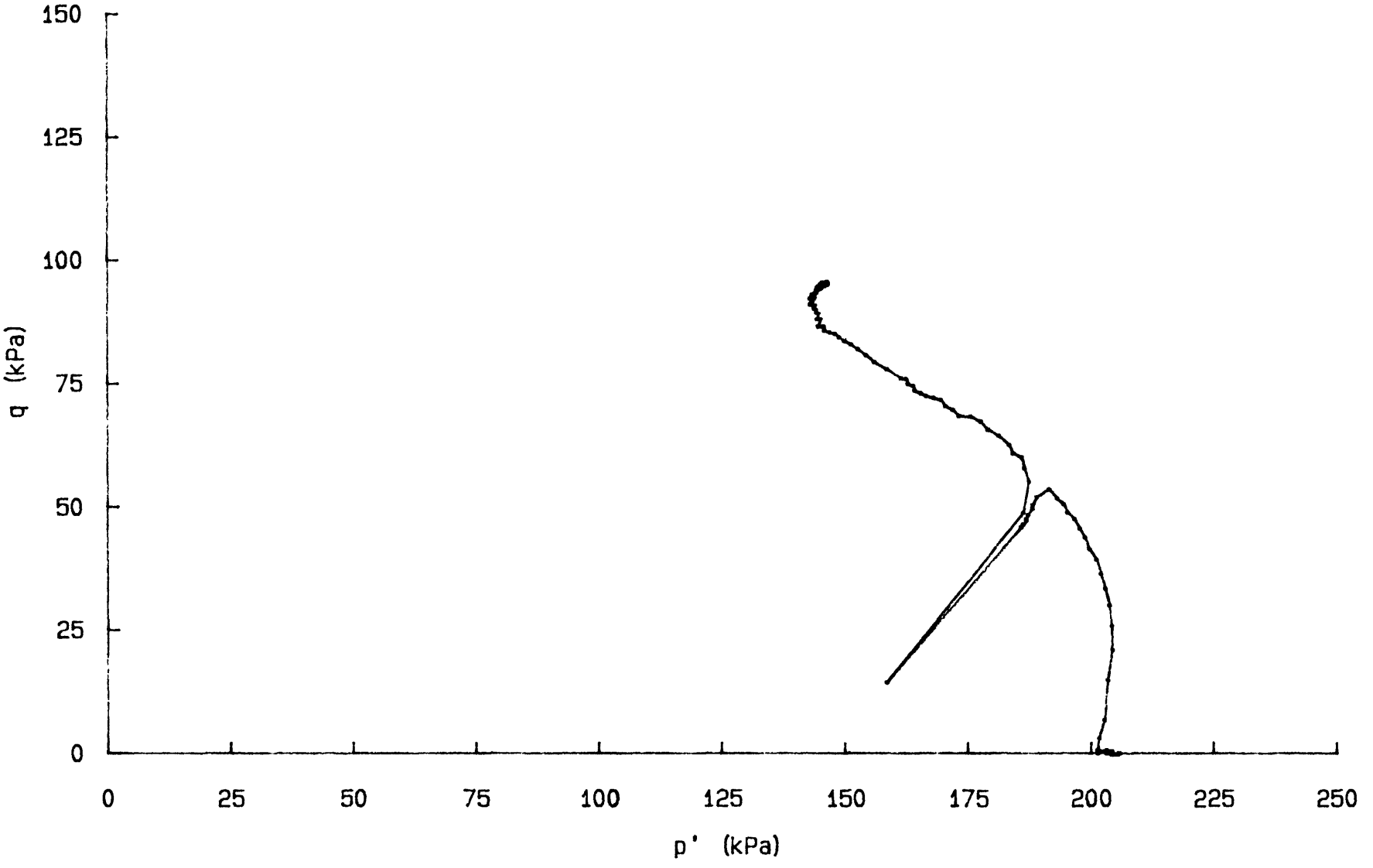

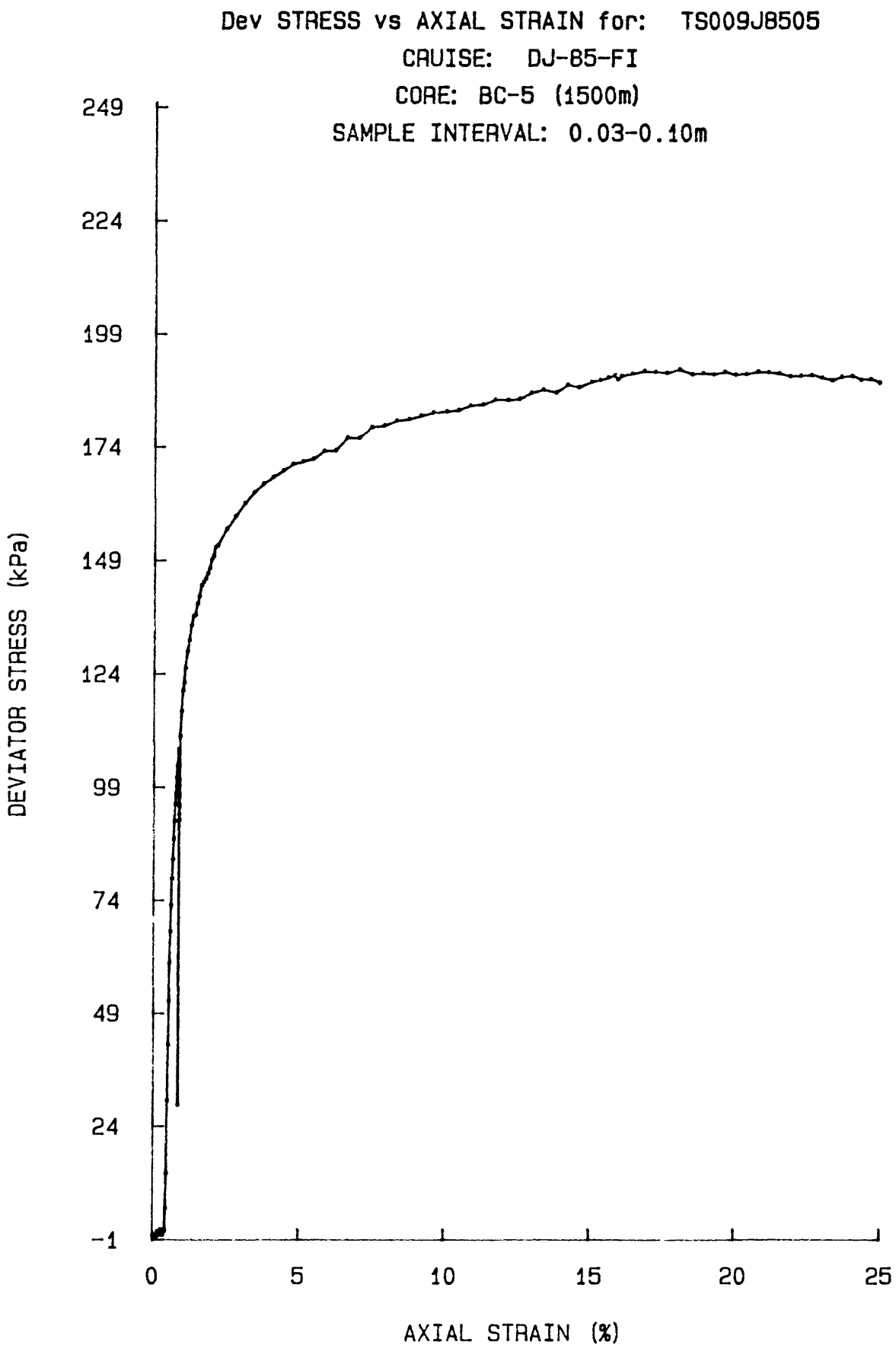
Dev STRESS vs AXIAL STRAIN for: TS009J8505
CRUISE: DJ-85-FI
CORE: BC-5 (1500m)
SAMPLE INTERVAL: 0.03-0.10m
DEVIATOR STRESS (kPa)
249
224
199
174
149
124
99
74
49
24
-1
0
5
10
15
20
25
AXIAL STRAIN (%)

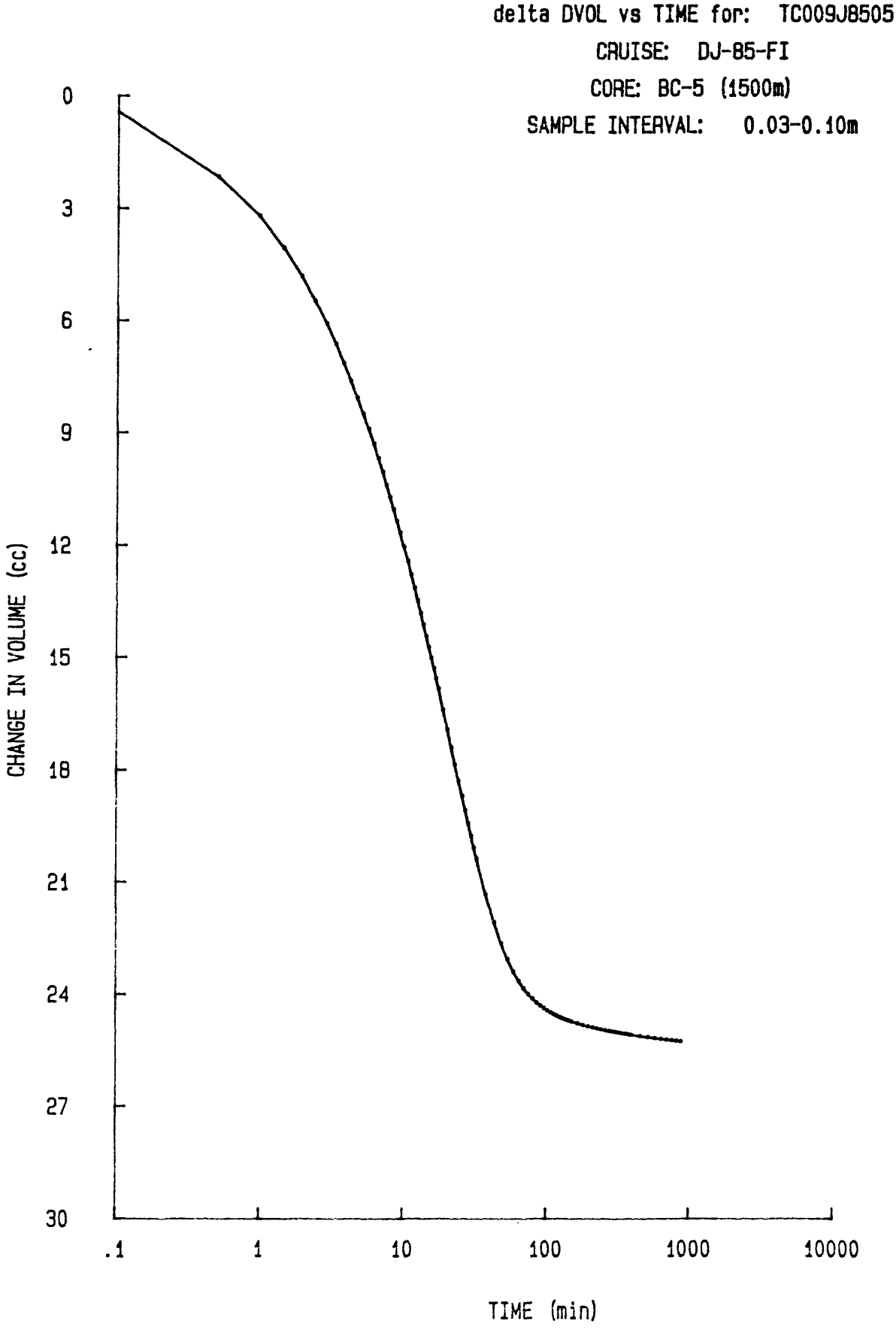
delta DVOL vs TIME for: TC009J8505
CRUISE: DJ-85-FI
CORE: BC-5 (1500m)
SAMPLE INTERVAL: 0.03-0.10m
CHANGE IN VOLUME (cc)
0
3
6
9
12
15
18
21
24
27
30
.1
1
10
100
1000
10000
TIME (min)